REPORT NO.
UCB/EERC-86/06
May 1986

EARTHQUAKE ENGINEERING RESEARCH CENTER

DETERMINATION OF PENETRATION RESISTANCE FOR COARSE-GRAINED SOILS USING THE BECKER HAMMER DRILL

by

LESLIE F. HARDER, Jr.
H. BOLTON SEED

A report on research sponsored by
the National Science Foundation

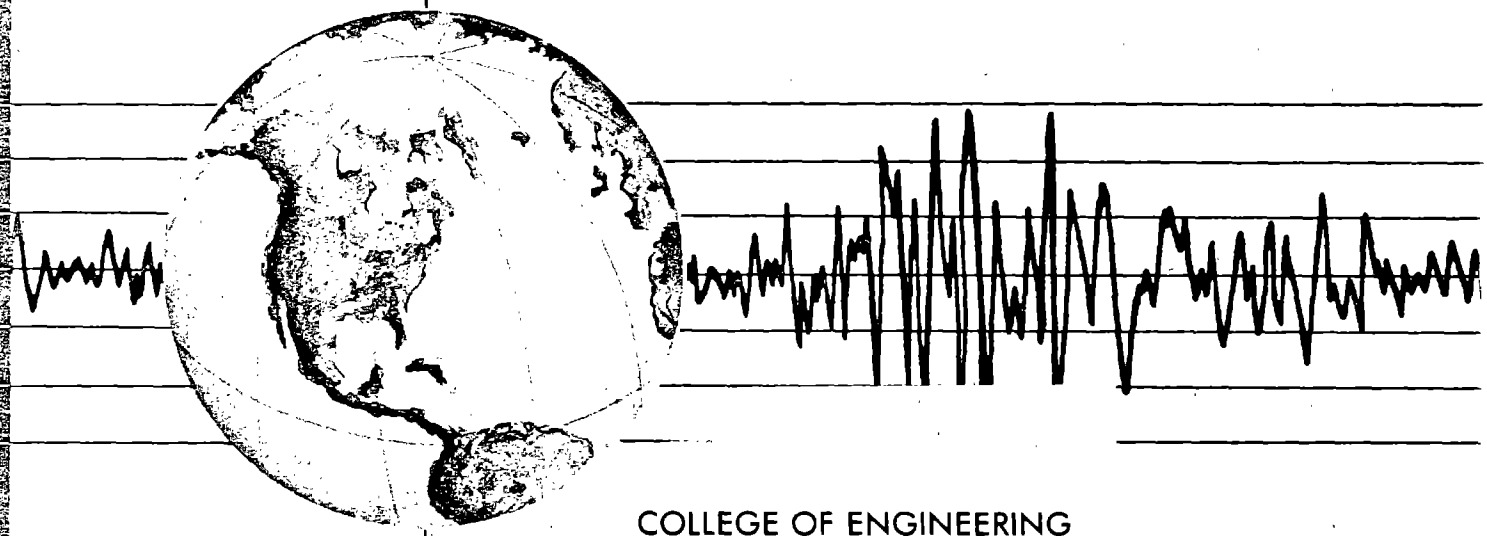

COLLEGE OF ENGINEERING

UNIVERSITY OF CALIFORNIA · Berkeley, California

50272-101

REPORT DOCUMENTATION PAGE	1. REPORT NO. NSF/ENG 86014	2.	3. Recipient's Accession No. PB87 124210/AS
4. Title and Subtitle: Determination of Penetration Resistance For Coarse-Grained Soils Using The Becker Hammer Drill			5. Report Date: May, 1986 6.
7. Author(s): Leslie F. Harder, Jr. and H. Bolton Seed			8. Performing Organization Rept. No. UCB/EERC-86/06
9. Performing Organization Name and Address: Earthquake Engineering Research Center, University of California, 1301 South 46th Street, Richmond, California 94804			10. Project/Task/Work Unit No. 11. Contract(C) or Grant(G) No. (C) NSF No. CEE-84-12366 (G)
12. Sponsoring Organization Name and Address: National Science Foundation, 1800 G. Street, N.W., Washington, D.C. 20550			13. Type of Report & Period Covered 14.

15. Supplementary Notes

16. Abstract (Limit: 200 words)

An investigation has been conducted on the use of a large dynamic penetrometer, developed by Becker Drills, Ltd., for determining the penetration resistance of gravelly soils.

The results show that variations in drilling equipment and procedures significantly influence the Becker Penetration Resistance. To reduce the potential for variability in test results, a set of procedures is recommended as a standard.

Using the recommended procedures, a new correlation between Becker Penetration Test resistance and Standard Penetration Test resistance has been developed. This new correlation has much less scatter than previous correlations and, by using data and experience developed in sands using the Standard Penetration Test, it provides a meaningful method for evaluating the probable behavior of gravelly deposits.

17. Document Analysis a. Descriptors

dynamic
penetrometer
penetration
gravelly soils
earthquake
seismic

b. Identifiers/Open-Ended Terms

Becker Penetration Resistance
Standard Penetration Test

c. COSATI Field/Group

18. Availability Statement: Release Unlimited	19. Security Class (This Report): Unclassified	21. No. of Pages: 148
	20. Security Class (This Page): Unclassified	22. Price

EARTHQUAKE ENGINEERING RESEARCH CENTER

DETERMINATION OF PENETRATION RESISTANCE FOR COARSE-GRAINED SOILS USING THE BECKER HAMMER DRILL

by

Leslie F. Harder, Jr.

and

H. Bolton Seed

Report No. UCB/EERC-86-06

May 1986

A report on research sponsored by
the National Science Foundation

College of Engineering
University of California
Berkeley, California

Abstract

An investigation has been conducted on the use of a large dynamic penetrometer, developed by Becker Drills, Ltd., for determining the penetration resistance of gravelly soils.

The results show that variations in drilling equipment and procedures significantly influence the Becker Penetration Resistance. To reduce the potential for variability in test results, a set of procedures is recommended as a standard.

Using the recommended procedures, a new correlation between Becker Penetration Test resistance and Standard Penetration Test resistance has been developed. This new correlation has much less scatter than previous correlations and, by using data and experience developed in sands using the Standard Penetration Test, it provides a meaningful method for evaluating the probable behavior of gravelly deposits.

Acknowledgements

This investigation was supported by Grant No. CEE-84-12366 from the National Science Foundation. The support of the Foundation for this research is greatly appreciated.

Information on previous Becker Penetration Test studies was kindly provided by O. Farris, M. Allen, L. Walker, W. Jones, I. Staal, and T. Dunne. Additional information regarding the diesel hammer operation was provided by Tony Last. Permission to perform the field studies and access at the various test sites were generously provided by Mr. L. H. Huntington, the California Department of Water Resources, the United States Navy, the Colorado Sand and Gravel Company, and the Big Lost River Irrigation District. Assistance in facilitating the field studies was provided by Cliff Lucas, Dean Smith, G. Reyes, D. Haynosch, R. Monroe, E. Shoebotham, D. Jensen, and R. Lundy. Additional assistance in handling field samples was provided by W. Hammond, R. Torres, D. Najima, R. Johnson, and C. Moody.

Finally we wish to acknowledge the generous help and cooperation provided by Becker Drills, Inc. The careful attention to details from Drillers Ken Arnold and Bill Jeskey is greatly appreciated.

TABLE OF CONTENTS

LIST OF FIGURES

LIST OF TABLES

Determination of Penetration Resistance for Coarse-Grained Soils Using the Becker Hammer Drill

by

Leslie F. Harder, Jr. and H. Bolton Seed

Chapter 1

INTRODUCTION

There are many cases in engineering practice where it is necessary to determine the engineering characteristics of gravelly and coarse-grained soils. Desirably this would be done in-situ, since the properties of cohesionless soils are known to be influenced significantly by sample disturbance. However, standard methods of in-situ soil exploration developed for sands, such as the standard penetration test (SPT), the cone penetration test (CPT), the self-boring pressuremeter, etc. give erroneous results in gravels because the soil particles are large compared to the dimensions of the test equipment. Furthermore, determining soil properties by laboratory testing is hampered by the fact that it is virtually impossible to take undisturbed samples of gravelly soils, except by in-situ freezing techniques, and these are enormously expensive.

In consequence, the engineering properties of gravels are more customarily determined by constructing test pits to extract samples for grain size distribution tests and for determining the in-situ density or relative density of the gravelly soil. Representative samples are then prepared in the laboratory to the same density or relative density as that of the field deposits and used to determine engineering properties such as strength, deformation, and compressibility characteristics. Alternatively, the engineering properties of the deposit are assessed on the basis of judgment, based on a knowledge of the

grain-size distribution and the density of the deposit. Only occasionally has in-situ testing been attempted or used for engineering property determinations of gravelly soils.

In many cases the above procedures have provided useful data for design studies. However, care must be exercised to insure that all relevant factors influencing the interpretation of the test data obtained from the reconstituted samples are considered in the final evaluation of properties. This involves consideration of changes in density, if it is necessary to change the gradation by scalping or adopting a parallel gradation curve for preparation of laboratory test specimens, and in some cases, consideration of other effects such as "ageing," which is likely to change the properties of any cohesionless soil over a long period of time.

In recent years it has been found necessary to explore other properties of gravelly deposits, in addition to the conventional determinations of strength, deformation and compressibility characteristics. These include the response of gravelly deposits to cyclic loading, which may be induced by earthquake shaking or wave action. It is only recently that the need for such studies and determinations has been recognized. Some years ago it was the conventional wisdom of the geotechnical engineering profession, for example, that gravelly soils were not susceptible to large increases in pore water pressure, leading possibly to liquefaction, under the effects of earthquake shaking. It was generally believed that gravelly soils, because of their high permeability, would be able to dissipate pore pressures virtually as fast as they could be generated by earthquake shaking, and thus were not vulnerable to liquefaction during earthquakes. Clearly this depends on the nature of the soil (sandy gravels for example, may not be significantly more pervious than sands); pore pressure dissipation also depends on the boundary drainage

conditions since a gravel is not free-draining if it is underlain and overlain by relatively impervious layers of other soils.

The concept that gravels were not vulnerable to liquefaction was also fostered by the better field performance of foundations on gravel, as compared with sands, in earthquakes such as the Alaska earthquake of 1964, and by laboratory tests, conducted under cyclic loading conditions, which showed that significantly higher stresses were required, even under undrained cyclic loading conditions, to induce high pore water pressures in gravelly soils than in sands. It has since been recognized that the higher laboratory strengths were due mainly to the effects of membrane compliance, and that when laboratory test results are corrected for this effect, the cyclic loading resistance of gravels is not very different from that for sands.

Finally and more importantly, there have been a number of cases in recent years where liquefaction of gravelly deposits has been observed to occur, with associated detrimental effects, during earthquakes. These events have prompted a review of earlier earthquake performance of gravelly soils and several cases of earthquake-induced liquefaction in gravelly soils are now recognized to have occurred.

Important cases of earthquake-induced liquefaction in gravelly soils include:

(1) The liquefaction of a gravelly-sand alluvial fan deposit in the 1948 Fukui earthquake (Ishihara, 1985).

(2) The flow slide at Valdez in an alluvial fan containing large zones of gravelly sand and sandy gravel in the 1964 Alaska earthquake (Coulter and Migliaccio, 1966).

(3) The slide in the upstream gravelly-sand shell of Shimen Dam in the 1975 Haicheng earthquake (Wang, 1984).

(4) The slide in the upstream sandy gravel slope protection layer of Baihe Dam in the 1974 Tangshan earthquake (Wang, 1984).

and (5) The liquefaction of gravelly soils in level ground at the Pence Ranch, and in sloping ground causing the Whiskey Springs Slide, both during the 1984 Mount Borah earthquake (Youd et al., 1985; Andrus et al., 1986).

In a number of these cases, the generation of soil "blows" at the ground surface showed that particles up to 1 inch size had been carried upward by flowing water, or that sand was washed out of sandy gravel deposits to form sand boils at the surface.

Recognition of these effects has led to a renewed interest in the liquefaction characteristics of gravelly soils and in methods of field exploration which can lead to meaningful determinations of their in-situ characteristics. Since the nature of gravelly soils is likely to involve many of the same problems in geotechnical investigations as sands, i.e. significant variability within relatively short distances and significant changes in properties due to sample disturbance, it has seemed desirable to explore the possibility of exploring the properties of gravelly soils using procedures which have proved successful for sandy soils; that is by the use of some type of penetration test which can be performed rapidly, at a number of locations in a deposit, to provide a representative index of overall characteristics. Clearly such a test would need to be much larger in scale than the relatively small-scale SPT or CPT tests used widely for investigating the liquefaction resistance and other properties of sands. In fact, a large scale version of either of these tests would seem to provide a useful basis for investigating the characteristics of gravelly soils. An added advantage of such an approach is that a large-scale version of, say, the SPT test should be just as

applicable in sands as the conventional SPT test and thus it should be possible to correlate the results of the test results with the extensive body of field performance data, such as liquefaction resistance and compressibility, through the development of correlations between the different test procedures. This would provide a direct basis for evaluating the field behavior of gravelly soils.

Fortunately such a large-scale type of penetration test already exists in the form of the Becker Penetration Test, developed in Canada in the later 1950's and now widely used for exploring the characteristics of deposits containing gravel and cobble-size particles. The test has also been used by several investigators for evaluating the penetration resistance of gravelly soils. This report, therefore, presents a review of previous attempts, and the results of an extensive new investigation conducted to develop a correlation between the results of the Becker Penetration Test and the Standard Penetration Test. The object of the study was to provide a meaningful correlation between the results of these different test procedures and thus facilitate the use of test data and experience already available for sands for evaluating the probable behavior of gravelly and other coarse-grained deposits.

Chapter 2

HISTORY OF THE BECKER PENETRATION TEST

The Becker Hammer Drill, shown in Figure 1, was developed by Becker Drills Ltd. in Alberta, Canada during the late 1950's as a method for rapidly penetrating deposits of gravels and cobbles. The method consists of driving a double-walled casing into the ground with a double-acting diesel pile hammer. During driving, air is forced down the annulus of the casing system to the drive bit. Soil particles entering the bit are then transported up the inner casing to the surface by the air flow and they are then collected in a cyclone as illustrated in Figure 2. The principal applications of the device in recent years have included gold-assaying of gravels, installation of piezometers in difficult soil conditions (e.g. Tarbela Dam foundation), and the characterization of coarse-particle deposits.

Equipment

The diesel hammer used on Becker drill rigs is an International Construction Equipment (ICE) Model 180; the hammer is rated at a maximum energy of 8100 foot-pounds per blow. This type of pile hammer is closed off at the top and part of its energy during driving is developed by the compression of air in the top of the hammer cylinder during the travel of the ram during each cycle. By measuring the pressure of this trapped air pressure (bounce chamber pressure), an estimate of the driving energy can be obtained for each blow. Correlations between potential hammer energy and bounce chamber pressure have been developed by the manufacturer and these will be discussed in a later section of this report.

The diesel hammer frame is mounted on rollers or wear blocks which move along guides on the drill rig mast. Delivering 92 blows per minute, it is not

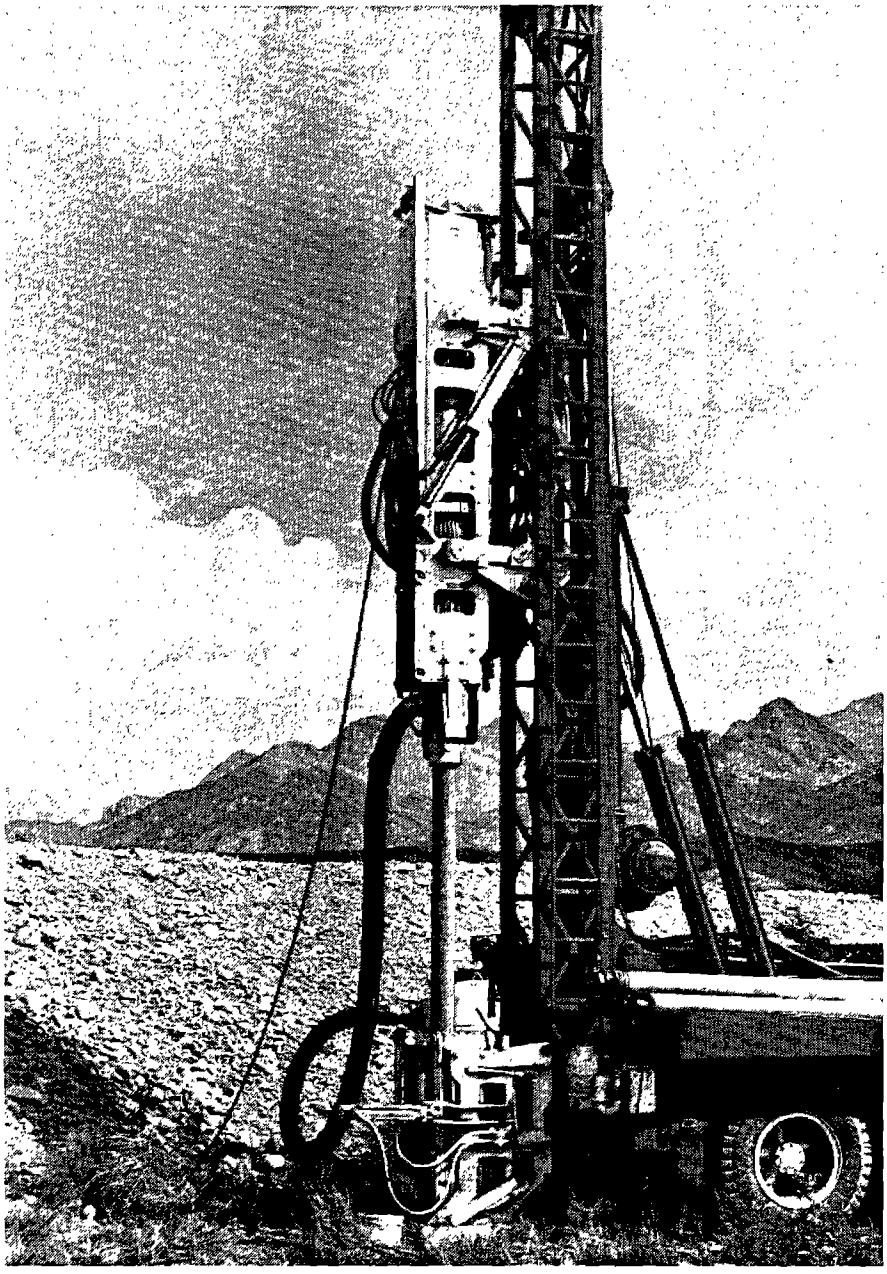

FIG. 1 PHOTOGRAPH OF BECKER HAMMER DRILL RIG

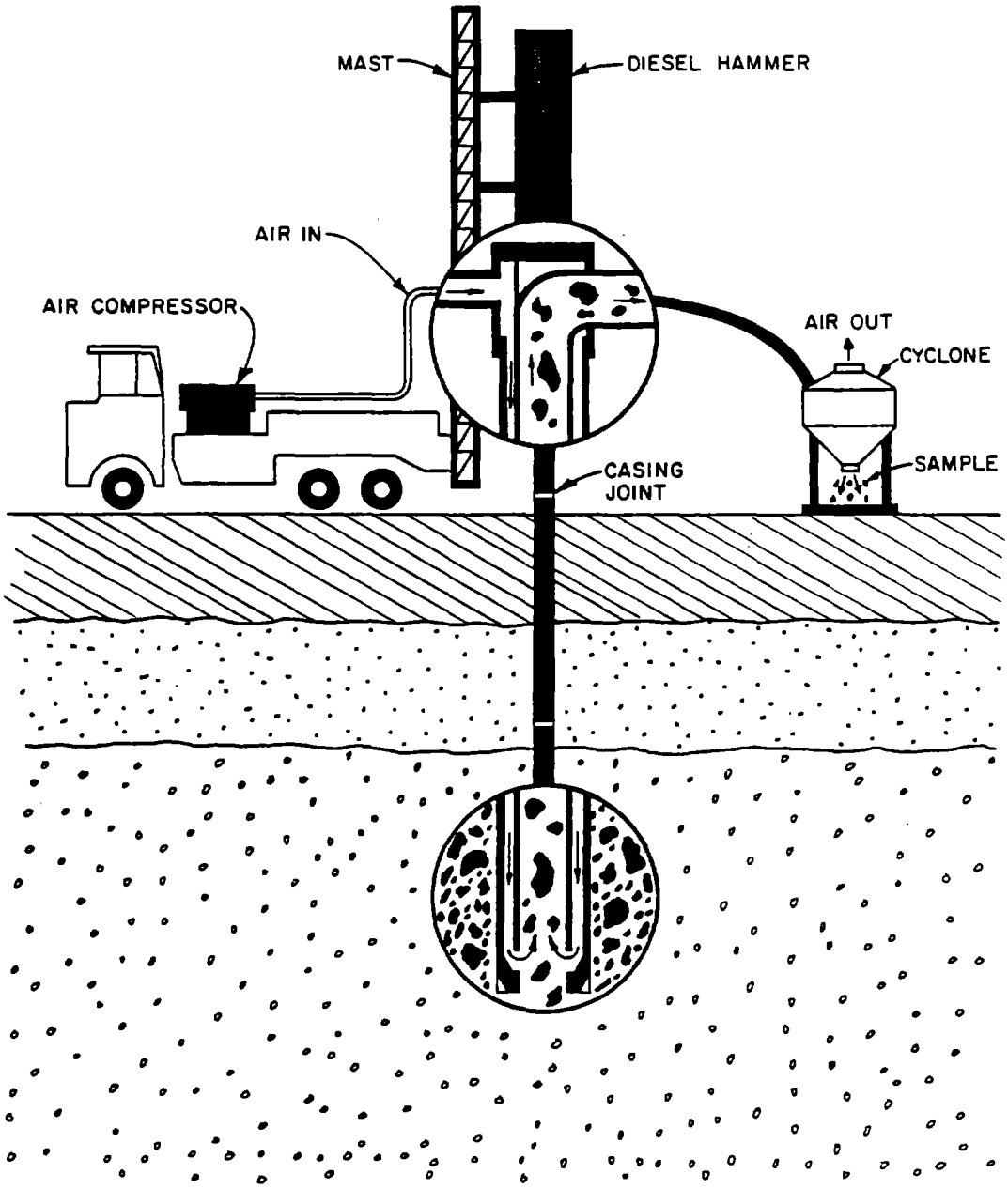

FIG. 2 SCHEMATIC DIAGRAM OF BECKER SAMPLING OPERATION

unusual for the hammer to achieve penetration rates of about 100 feet an hour. On completion of each sounding, the casing is gripped with tapered slips and raised by hydraulic grips. It usually requires about 40 minutes to withdraw 100 feet of casing from the ground.

The double-walled casing is composed of two heavy pipes arranged concentrically (see Figure 3). The inner pipe floats inside the outer pipe, separation being provided by neoprene cushions, and only the outer pipe absorbs the direct impact of the hammer. The casing is provided in 8 to 10-foot lengths, and segments are connected with threaded joints in the outer pipe. An "O" ring seal is used on one end of each inner pipe segment to avoid leaks between the outer and inner pipes. Casing pipes are available in three sizes as follows:

5.5-inch O.D. x 3.3-inch I.D. (Original size)

6.6-inch O.D. x 4.3-inch I.D.

9.0-inch O.D. x 6.0-inch I.D.

Drill bits have two basic shapes: crowd-in bits and crowd-out bits. A crowd-in bit is used to recover as much soil material as possible. A crowd-out bit is used when driving might be difficult and/or when soil recovery is not as important. Figure 4 shows photographs of some of the more commonly used drill bits. A comparison of the 6.6 inch-O.D. Becker crowd-out bit and the 2.0-inch O.D. SPT sampling shoe is shown in Figure 5.

Becker Penetration Test

The Becker Penetration Test consists basically of counting the number of hammer blows required to drive the casing one foot into the ground. By counting blows for each foot of penetration, a more or less continuous record of penetration resistance can be obtained for an entire soil profile. This test was originally called the "Becker Denseness Test" and was developed in

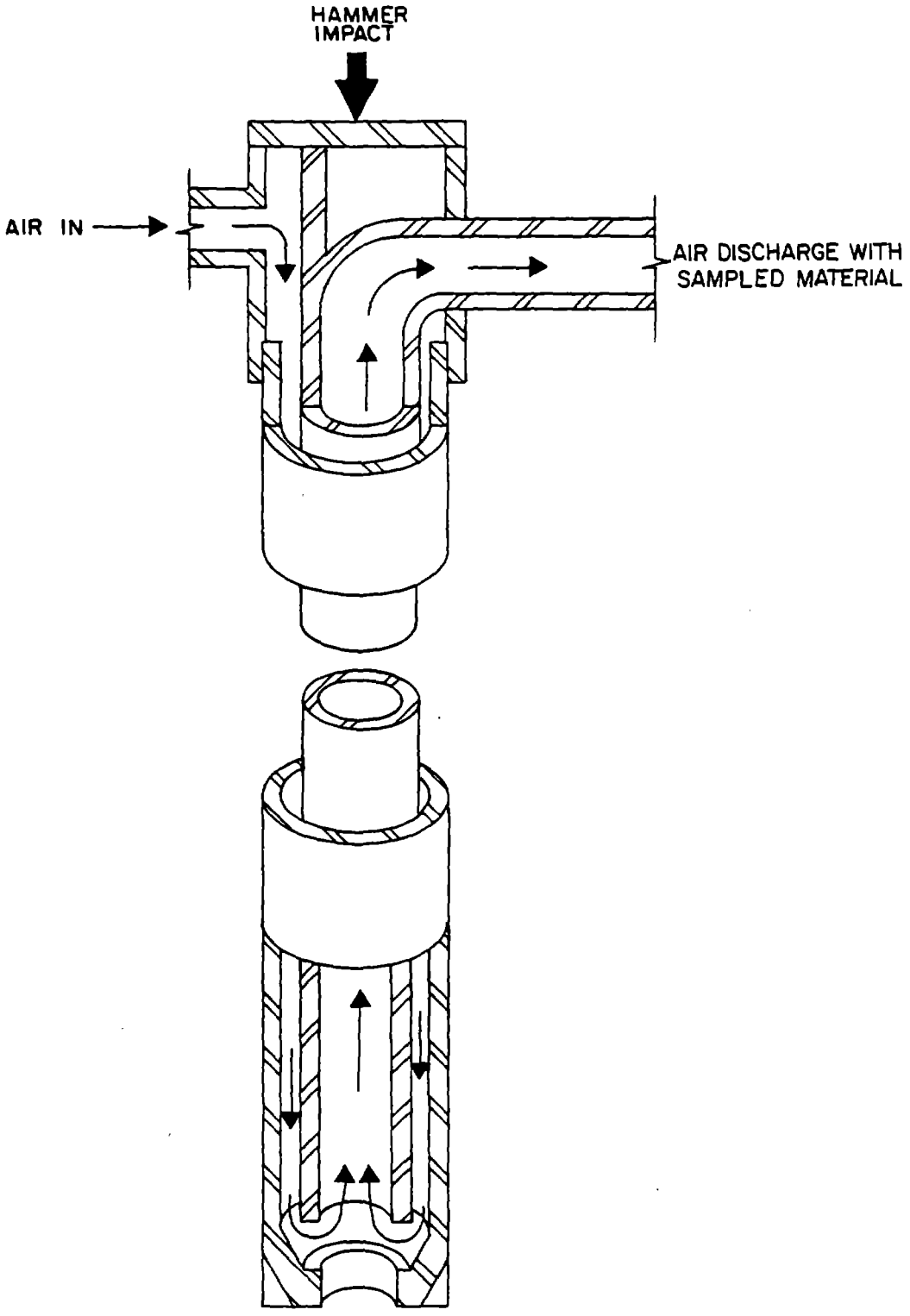

FIG. 3 REVERSE CIRCULATION PROCESS USED WITH BECKER HAMMER DRILL AND OPEN DRILL BITS (adapted from Becker Drills, Inc. literature)

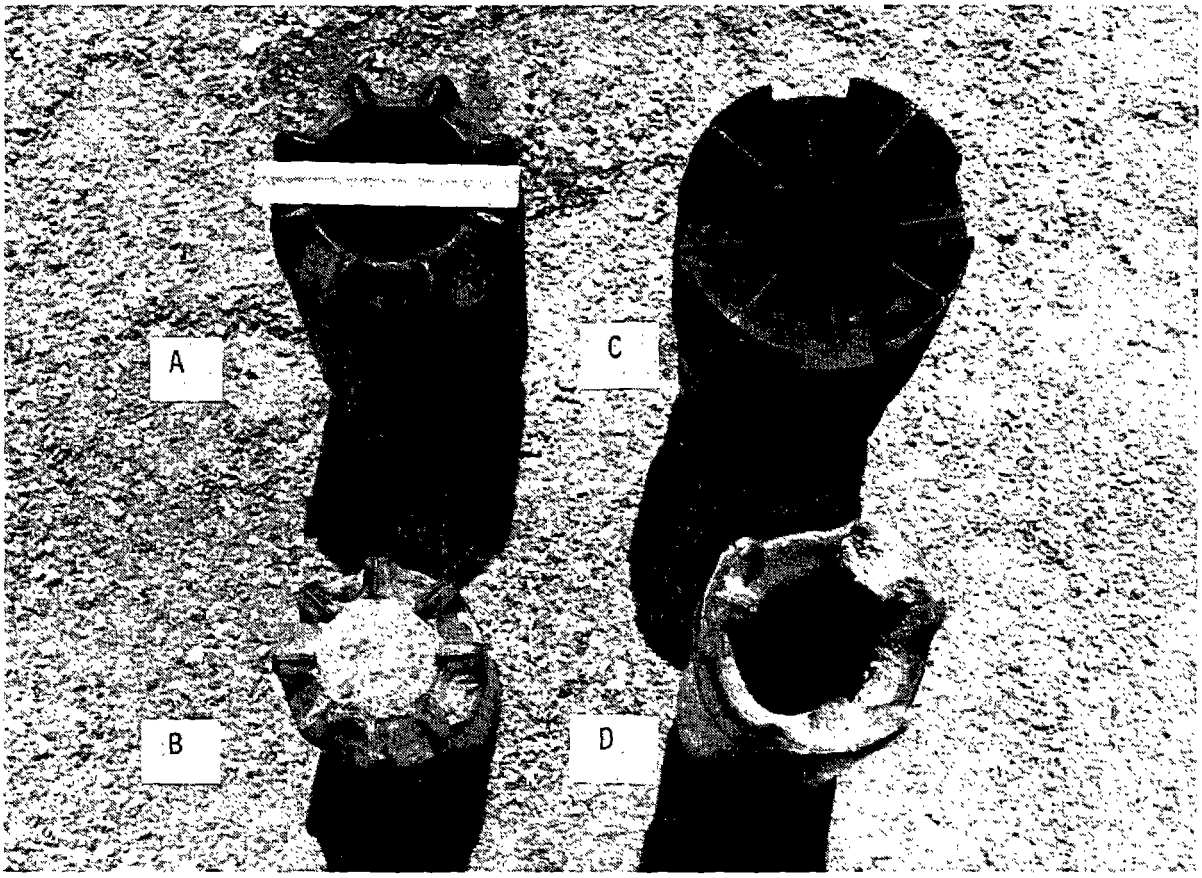

A. 6.6-inch O.D. Open 8-tooth Crowd-out Bit

B. 5.5 inch O.D. Closed 8-tooth Crowd-out Bit

C. 7.3-inch O.D. Open Felcon Crowd-in Bit
(Used with 6.6-inch O.D. Casing)

D. 5.5-inch O.D. Open 3-web Crowd-in Bit

FIG. 4 TYPICAL DRILL BITS USED WITH BECKER HAMMER DRILL RIGS

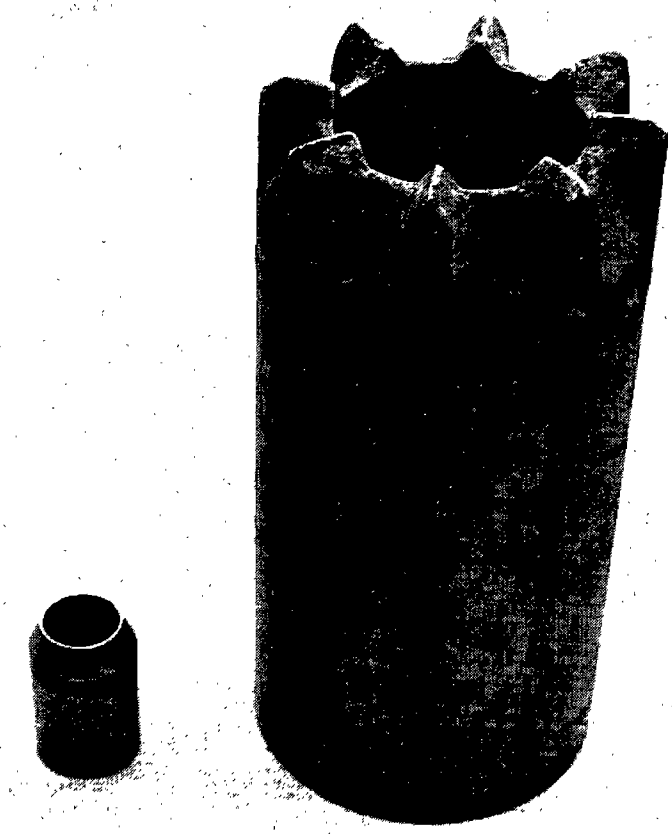

FIG. 5 PHOTOGRAPH COMPARING 2-INCH O.D. SPT SAMPLING SHOE WITH 6 5/8-INCH O.D. CROWD-OUT BECKER DRILL BIT

Canada by using a plugged 8-tooth crowd-out bit with 5.5-inch O.D. casing. The plugged bit was employed because it was found that open-bit soundings in saturated sands often gave erratic results. Over the years, however, Becker penetration testing has employed both open and plugged bits together with both 5.5-inch and 6.6-inch O.D. casing sizes.

On a number of investigations the Becker Penetration Test has often been used for the purpose of obtaining equivalent Standard Penetration Test (SPT) blowcounts and using correlations between SPT resistance and field behavior to predict performance. During the last 13 years, several correlations between Becker blowcounts and Standard Penetration Test (SPT) blowcounts have been developed. Figures 6 through 9 present four correlations between Becker and SPT blowcounts developed by different investigators, and Table 1 summarizes some of the information pertinent to each correlation. In Figure 10 all four correlations are presented together on the same plot. In general there is much scatter in the test data and there are wide variations in the proposed correlations. Thus, for example, a Becker blowcount of 30 might be considered to be equivalent to a SPT blowcount ranging between 30 and 80, depending on which correlation is used.

The great variability of Becker-SPT correlations is due in large measure to the fact that the different studies often employed different Becker and SPT procedures and equipment, as well as different methods of data interpretation. In addition, the studies involved the following deficiencies:

1. Except for the studies performed by Geotechnical Consultants, Inc., no attempt was made to monitor and correct for variations in energy developed by the diesel hammer used for conducting the Becker Penetration Test.

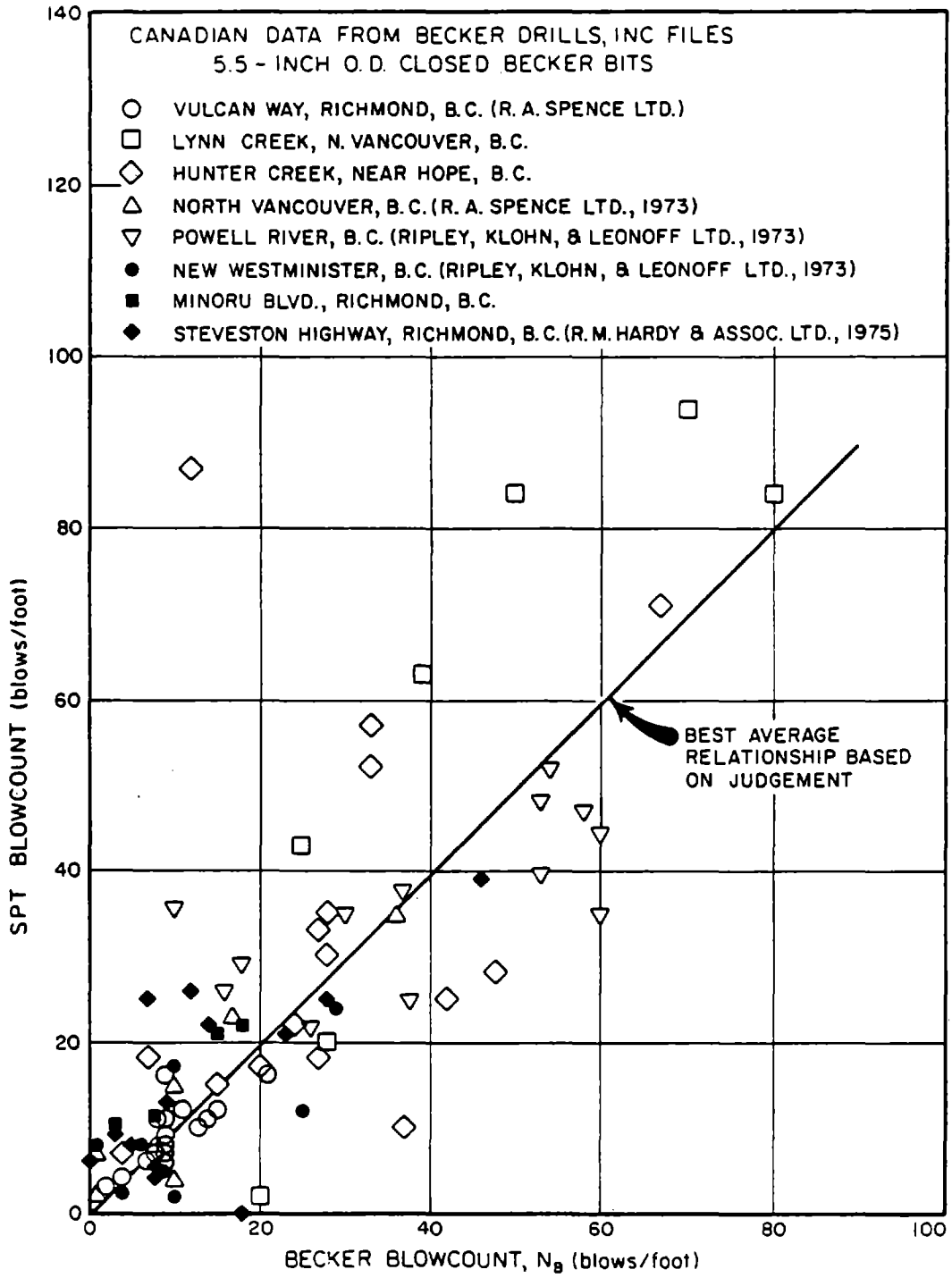

FIG. 6 CORRELATION BETWEEN BECKER AND SPT BLOWCOUNTS DEVELOPED FROM CANADIAN DATA OBTAINED FROM BECKER DRILLS, INC. FILES

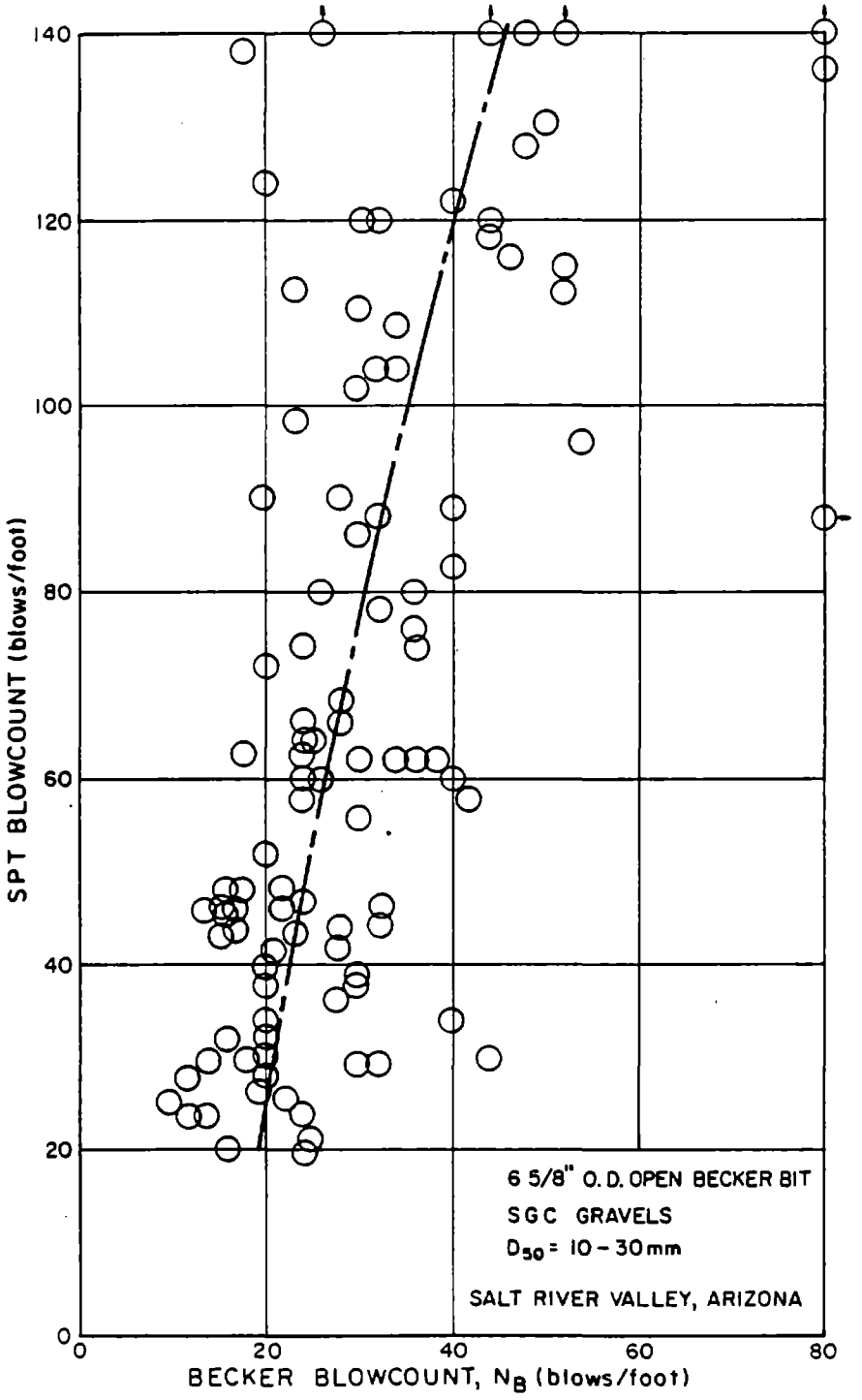

FIG. 7 CORRELATION BETWEEN BECKER AND SPT BLOWCOUNTS DEVELOPED BY SERGENT, HAUSKINS & BECKWITH (1973)

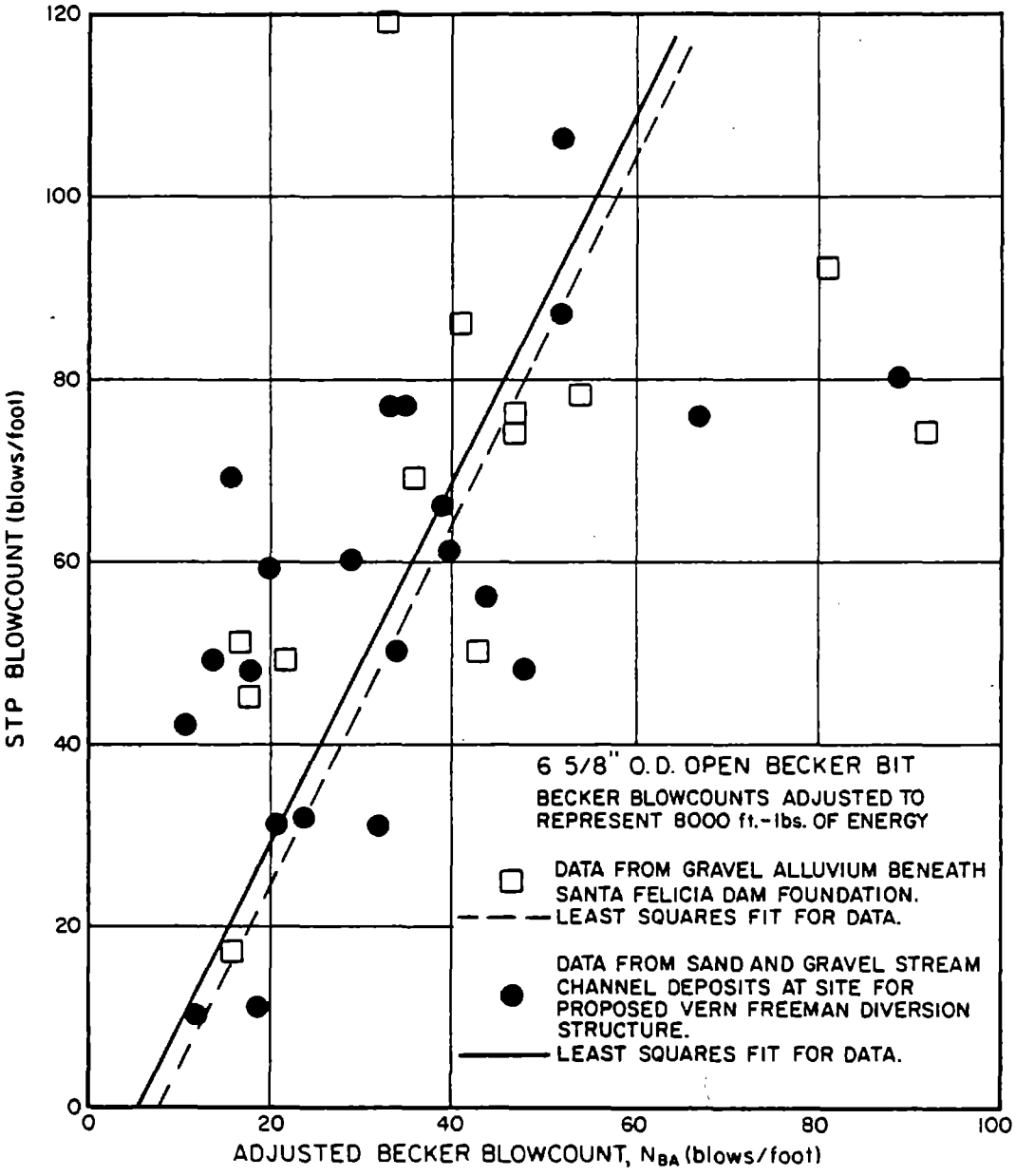

FIG. 8 CORRELATIONS BETWEEN BECKER AND SPT BLOWCOUNTS DEVELOPED BY GEOTECHNICAL CONSULTANTS, INC. (1981, 1983)

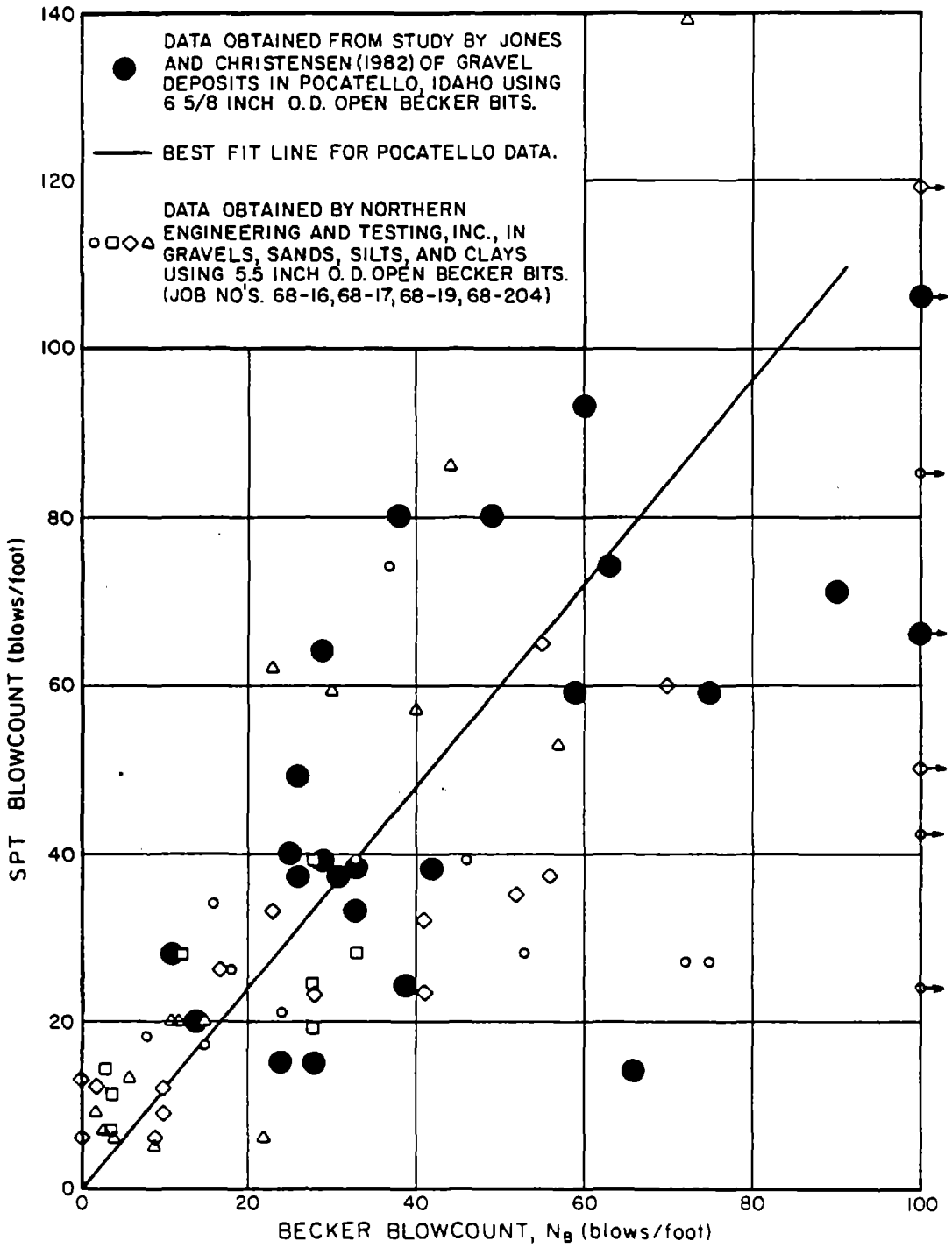

FIG. 9 CORRELATION BETWEEN BECKER AND SPT BLOWCOUNTS DEVELOPED BY JONES AND CHRISTENSEN (1982)

TABLE 1: Existing Correlations Between BECKER and SPT Blowcounts

CORRELATION	SOIL TYPE	CASING O.D.(in.)	DRILL BIT CONFIGURATION
1. CANADIAN DATA FROM BECKER DRILLS, INC. FILES			
A. Vulcan Way, Richmond, BC (R. A. Spence Ltd.)	Silty & Clayey Silts	5.5	Closed
B. Lynn Creek, N. Vancouver, BC	Gravelly Sands	5.5	Closed
C. Hunter Creek, Near Hope, BC	Sands & Gravels	5.5	Closed
D. North Vancouver, BC (R. A. Spence Ltd.)	Gravelly & Silty Sands	5.5	Closed
E. Powell River, BC (Ripley, Klohn, & Leonoff Ltd.)	Gravelly Sands	5.5	Closed
F. New Westminster, BC (Ripley, Klohn, & Leonoff Ltd.)	Sands & Silts	5.5	Closed
G. Minoru Blvd., Richmond, BC	Sands	5.5	Closed
H. Steveston Hwy., Richmond, BC (R.M. Hardy & Assoc, Ltd.)	Sands & Silts	5.5	Closed
2. Sargent, Hauskins & Beckwith (1973) (Salt River Valley, Arizona)	Gravels (D_{50}= 10-30 mm)	6.6	Open
3. Geotechnical Consultants, Inc. (1981, 1983)			
A. Santa Felicia Dam Foundation, California	Gravels (D_{50}= 4-10 mm)	6.6	Open *
B. Vern Freeman Diversion Structure, California	Sands and Gravels	6.6	Open *
4. Jones and Christensen (1982)			
A. Great Western Malting Facility, Pocatello, ID	Silts and Gravels	6.6	Open
B. Northern Engineering & Testing, Inc. Files (Job Nos. 68-16, 68-17, 68-19, 68-204)	Sands, Gravels, Baked Shale	5.5	Open

NOTE: * Denotes that Geotechnical Consultants, Inc. measured bounce chamber pressures and used the the ICE energy calibration charts to adjust measured Becker blowcounts to represent values consistent with an 8000 ft-lb. energy level.

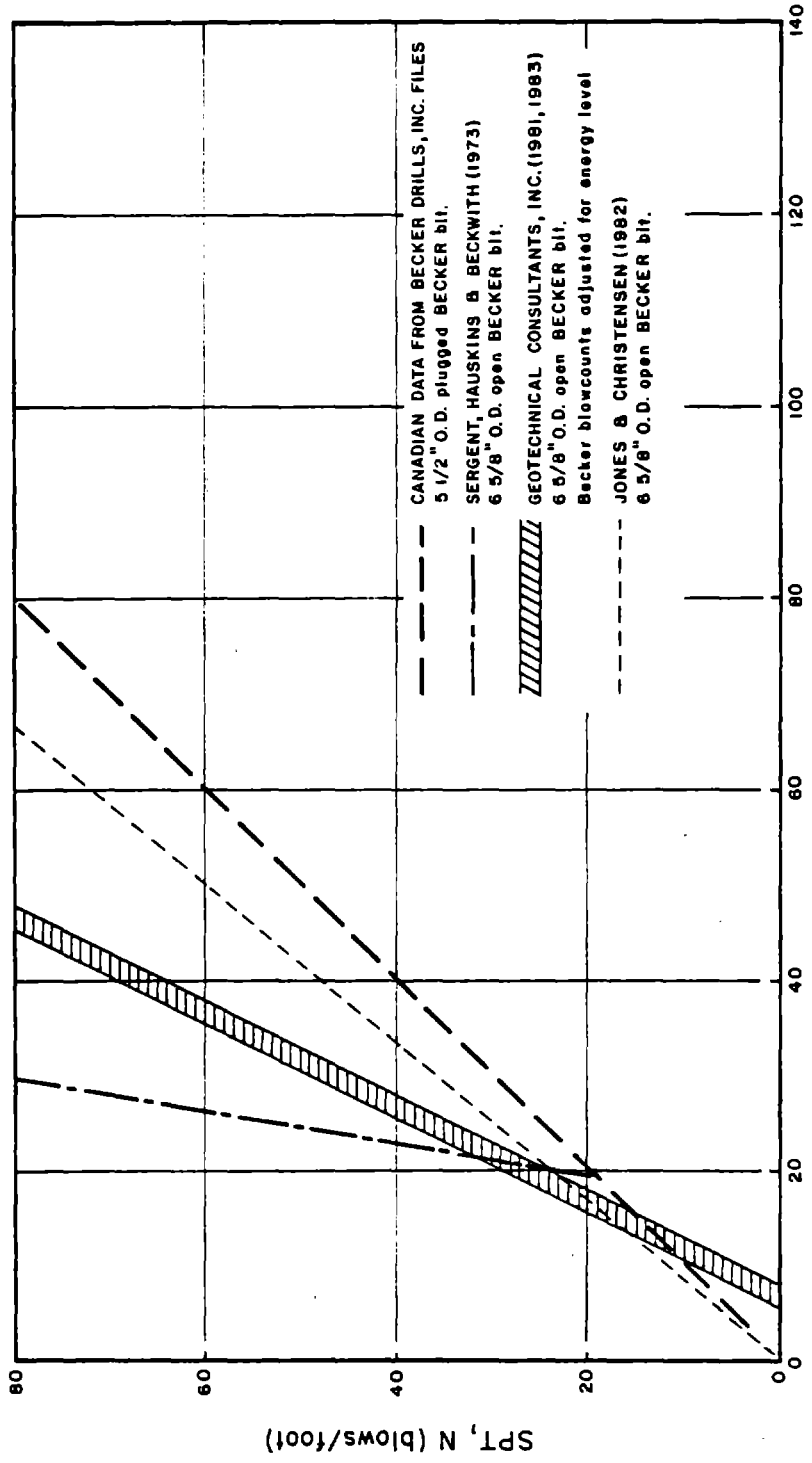

FIG. 10 PREVIOUS CORRELATIONS BETWEEN BECKER BLOWCOUNT AND SPT BLOWCOUNT

2. No attempt was made to account for variations in equipment and procedures used to perform the SPT. Many of these studies employed the Becker "free-fall" SPT hammer and/or non-standard SPT samplers to perform the SPT tests.
3. Many of the correlations employed Becker soundings with open-bits and air recirculation to conduct the Becker Penetration Test. This could have led to erratic and erroneous results due to the loosening and removal of soil ahead of the bit. In some of the correlations, the SPT was performed through open-bit Becker casing thus compounding the problem.
4. Most of the correlations were performed in soils having relatively large gravel and cobble particles. SPT values in soils having such large particles leads to highly questionable results, with judgment indicating that the resulting SPT values would be too high to be used with correlations developed for sand and silty sand deposits.

Never-the-less the studies do indicate that the penetration resistance measured by the Becker Drill procedure has the potential for development as an index of soil penetrability and that if tests were performed under suitably standardized conditions, a useful correlation between SPT and Becker test blowcounts could be developed. Accordingly a new investigation has been conducted with the objective of providing such a correlation.

Chapter 3

FIELD STUDIES OF VARIABLES AFFECTING THE RESULTS OF BECKER PENETRATION TESTS

General

The principal purpose of the field investigations described in this chapter was to obtain a better correlation between Becker blowcounts and SPT blowcounts. Previous correlations were generally performed in gravelly soils where the particle sizes were too large for the SPT to give a meaningful result. Therefore, to develop an improved correlation, Becker and SPT tests were performed in sands and silts at three different sites:

Salinas, California

Thermalito, California

San Diego, California

Because of variations in SPT hammer energies and sampler configurations, the SPT blowcounts obtained at these sites were corrected to equivalent N_{60} blowcounts using the procedures outlined by Seed et al. (1985). The N_{60} blowcount represents a SPT blowcount obtained in a test where the hammer energy delivered into the drill rods is equal to 60 percent of the theoretical free-fall energy of a 140 lb hammer falling 30 inches. It is also representative of a blowcount obtained with a 2-inch O.D. split spoon sampler having a constant I.D. of 1-3/8 inches (i.e. if space for liners is provided in the sampler barrel, then liners are used).

Since the Becker drill rig is a relatively unfamiliar device to many and has not been extensively investigated, it was also necessary to determine the influence of different test parameters on the Becker blowcounts. The parameters studied included bit diameter, bit type (open or closed), drill-rig type, diesel hammer energy, and casing friction. Some of these parameters

were studied at the three sites listed above while other studies were performed at sand and gravel sites in Denver, Colorado and in Mackay, Idaho. A summary of the field explorations is presented in Table 2.

Test Sites

The three sand/silt sites chosen to develop the Becker/SPT correlation were picked because the sites already had good quality SPT tests performed in relatively limited areas and because the soils appeared to have relatively high uniformity (i.e. about the same blowcount) over a significant horizontal distance. The Denver and the Mackay sites were chosen to investigate the influence of several test parameters partly because the rig was already in those areas at the time and because the soils at the two sites were also thought to be relatively uniform in horizontal extent.

Salinas Test Site, California

The Salinas test site is located on the southern bank of the Salinas River near Highway 68 (Figure 11). The site has been used extensively as a testing ground for research on field exploration tools and techniques. Research groups have included the United States Geologic Survey (USGS), University of California-Berkeley (UCB), and the Earth Resources Technology Corporation (ERTEC). According to the ERTEC (1981) investigations (Reference 6), silt and sand exists in the upper 35 feet at this site. These deposits are believed to have been deposited by the Salinas River and are of Holocene age. Below about 35 feet the sediments consist of interbedded sands, silts, and clays.

In addition to several cone penetrometer soundings, ERTEC drilled 8 SPT boreholes at the Salinas site. These SPT tests were generally carried out in the silt and sand within the upper 35 feet and provided an excellent

Table 2: Summary of Becker Soundings Performed For Developing Becker-SPT Correlation

SITE	Date	Drill Rig	Sounding Type	Max. Depth	Number
SALINAS, CA **	11/19/84	AP-1000 (#057)	6.6-in. open CO bit, full throttle	39 ft.	2*
	11/19/84	AP-1000 (#057)	6.6-in. closed CO bit, full throttle	38 ft.	2*
	8/28-29/85	AP-1000 (#057)	6.6-in. closed CO bit, full throttle	99 ft.	3
	8/29/85	AP-1000 (#057)	6.6-in. closed CO bit, red. throttle	99 ft.	4
THERMALITO, CA **	11/21/84	AP-1000 (#057)	6.6-in. open CO bit, full throttle	29 ft.	2
	11/21/84	AP-1000 (#057)	6.6-in. closed CO bit, full throttle	29 ft.	2
SAN DIEGO, CA **	4/18/85	B-180 (#011)	6.6-in. open CO bit, full throttle	52 ft.	2
	4/18/85	B-180 (#011)	6.6-in. closed CO bit, full throttle	52 ft.	2
DENVER, CO	6/13/85	AP-1000 (#057)	6.6-in. closed CO bit, full throttle	55 ft.	2
	6/13/85	B-180 (#055)	6.6-in. closed CO bit, full throttle	55 ft.	2
	6/14/85	AP-1000 (#057)	5.5-in. closed CO bit, full throttle	55 ft.	2
	6/14/85	AP-1000 (#057)	5.5-in. open CO bit, full throttle	55 ft.	2
	6/14/85	AP-1000 (#057)	5.5-in. open CI bit, full throttle	55 ft.	2
	6/27-28/85	AP-1000 (#057)	6.6-in. closed CO bit, full throttle	55 ft.	5
	6/28/85	AP-1000 (#057)	6.6-in. closed CO bit, red. throttle	55 ft.	2
	6/28/85	AP-1000 (#057)	6.6-in. open CO bit, full throttle	49 ft.	1
	6/28/85	AP-1000 (#057)	7.3-in. open CI bit, full throttle	49 ft.	2
MACKAY, ID	8/21/84	AP-1000 (#057)	6.6-in. open CO bit, full throttle	43 ft.	1
	8/21/84	AP-1000 (#057)	6.6-in. closed CO bit, full throttle	45 ft.	1
	7/17/85	AP-1000 (#057)	7.3-in. open CI bit, full throttle	39 ft.	1
	7/17/85	AP-1000 (#057)	6.6-in. open CO bit, full throttle	38 ft.	2
	7/17/85	AP-1000 (#057)	6.6-in. closed CO bit, full throttle	37 ft.	2
	7/17-18/85	AP-1000 (#057)	6.6-in. closed CO bit, red. throttle	38 ft.	3

NOTES: * Denotes no bounce pressure readings taken
** Denotes a sand/silt site where SPT blowcounts were available
CO Denotes a crowd-out bit
CI Denotes a crowd-in bit

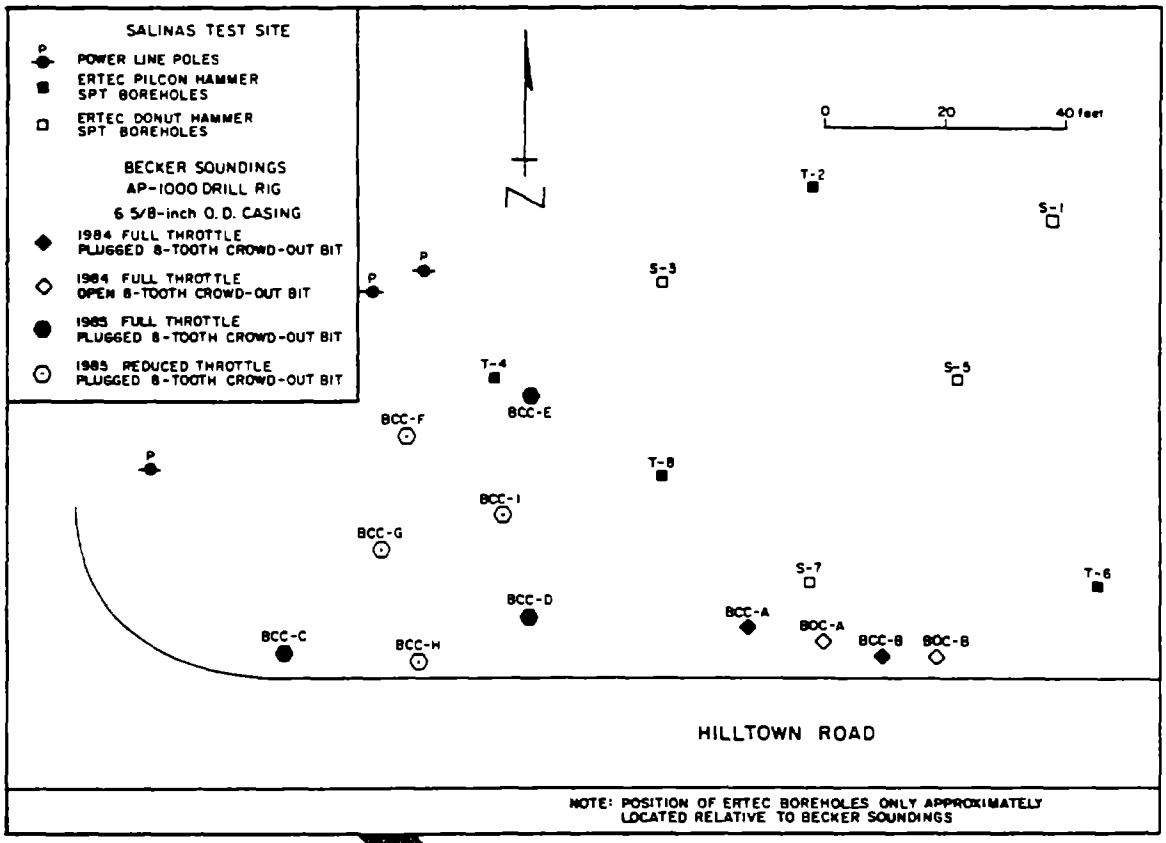

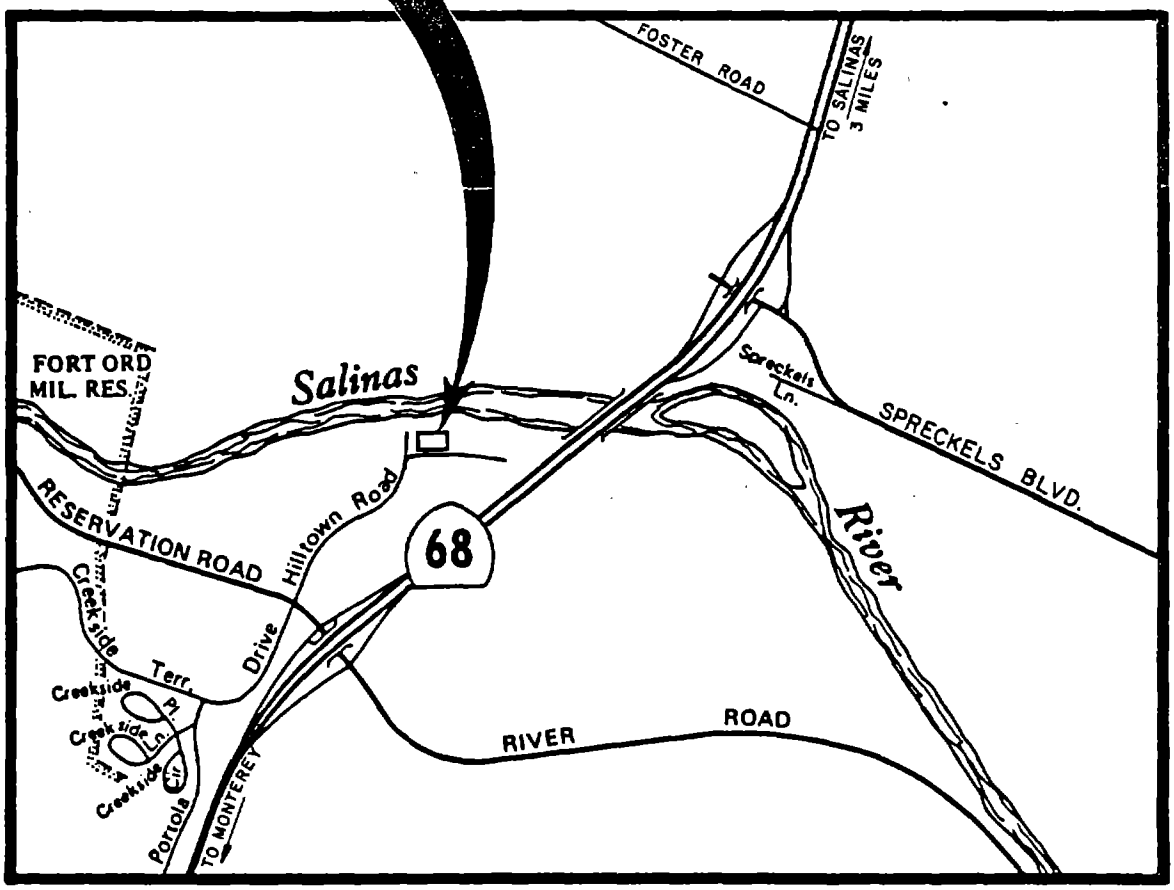

FIG. 11 GENERAL LAYOUT OF BORINGS AND SOUNDINGS AT SALINAS TEST SITE

opportunity to calibrate the Becker apparatus. For four of the ERTEC boreholes, the SPT tests were carried out with a Pilcon trip hammer, a hammer type which has been found to give reasonably consistent energy levels near 60 percent of the theoretical free-fall value (Liang, 1983; Decker et al., 1984; and ERTEC, 1984). The other four boreholes employed a non-standard donut hammer with a rope and cathead release. In general, the non-standard donut hammer gave much higher SPT blowcounts than did the Pilcon trip hammer. Since the energy characteristics of the second hammer system were unknown, only the SPT blowcounts obtained with the trip hammer were used in this investigation. All ERTEC borings at this site employed a SPT split-spoon sampler with room for liners, but with no liners used. As discussed by Seed et al., (1985), the effect of removing the liners is thought to decrease the blowcount by about 10 percent for blowcounts around 10 and about 30 percent for blowcounts around 35 or more. Since most of the Salinas blowcounts were less than 20, to correct the ERTEC blowcounts to equivalent N_{60} values, a correction factor for energy level of 1.00 and a correction factor for sampler geometry averaging about 1.15 were used.

The initial explorations at this site with the Becker Penetration Test were carried out in November 1984 and consisted of two Becker Open Casing (BOC) soundings and two Becker Closed Casing (BCC) soundings. The gradation curves for the samples obtained in the BOC explorations are shown in Figure 12. Although these initial soundings were performed with the diesel hammer at full throttle, the bounce chamber pressure gage was not available at the time and, therefore, the actual bounce pressures were not determined. Since subsequent studies revealed that the bounce chamber pressure was a very important parameter, 7 additional BCC soundings with measurements of bounce pressures were made in August 1985. Four of these later BCC soundings were conducted

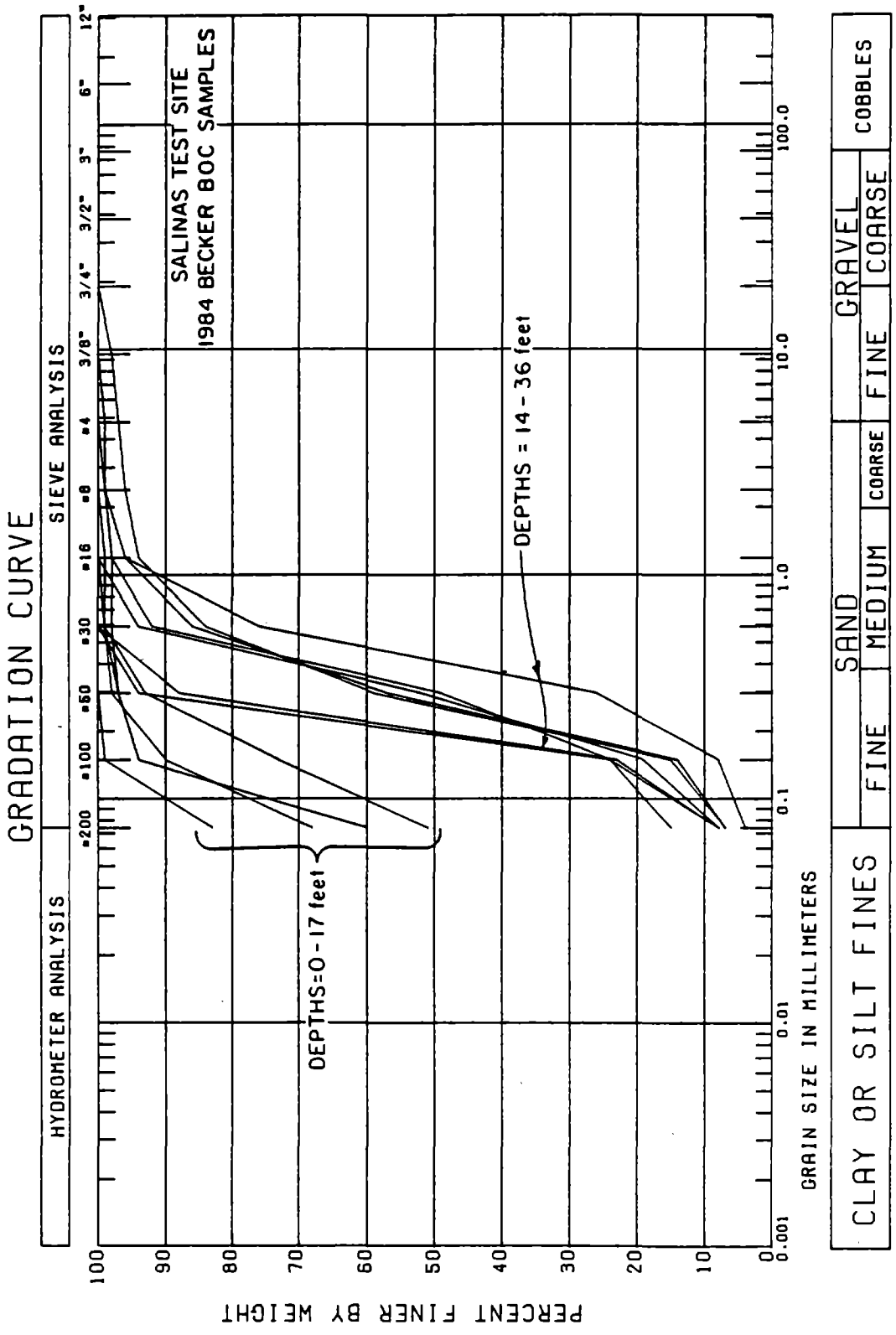

FIG. 12 GRADATION CURVES FOR BECKER SAMPLES OBTAINED AT THE SALINAS TEST SITE

with reduced throttle settings in order to study the effect of reduced energy on the Becker blowcount.

Thermalito Test Site

The Thermalito test site is located at Thermalito Afterbay Dam, near Oroville, California. This site is located near the downstream toe of the embankment at Station 104. The foundation at this site consists of fluvial deposits formed during the Pleistocene. The California Department of Water Resources had previously drilled a number of SPT boreholes at this site (Reference 3). There were 9 boreholes at this site which employed a safety hammer and 4 which employed a donut hammer for performing the SPT tests. For calibration purposes, it was decided to use only the results from the 9 safety hammer tests. Velocity measurements indicated that the SPT hammers had velocities just prior to anvil impact that were equivalent to a kinetic energy equal to 70 percent of the theoretical free-fall value. Since safety hammers are generally able to transmit between 90 to 95 percent of the kinetic energy through the anvil, a rod energy equivalent to 63 percent of the theoretical free-fall value was used to interpret the results of these tests. Thus, the Thermalito SPT blowcounts required a correction factor of 1.05 for energy level. As no liners were used in the SPT sampling tubes and the blowcounts were between 20 and 40, a correction factor of 1.2 to 1.3 for sampler configuration was also employed to correct the blowcounts to equivalent N_{60} blowcounts.

Becker explorations were performed at Station 104 in November 1984. Two Becker open-casing (BOC) soundings and two Becker closed-casing (BCC) soundings were performed in the vicinity of the previous SPT borings (Figure 13). The soil of interest at this site is a 20-foot thick layer of fine to medium sand lying beneath an 8-foot thick cap of compact silt. Figure 14 presents

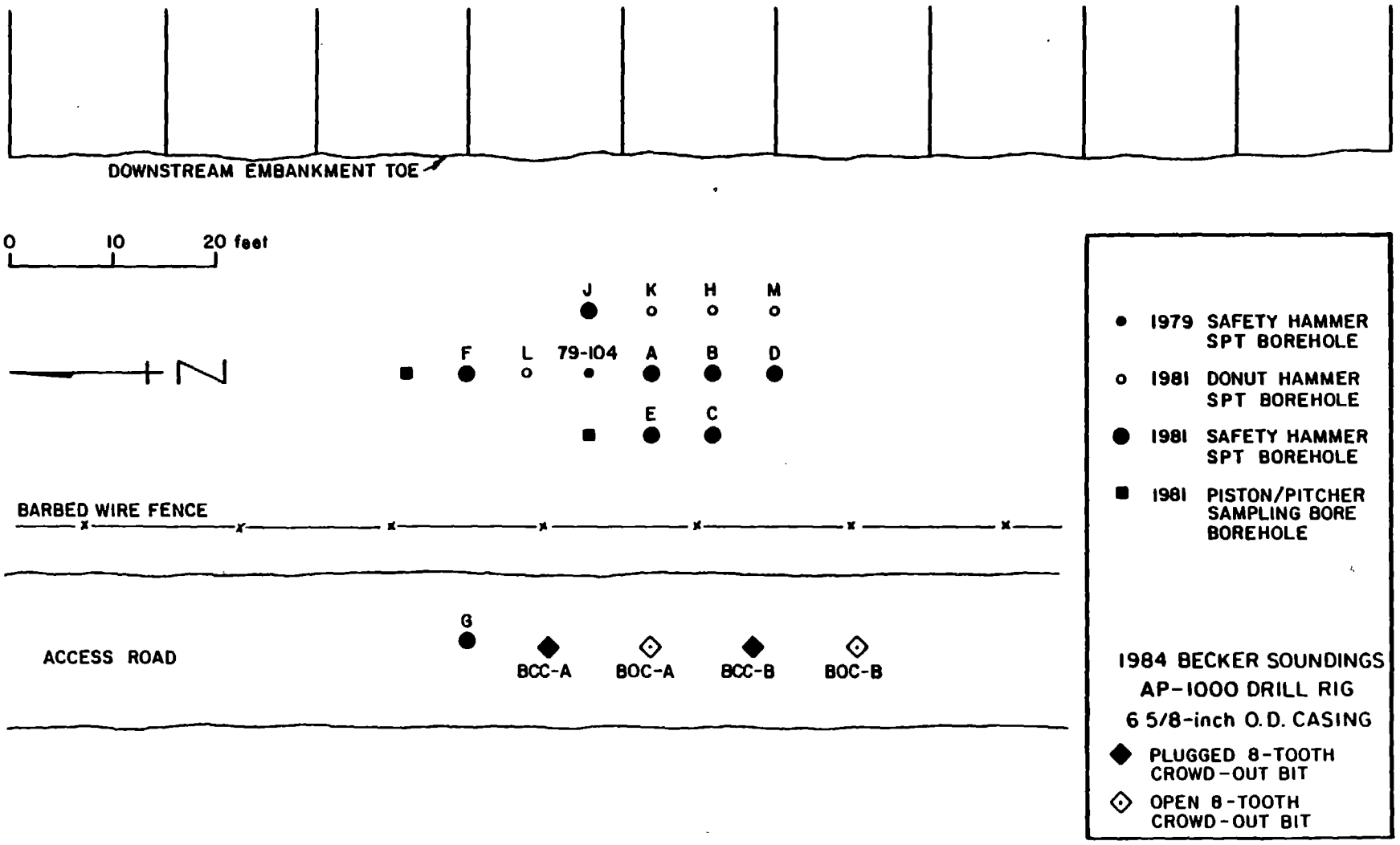

FIG. 13. GENERAL LAYOUT OF BORINGS AND SOUNDINGS AT THERMALITO TEST SITE

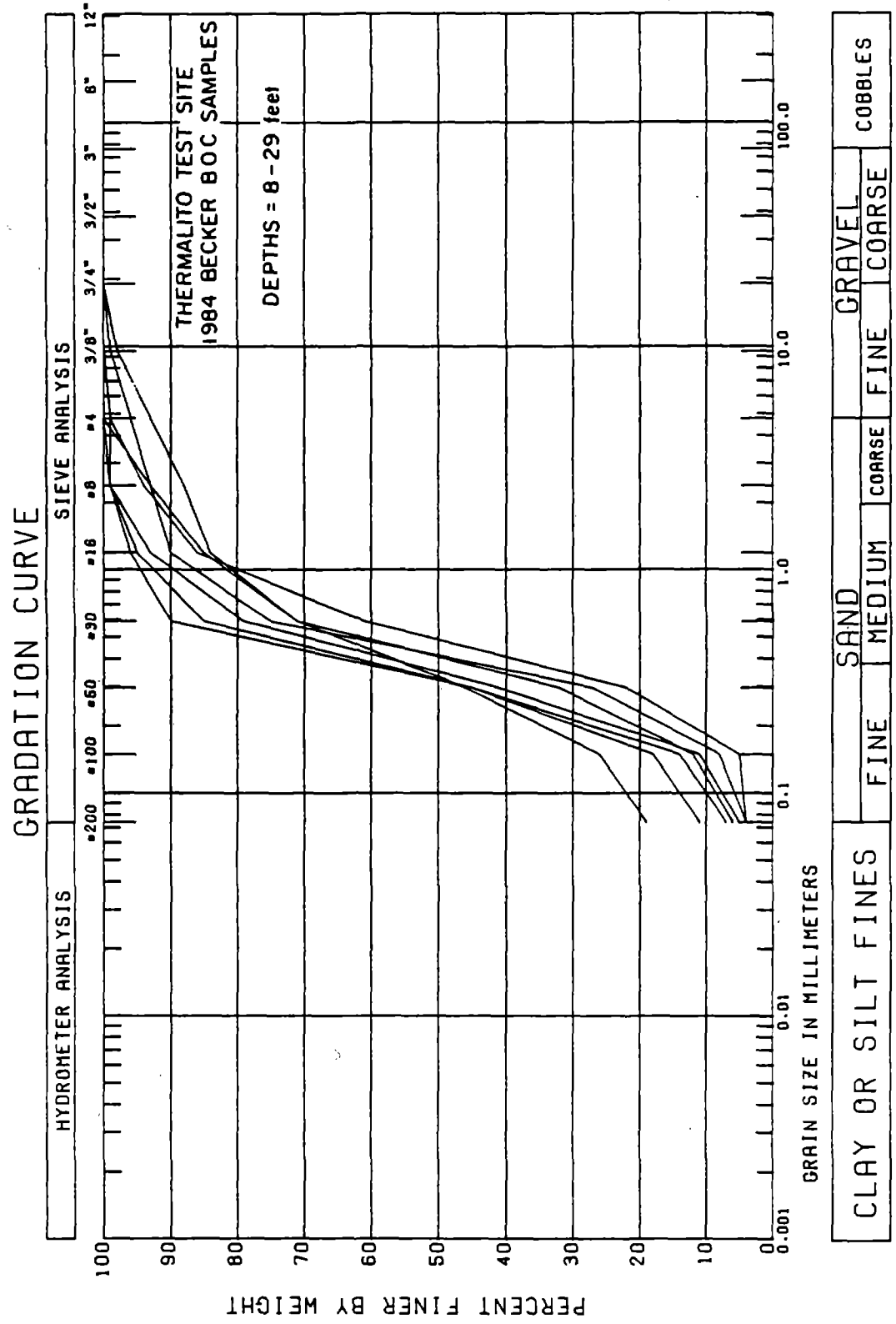

FIG. 14 GRADATION CURVES FOR BECKER SAMPLES OBTAINED AT THE THERMALITO TEST SITE

gradation curves for samples obtained from the sand layer by the Becker BOC sampling operations.

San Diego Test Site

The San Diego test site is located on North Island Naval Air Station in a parking lot immediately south of Building 652, (Figure 15). According to a study by ERTEC (1981) the site is in an area where artificial fill was placed across a channel in 1945 in order to link North and Coronado Islands. Both the fill and the underlying near-surface deposits consist chiefly of sands and silty sands. Gradation tests performed by ERTEC (Reference 6) indicated that these sands generally had between 7 and 24 percent finer than the No. 200 sieve (0.074 mm) and roughly 2 to 4 percent clay fines (finer than 0.002 mm).

As with the Salinas site, ERTEC had made extensive use of the site to perform field studies and had made 4 SPT boreholes using the Pilcon trip hammer and 4 SPT boreholes using the non-standard donut hammer/rope-and-cathead system. As for the Salinas site, only the trip hammer blowcounts were used in the current study to develop a correlation with Becker blowcounts (see section on Salinas Test Site, California). As described for the Salinas site, to correct the measured results to equivalent N_{60} blowcounts, no correction factor for SPT hammer energy was required. However, because the SPT blowcounts at the San Diego site ranged from very small to very large values, the correction factors required to allow for the omission of liners from the sampling tube ranged from 1.00 to 1.35.

In April 1985, two BOC and two BCC soundings were carried out. Unlike the explorations at Salinas and Thermalito which used an AP-1000 Becker drill rig, the soundings at San Diego used a B-180 Becker drill rig.

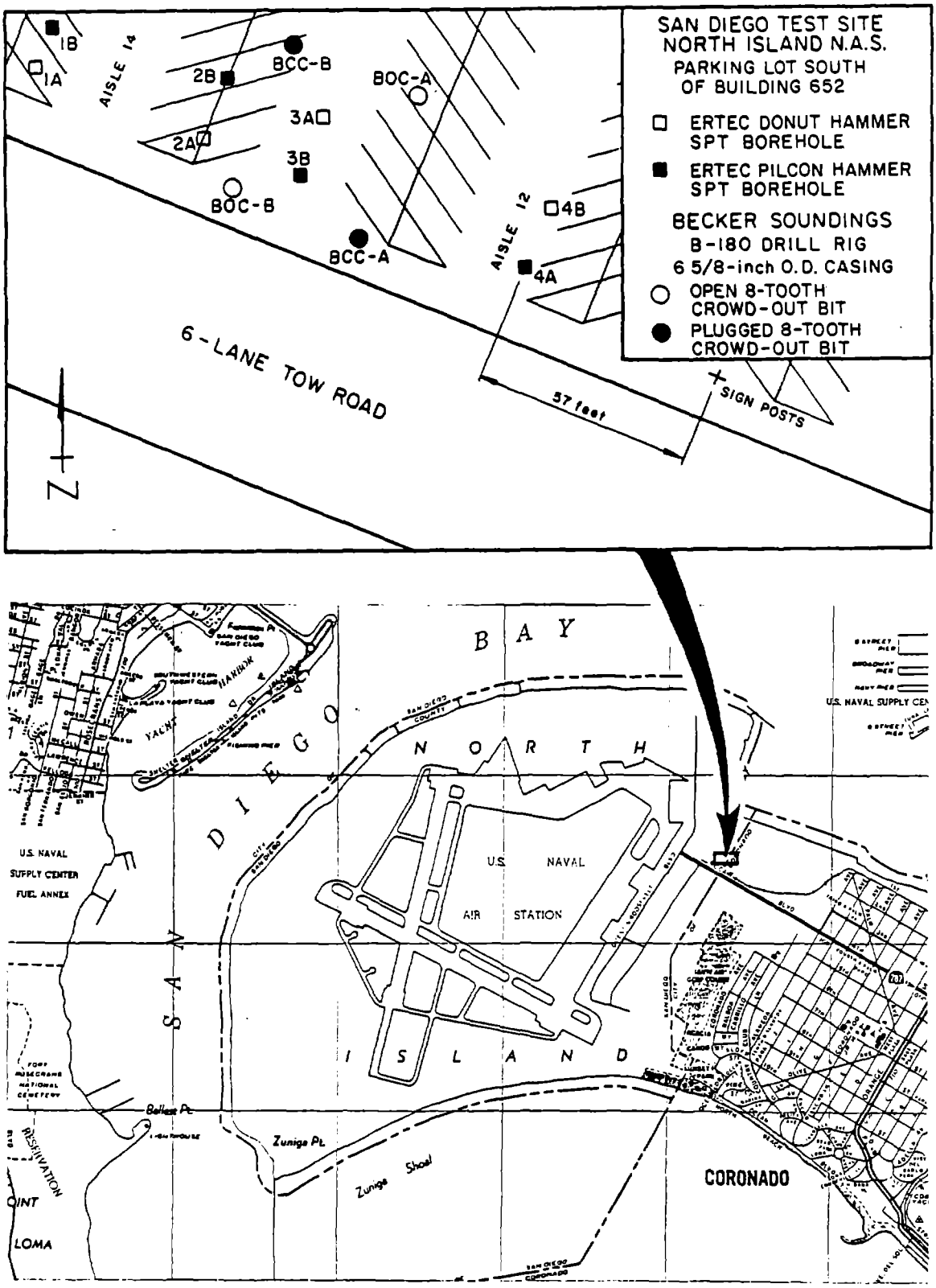

FIG. 15 GENERAL LAYOUT OF BORINGS AND SOUNDINGS AT SAN DIEGO TEST SITE

Denver Test Site

The Denver test site is located on the northeast edge of town in a sand and gravel pit owned by the Colorado Sand and Gravel Company. The deposits tested consisted of a partially cemented gravelly sand in the upper 42 feet. Figure 16 shows a photograph of this material exposed in an adjacent cut. Below 42 feet, the material changed to a sandy clay which became more sandy between 52 and 55 feet.

Becker soundings were made in the period June 13-14, 1985 and again on June 27-28, 1985. The purpose of these soundings was to investigate the effects of various test parameters on the resulting Becker blowcounts. The parameters studied at this site included bit diameter, open-bit vs. closed-bit, drill rig type, and diesel hammer throttle setting. In all, 13 plugged bit and 7 open-bit soundings were performed. Figure 17 shows the general layout of the soundings.

Three of the closed-bit soundings performed using the June 27/28 test period (BCC-5, BCC-7, and BCC-9) were not used in determining the effects of test parameters. Because the location of the first group of soundings was only approximately known, sounding BCC-5 was apparently located over or near a previous sounding. This was believed to be the case because the blowcounts from this sounding were low and inconsistent with other soundings performed in the same manner. Therefore, the blowcounts from this sounding were not used. The results of soundings BCC-7 and BCC-9 were not used because a special bypass valve had been installed in the hydraulic system supporting the hammer to the mast and had been open at the time these tests were made. When open, this valve was intended to allow the hydraulic fluid to flow faster and enable the hammer to keep up with the descending casing. If successful, this would have increased hammer efficiency, and the blowcount would have decreased.

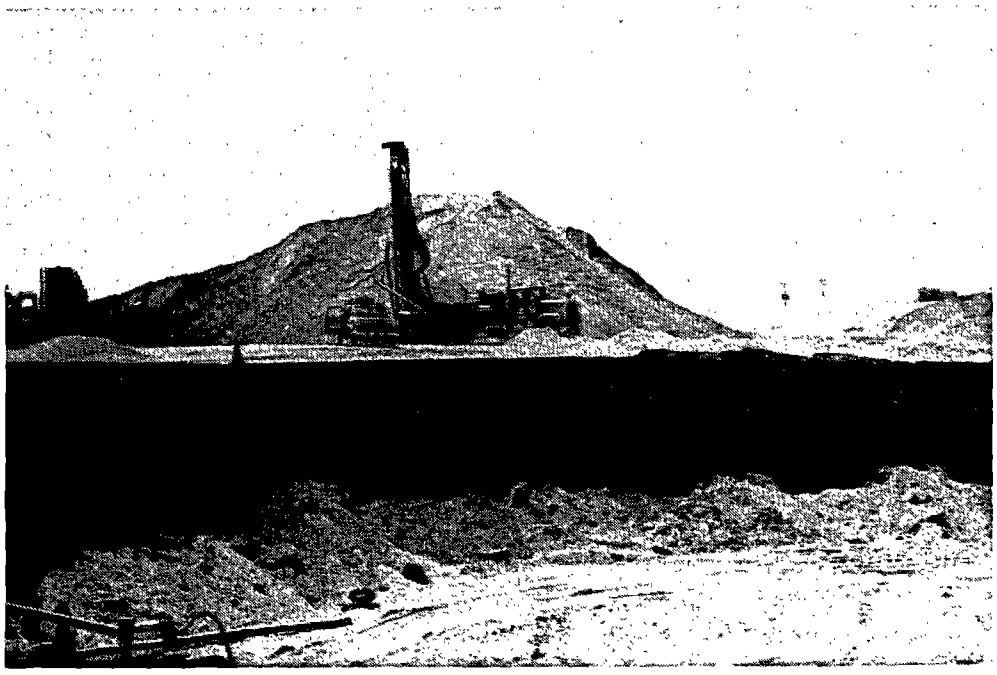

a) Denver Test Site

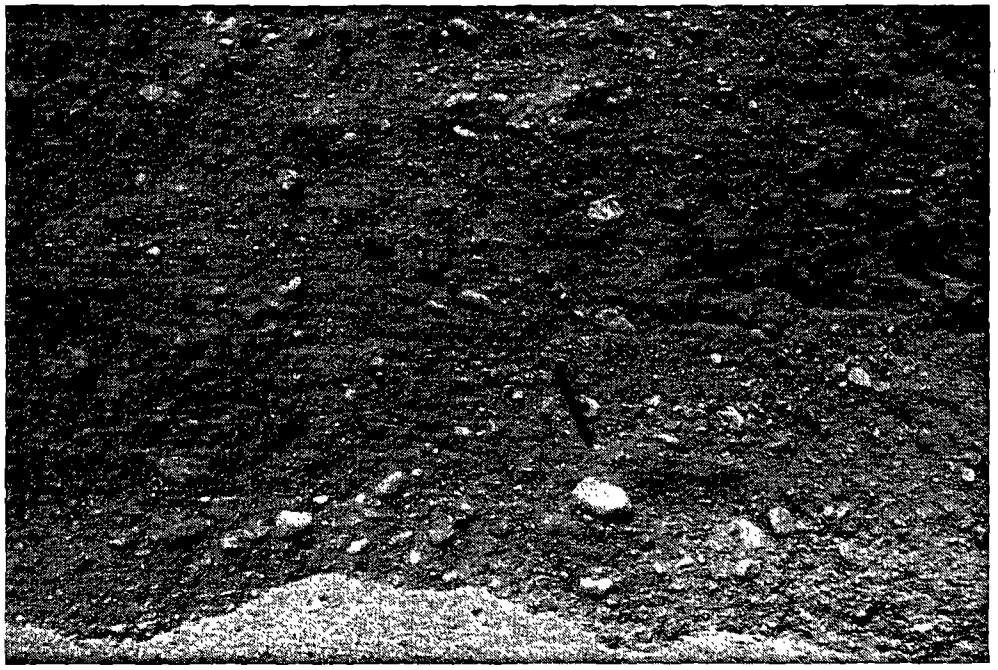

b) Gravelly Sand Exposed in Adjacent Cut

FIG. 16 PHOTOGRAPHS ILLUSTRATING DENVER TEST SITE AND MATERIALS

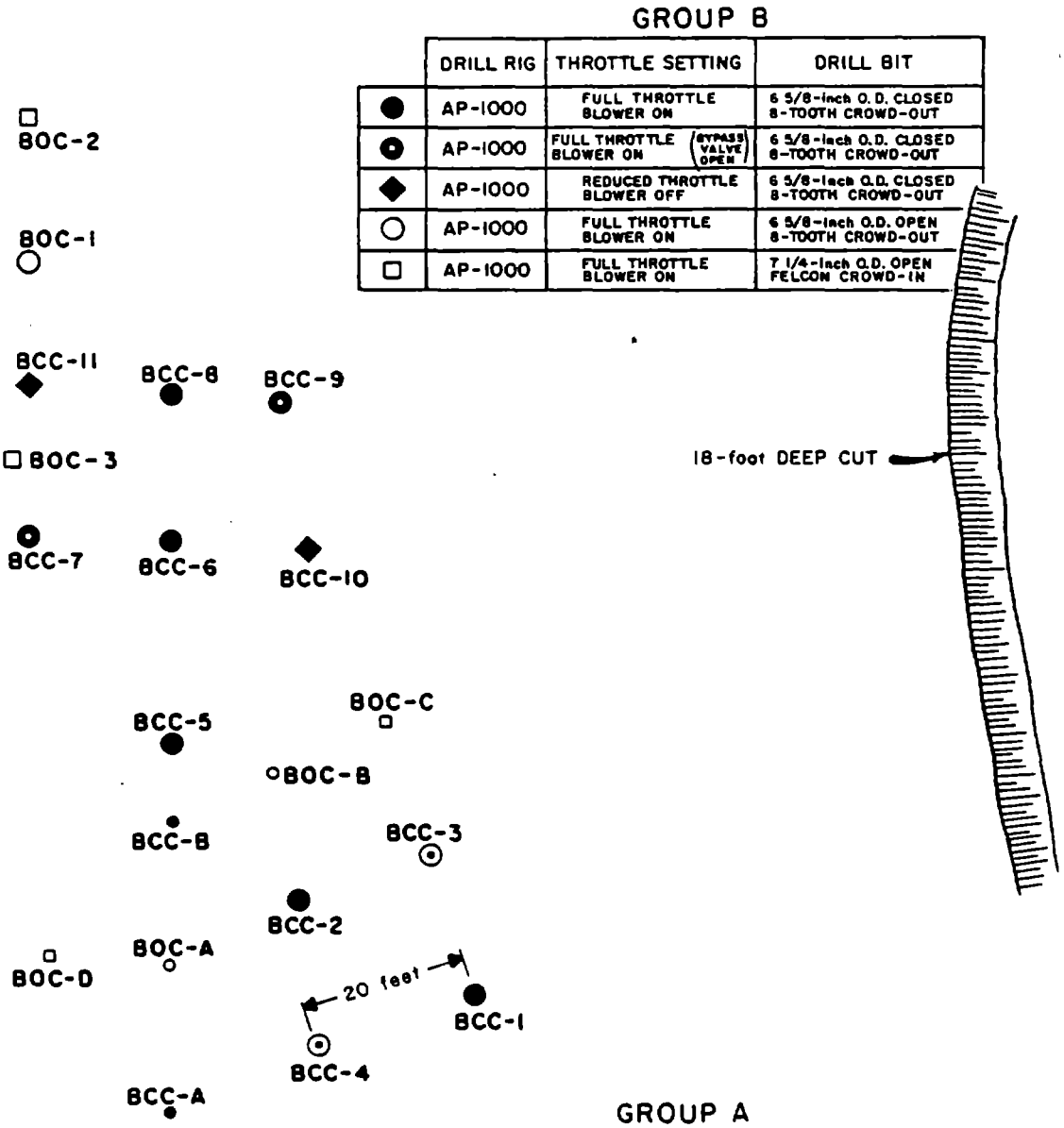

GROUP B

	DRILL RIG	THROTTLE SETTING	DRILL BIT
●	AP-1000	FULL THROTTLE BLOWER ON	6 5/8-inch O.D. CLOSED 8-TOOTH CROWD-OUT
◉	AP-1000	FULL THROTTLE BLOWER ON (BYPASS VALVE OPEN)	6 5/8-inch O.D. CLOSED 8-TOOTH CROWD-OUT
◆	AP-1000	REDUCED THROTTLE BLOWER OFF	6 5/8-inch O.D. CLOSED 8-TOOTH CROWD-OUT
○	AP-1000	FULL THROTTLE BLOWER ON	6 5/8-inch O.D. OPEN 8-TOOTH CROWD-OUT
□	AP-1000	FULL THROTTLE BLOWER ON	7 1/4-inch O.D. OPEN FELCON CROWD-IN

GROUP A

	DRILL RIG	THROTTLE SETTING	DRILL BIT
⊙	B-180	FULL THROTTLE BLOWER ON	6 5/8-inch O.D. CLOSED 8-TOOTH CROWD-OUT
●	AP-1000	FULL THROTTLE BLOWER ON	6 5/8-inch O.D. CLOSED 8-TOOTH CROWD-OUT
•	AP-1000	FULL THROTTLE BLOWER ON	5.5-inch O.D. CLOSED 8-TOOTH CROWD-OUT
o	AP-1000	FULL THROTTLE BLOWER ON	5.5-inch O.D. OPEN 8-TOOTH CROWD-OUT
□	AP-1000	FULL THROTTLE BLOWER ON	5.5-inch O.D. OPEN 3-WEB CROWD-IN

FIG. 17 GENERAL LAYOUT OF BECKER SOUNDINGS AT DENVER TEST SITE

Although the new valve failed to make any significant difference, it was decided for consistency not to use the results from these two soundings.

Mackay Dam Test Site

The Mackay test site is located between Stations 7 and 9 on the crest of Mackay Dam. Mackay Dam is located in central Idaho and was built between 1909 and 1917. The principal method of construction consisted of dumping sandy gravel in roughly 25-foot thick lifts. The explorations at this test site were performed in conjunction with the studies of the performance of Mackay Dam during the 1983 Mount Borah Earthquake (M_s=7.3). The soundings performed in this test area were made to investigate the effect of driving an open-bit vs. a closed-bit, and to study the effect of hammer energy on Becker blowcount. Figure 18 shows a plan view of the arrangement of soundings in the test area. Details of the history of the dam, materials, performance during the earthquake, and other explorations are presented elsewhere (Harder, 1986).

Effect of Closed vs. Open-Bits on Becker Blowcount

Becker Drills, Inc. literature and staff recommend using a closed-bit to obtain reliable Becker blowcounts. Previous studies conducted in gravelly sands in Canada have indicated that a closed-bit gives blowcounts roughly twice the values obtained with an open-bit. The correlations provided by the company literature and file (Figure 6) are based on soundings performed with 5.5-inch closed crowd-out drill bits. However, samples cannot be obtained using a closed-bit. Thus, rather than perform and pay for two soundings at each drilling location, most firms and agencies have opted to use mainly open-bit soundings. By this means, both samples and blowcounts are obtained from the same sounding. However the use of open-bit soundings often leads to overly conservative and unreliable blowcounts.

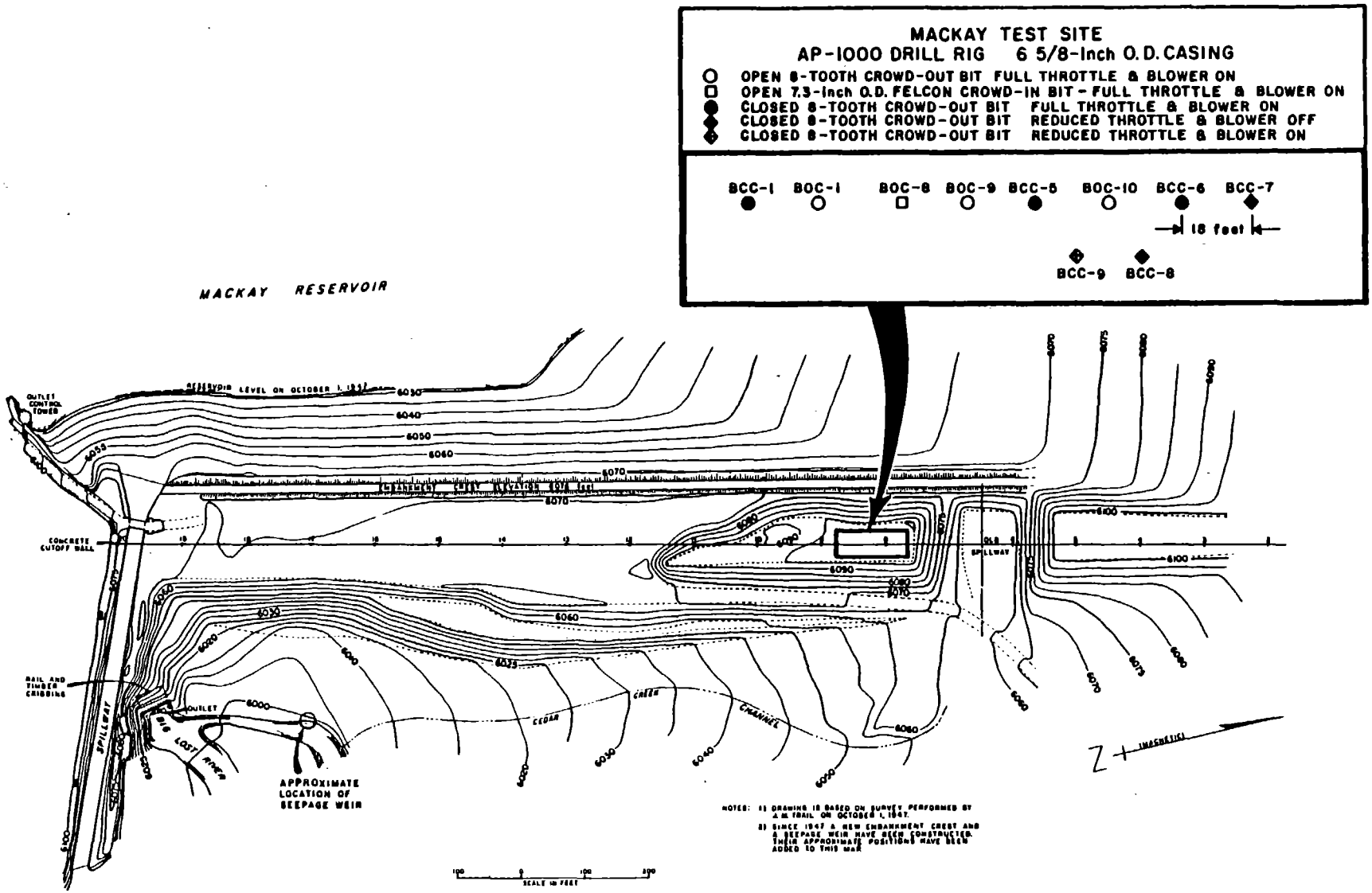

FIG. 18 GENERAL LAYOUT OF BECKER SOUNDINGS AT MACKAY TEST SITE

Figure 19 presents uncorrected blowcounts from two 6.6-inch, closed, crowd-out bit soundings performed at the San Diego test site. Also shown in this figure are uncorrected SPT blowcounts performed in the same general area by ERTEC (1981). This figure shows excellent agreement in both the trend and general magnitude of the blowcounts from both types of penetrometers. However, as shown in Figure 20, Becker blowcounts from two open crowd-out bit soundings performed in the same area do not compare well with the blowcounts from the closed-bit soundings. Although reasonable agreement is obtained between the two sets of Becker data in the upper 30 feet, the blowcounts from the open-bit soundings drop to much lower values than those for the closed-bit soundings below this depth. For one open-bit sounding, BOC-A, the blowcounts actually drop to zero at depths where the closed-bit soundings and the SPT blowcounts indicated a dense soil. The open-bit soundings are clearly too low below the 30-foot depth.

The experience of open-bit soundings giving erroneously low blowcounts was also repeated for the fine sands at the Salinas and Thermalito test sites. Figure 21 shows that one of the BOC soundings at Salinas developed unreasonably low blowcounts between a depth interval of 25 to 35 feet. Figure 22 shows that both BOC soundings at Thermalito gave unreasonably low blowcounts between a depth interval of 20 to 29 feet.

The fact that open-bit soundings give erroneously low values in sands can be attributed to the recirculation process drawing up excessive amounts of sand into the casing and out of the hole. This creates a loosening and removal of sand ahead of the bit and leads to a relatively low blowcount. The loosening and removal is further encouraged below the water table where the water tends to flow up, under relatively high gradients, into the bottom of the casing. The situation is analogous to performing SPT tests in a borehole

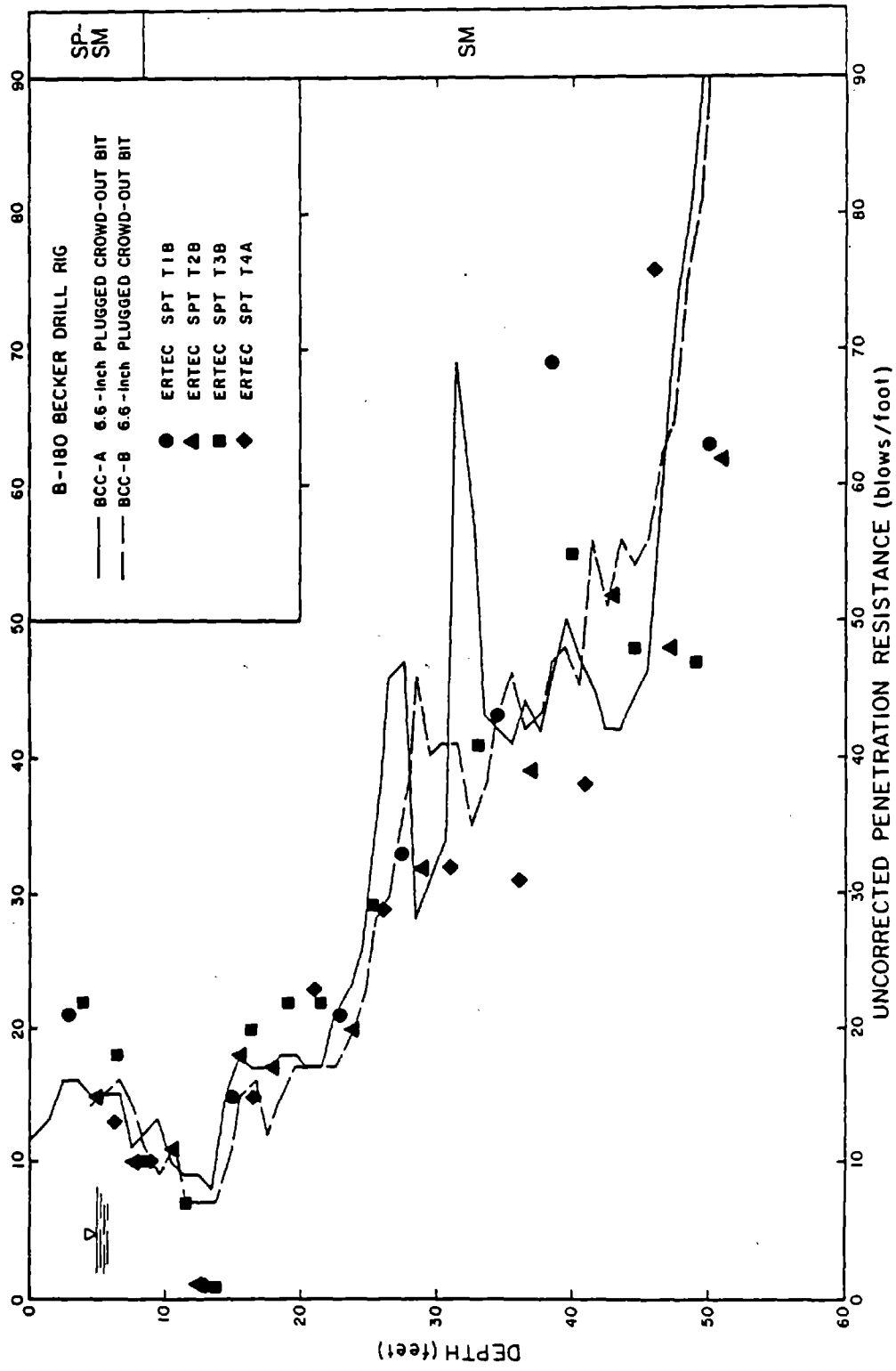

FIG. 19 UNCORRECTED BLOWCOUNTS FROM SPT AND CLOSED BIT BECKER PENETRATION TESTS PERFORMED AT THE SAN DIEGO TEST SITE

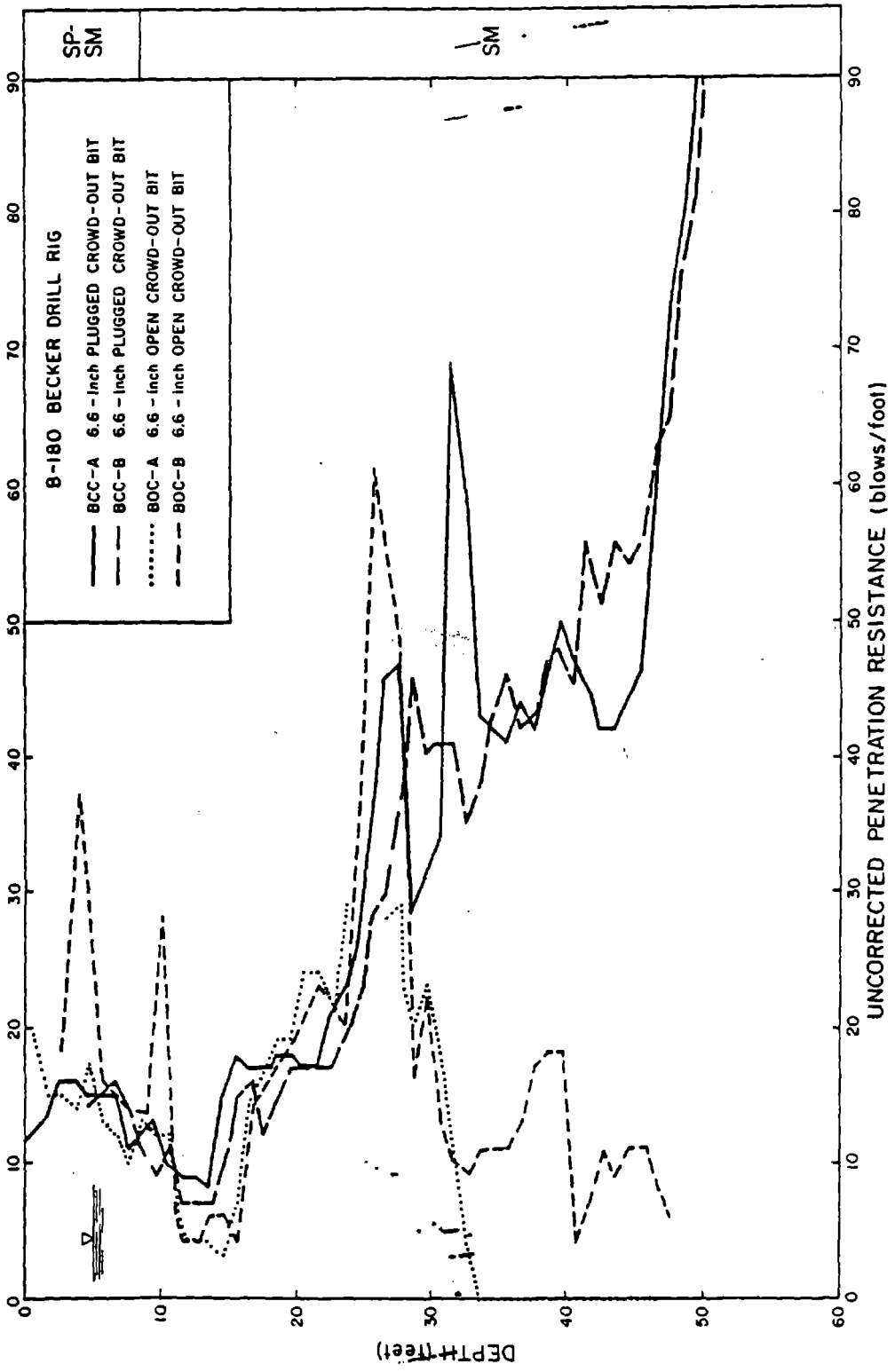

FIG. 20 COMPARISON OF UNCORRECTED BECKER BLOWCOUNTS FROM OPEN AND CLOSED BIT PENETRATION TESTS PERFORMED AT THE SAN DIEGO TEST SITE

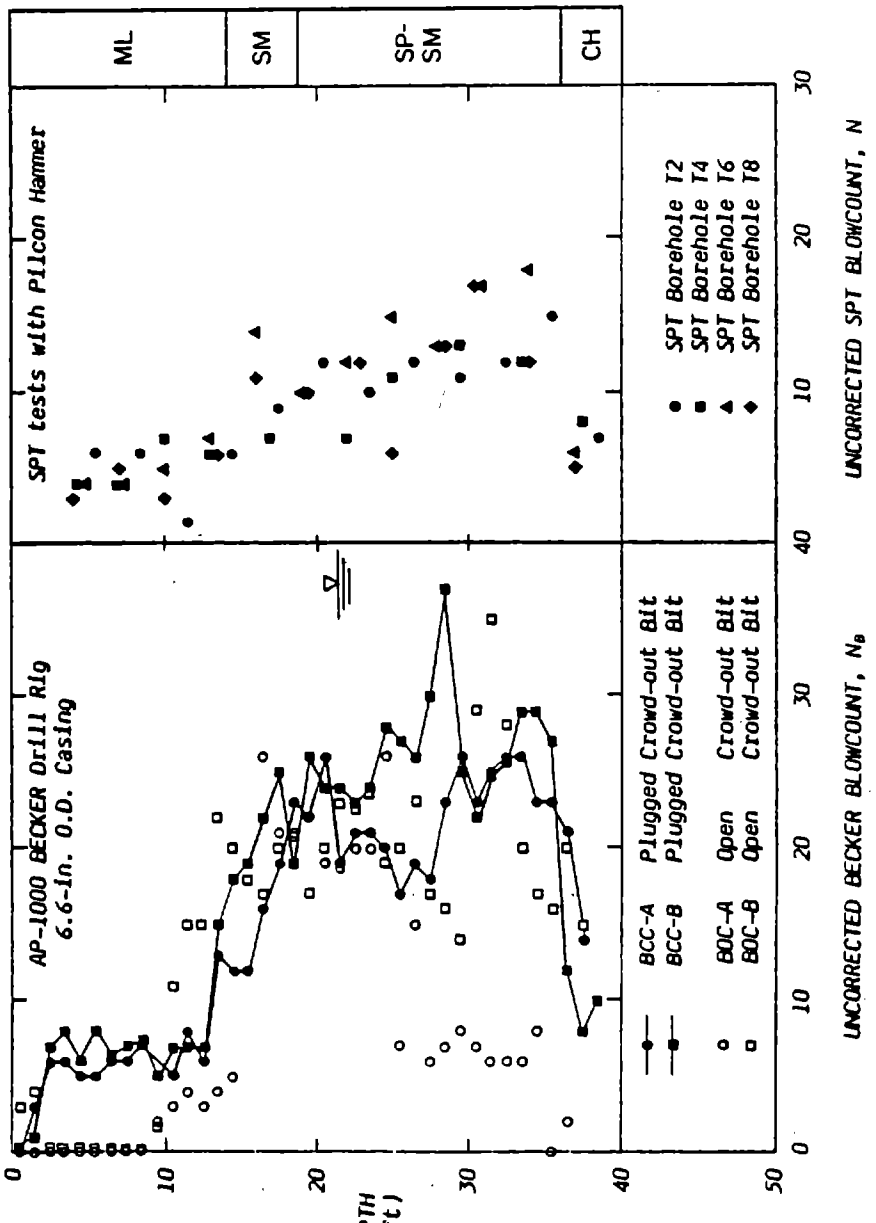

FIG. 21 UNCORRECTED BLOWCOUNTS FROM SPT AND BECKER PENETRATION TESTS PERFORMED AT THE SALINAS TEST SITE

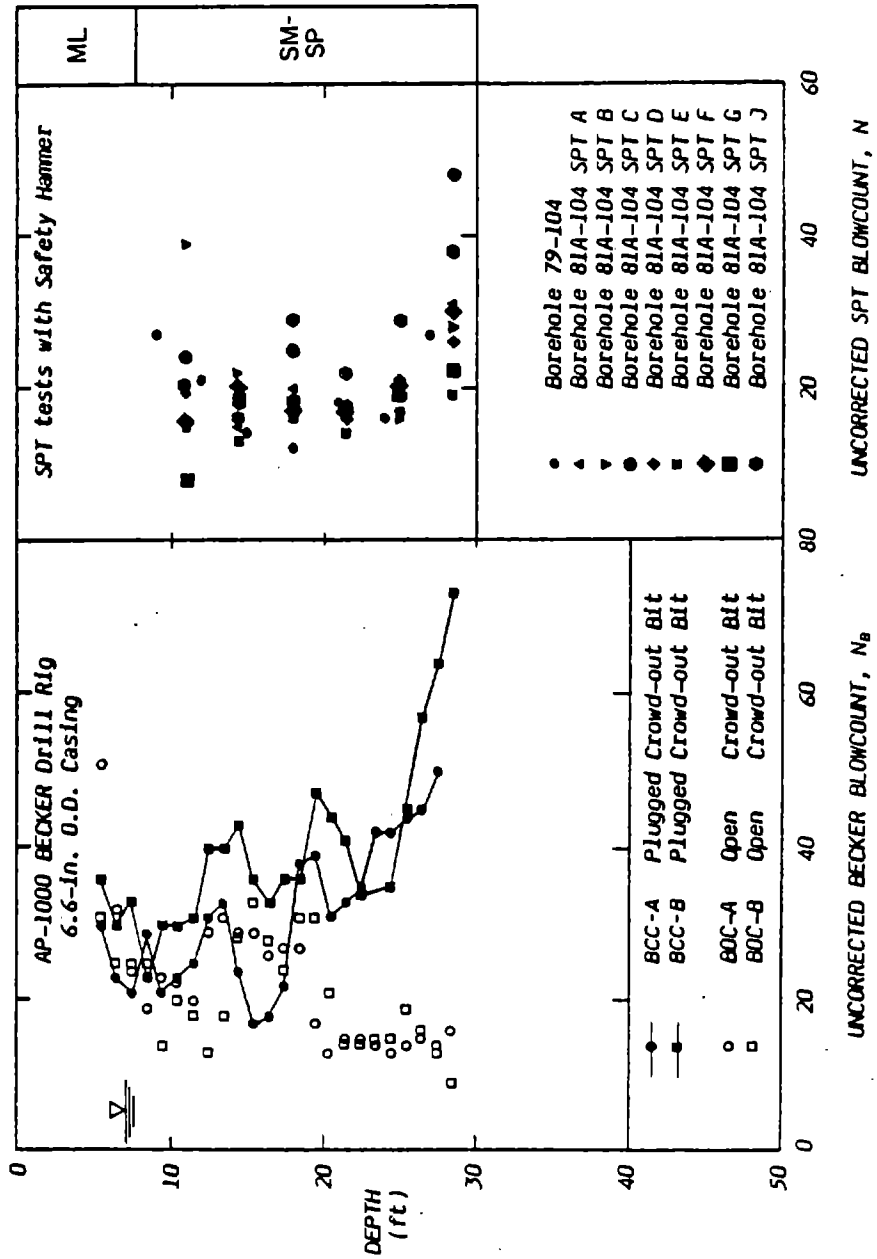

FIG. 22 UNCORRECTED BLOWCOUNTS FROM SPT AND BECKER PENETRATION TESTS PERFORMED AT THE THERMALITO TEST SITE

where neither water nor drilling mud has been used to stabilize the sand at the bottom of a hole.

Confirmation that the recirculation process was loosening the sand below the bit was achieved by performing a SPT test through the Becker casing at San Diego. The depth chosen for this test was at approximately 7 feet, where the ERTEC trip hammer tests indicated an uncorrected SPT blowcount of 10 (See Figure 19). When the Becker drill bit reached a depth of 7.2 feet, the recirculation process was stopped and the SPT split spoon sampler was inserted down the inner casing. After placing the sampler into the casing, the bottom of the split spoon reached a depth of 7.4 feet and sank another inch when the Becker SPT hammer was attached to the sampling rod (i.e. before driving, the bottom of the sampler was approximately 3 inches beyond the bottom of the Becker bit). The resulting SPT blowcount was only 3, a value less than a third of that predicted by the ERTEC results (Figure 23). This result indicates that previous SPT-Becker blowcount correlations where SPT tests were performed through the Becker casing may have utilized erroneous results.

The heave problem at the bottom of a hole is apparently not limited to fine sand. Figures 24 and 25 compare uncorrected blowcounts from open and closed-bit soundings performed at the Denver test site, where the soil is a gravelly sand down to about 42 feet with a sandy clay lying at lower depths. Figure 24 compares blowcounts obtained with 6.6-inch O.D. casing and bits and Figure 25 compares blowcounts obtained with 5.5-inch O.D. casing and bits. In both figures, the open-bit soundings give consistently lower blowcounts than do the closed-bit soundings.

The overall effects of bit diameter and configuration (open vs. closed) are readily summarized by the data in Figure 26, which shows the blowcounts measured in four of the Denver soundings. Each of the four soundings

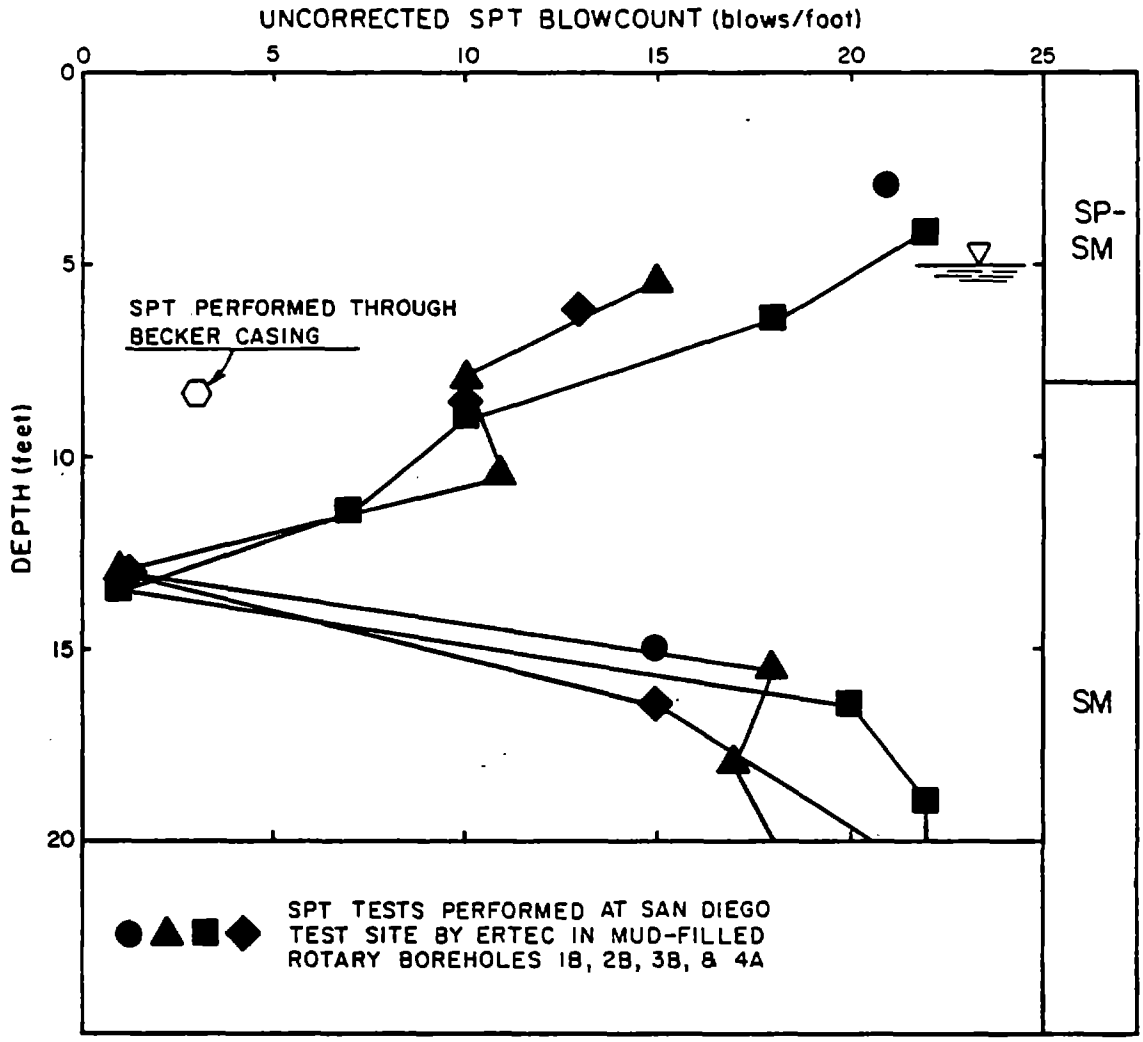

FIG. 23 COMPARISON OF SPT BLOWCOUNT PERFORMED THROUGH THE BECKER CASING WITH SPT BLOWCOUNTS PERFORMED IN MUD-FILLED ROTARY BOREHOLES

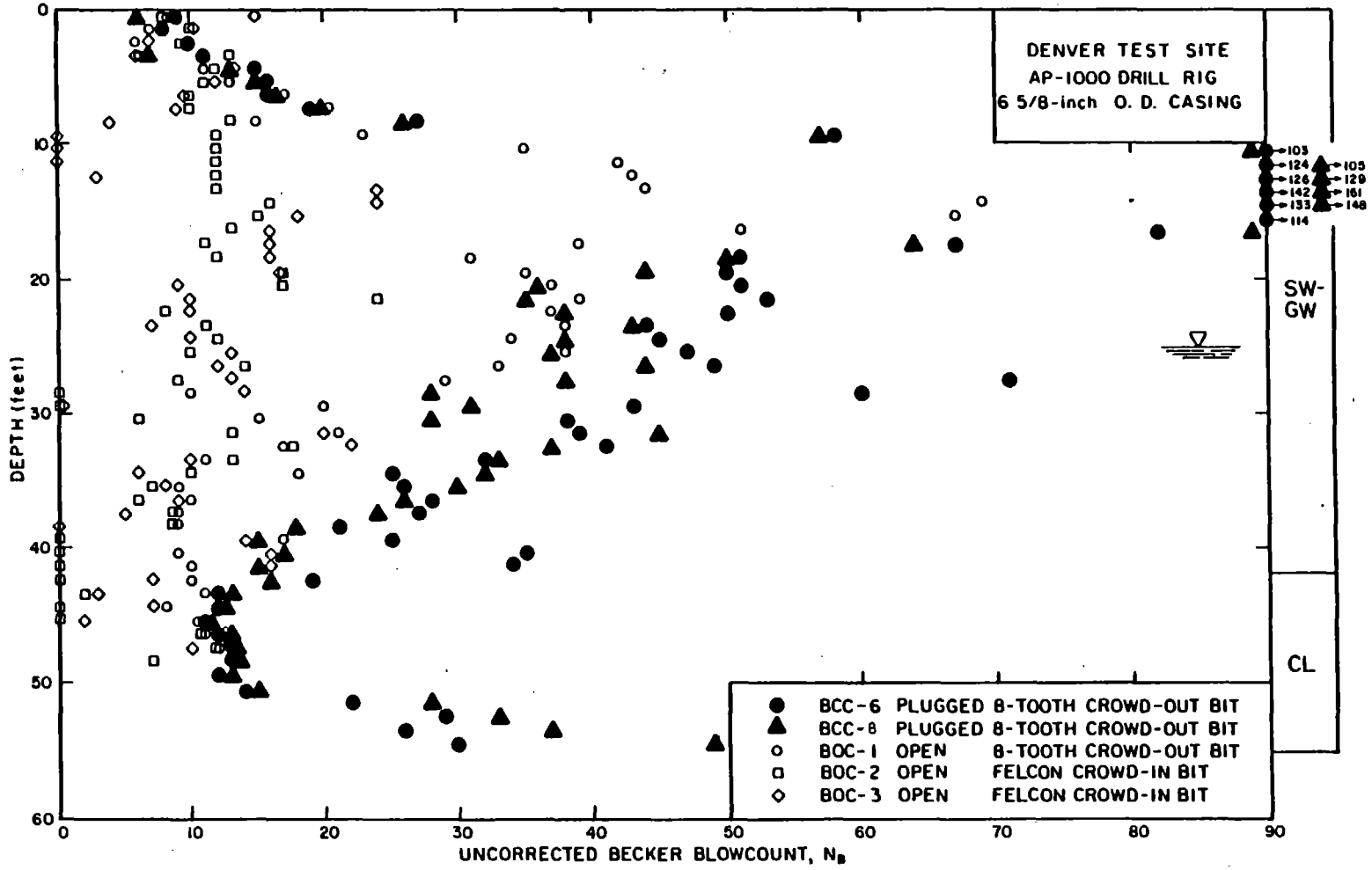

FIG. 24 COMPARISON OF UNCORRECTED BECKER BLOWCOUNTS FROM 6.6-INCH OPEN AND CLOSED BIT SOUNDINGS PERFORMED AT THE DENVER TEST SITE

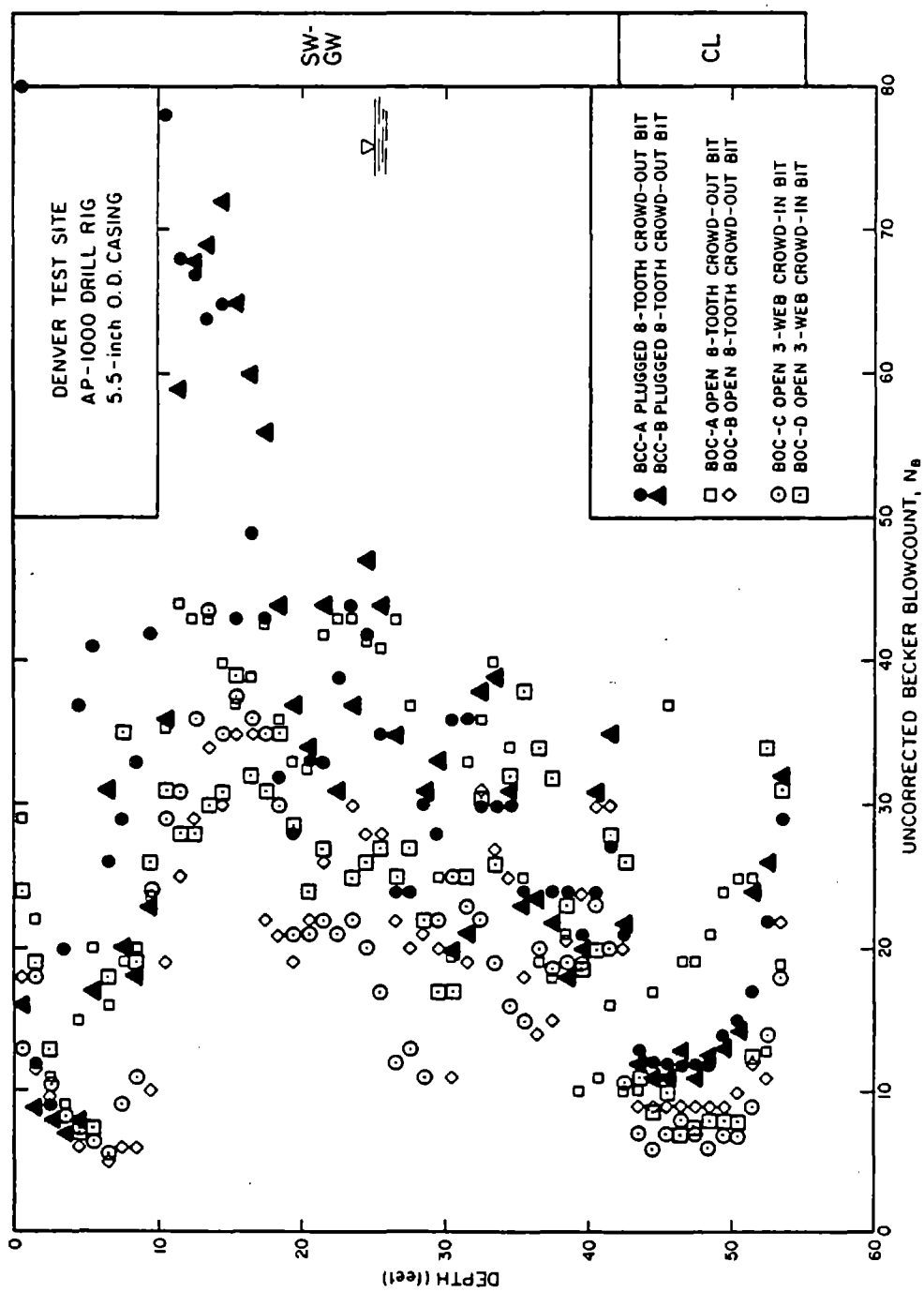

FIG. 25 COMPARISON OF UNCORRECTED BECKER BLOWCOUNTS FROM 5.5-INCH OPEN AND CLOSED BIT SOUNDINGS PERFORMED AT THE DENVER TEST SITE

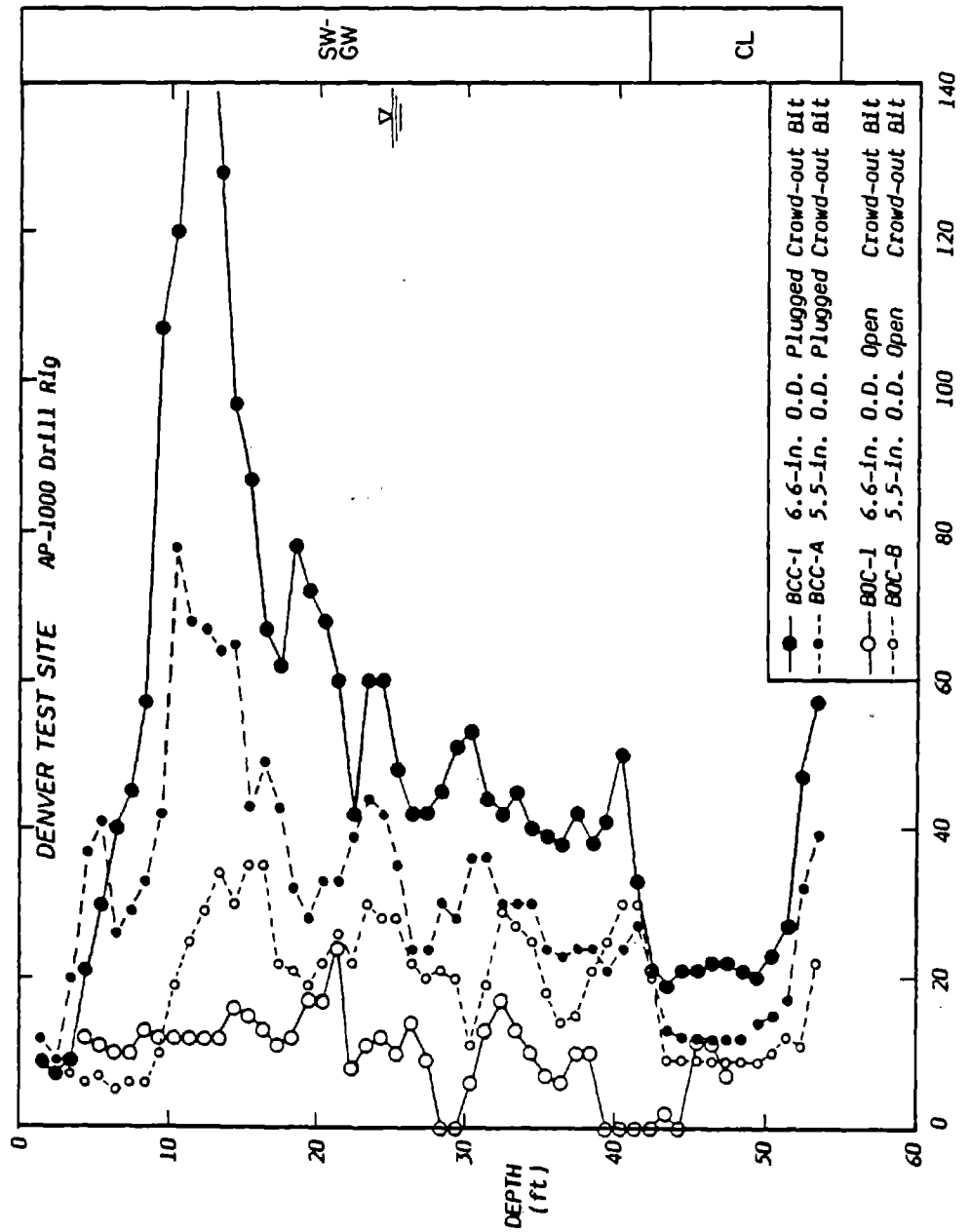

FIG. 26 EFFECT OF BIT DIAMETER AND CONFIGURATION ON BECKER BLOWCOUNT

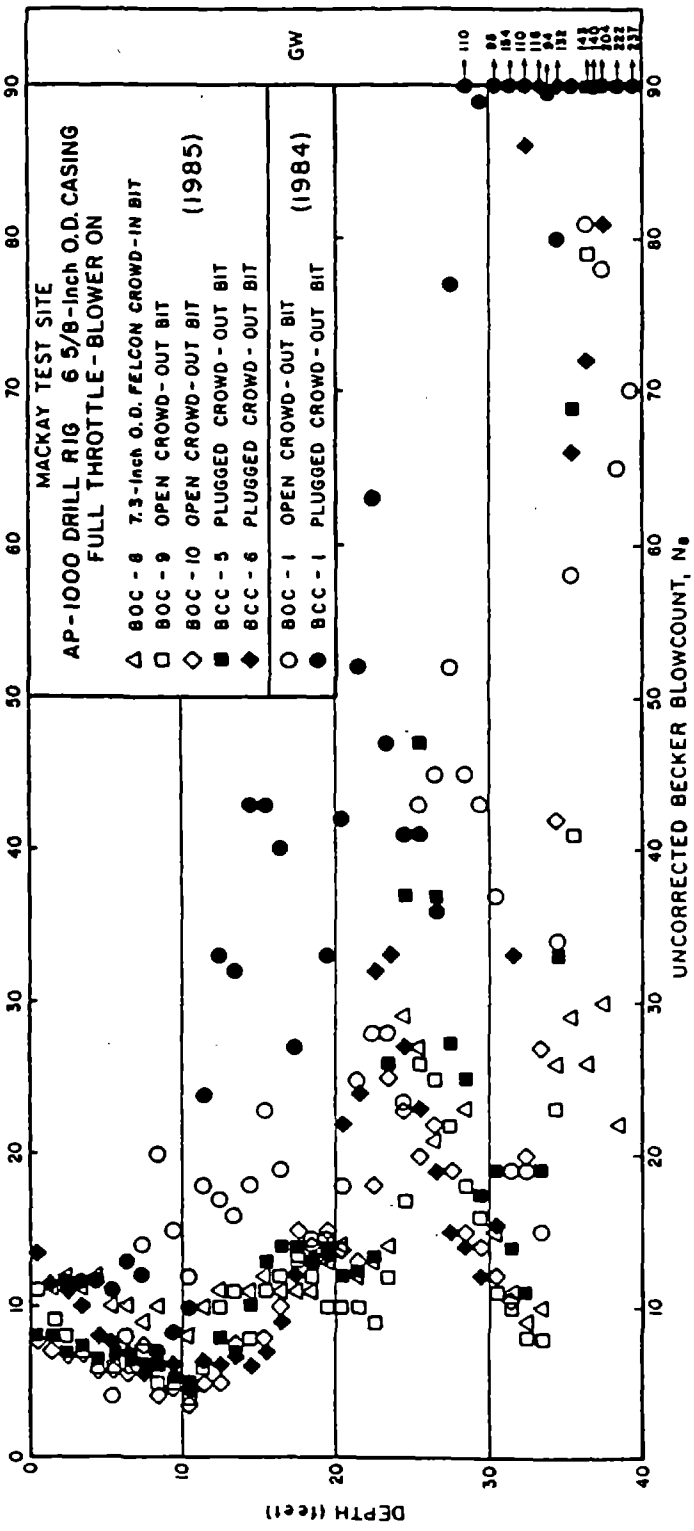

FIG. 27 COMPARISON OF UNCORRECTED BECKER BLOWCOUNTS FROM 6.6-INCH OPEN AND CLOSED BIT SOUNDINGS PERFORMED AT THE MACKAY TEST SITE

represents a different combination of bit size and configuration. As expected the closed 5.5-inch bit gives a significantly lower blowcount than does the closed 6.6-inch bit. However, a seemingly inconsistent result is indicated by the fact that the larger 6.6-inch open-bit produced a significantly lower blowcount than did the 5.5-inch open-bit. At times, the blowcount from the 6.6-inch open-bit reached zero despite the fact that the plugged bit of the same size gave blowcounts greater than 40 at the same depths. A possible explanation why the larger open-bit gave lower blowcounts than the smaller open-bit is the fact that the larger bit also has a larger inside diameter (4.3 inches vs. 3.3 inches). The larger inside diameter may more easily transmit the gravel particles which range up to about 2 to 3 inches in the gravelly sand at this site. For the smaller inside diameter, the gravel particles are more likely to block or partially block the bit opening, thus making the open-bit act more like a plugged or closed-bit.

There is probably a critical grain size or gradation where the particles are sufficiently large to plug or to arch across the bit opening causing open-bit blowcounts to be essentially the same as closed-bit blowcounts. The particle sizes required for adequate arching or blocking are apparently at least as large as those in a sandy gravel. This observation is based on the fact that at Mackay Dam the open-bit and closed-bit soundings gave essentially the same blowcounts (Figure 27). The soil at Mackay Dam is basically a silty, sandy, gravel with approximately 65 percent of the grains retained on the No. 4 sieve (D_{50} = 6 - 20 mm) and maximum particle sizes up to about 3 to 6 inches. A similar result was found at Folsom Dam where open and closed-bit soundings were carried out in the embankment shell and foundation. For the soundings in the shell material having a gravel content of about 70 percent (i.e. only about 30 percent passing the No. 4 sieve), open and closed-bit

soundings gave about the same blowcounts after correcting for energy effects. However, for the soundings in the gravelly sand foundation where the gravel content was generally between only 10 and 60 percent, the open-bit soundings were often significantly lower than the closed-bit soundings (Reference 10).

The results presented in this section clearly show that open-bit soundings often give erroneously low blowcounts, particularly for saturated sandy soils. Although gravels apparently have large enough particle sizes that arching and plugging often causes open-bit soundings to have the same penetration resistance as plugged bit soundings, it may not always be known if sufficient gravel sizes exist to assure that representative blowcounts are obtained. Therefore, it is recommended that only plugged bit soundings be used to characterize soil deposits.

Effect of Diesel Hammer Energy on Becker Blowcount

Most engineers used to working with SPT tests believe that the energy imparted to the sampling rods is more or less constant regardless of the blowcount of the soil being investigated. For example, although there is some variability with operator and testing conditions, it is now common to regard a SPT safety hammer used with a rope and cathead release as generally giving about 60 percent of its theoretical free-fall energy. This 60 percent energy level is considered applicable regardless of whether the SPT blowcount is 2 or 50.

Constant energy conditions are not a feature of the double-acting diesel hammers used in the Becker Penetration Test. One obvious reason for this is that the energy is dependent upon combustion conditions; thus anything that affects combustion, such as fuel quantity, fuel quality, air mixture and pressure all have a significant effect on the energy produced. For example,

the operator of the Becker drill rig has control of a throttle that controls the amount of fuel injected into the combustion chamber (see Figure 28). That throttle can be adjusted to a variety of settings and the amount of combustion energy can be varied significantly. The procedure is analogous to the use of an accelerator in an automobile: the more fuel provided, the faster the casing will move into the ground (i.e. the lower are the blowcounts). Although the operator generally prefers to operate at as high a throttle setting as possible in order to get the job done sooner, some operators use a reduced throttle setting near the surface or in soft zones.

The amount of kinetic energy delivered by the ram at impact depends on the amount of combustion energy developed on the previous blow to drive the ram back up the cylinder. As shown in Figure 29A, the interior of a double-acting diesel pile hammer is closed off at the top to allow a smaller stroke and a faster driving rate. At the top, trapped air in the compression cylinder and bounce chamber acts as a spring. The amount of potential energy within the ram at the top of its stroke can be estimated by measuring the peak pressure induced in the bounce chamber. Figure 30 shows a drawing of the monitoring gauge used to measure the bounce chamber pressure. The higher the bounce chamber pressure becomes, the higher is the potential energy of the ram. Also shown in Figure 29 is a correlation between potential energy and bounce chamber pressure developed by ICE.

Another reason why the energy is not a constant with the Becker Hammer Drill is that the energy developed is dependent on the blowcount of the soil being penetrated. The dependency of hammer energy on blowcount can be demonstrated by comparing Becker blowcounts to the bounce chamber pressures measured during driving. Shown in Figure 31 is a situation where the hammer, operating at a bounce pressure of 20 psi, produces a blowcount in the ground

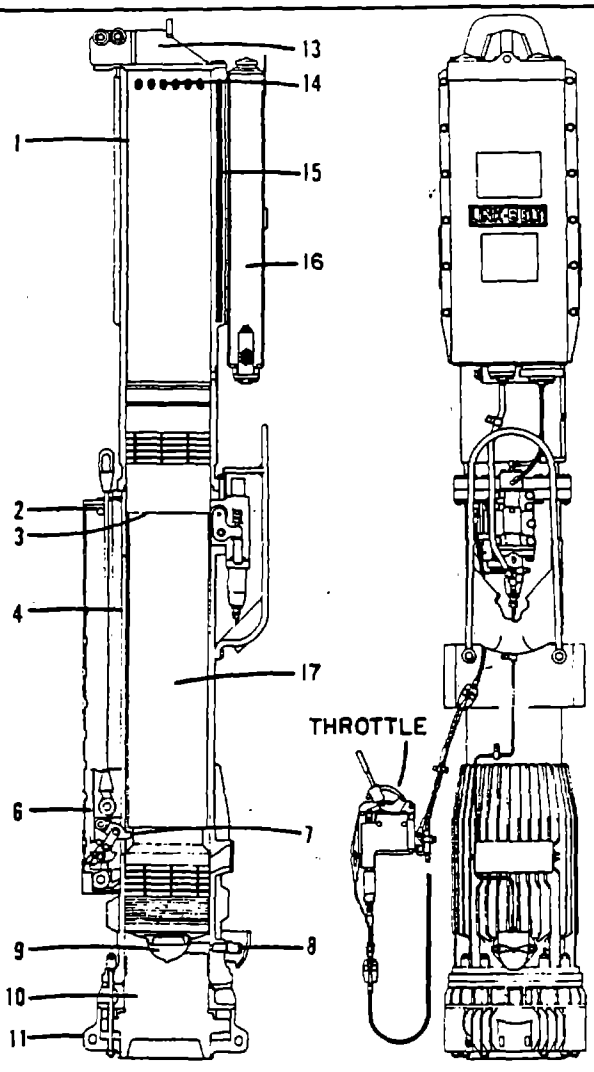

Diesel Pile Hammer

(1) Upper Cylinder
(2) Lifting Pin
(3) Cam Surface
(4) Lower Cylinder
(5) Starting Fluid Injector
(6) Starting Device
(7) Lifting Lever
(8) Injector
(9) Combustion Chamber
(10) Anvil
(11) Anvil Retainer
(12) Lifting Eye
(13) Cylinder Head
(14) Chamber Ports
(15) Bounce Chamber
(16) Fuel Tank
(17) Ram

FIG. 28 ICE MODEL 180 DIESEL PILE HAMMER (adapted from ICE literature)

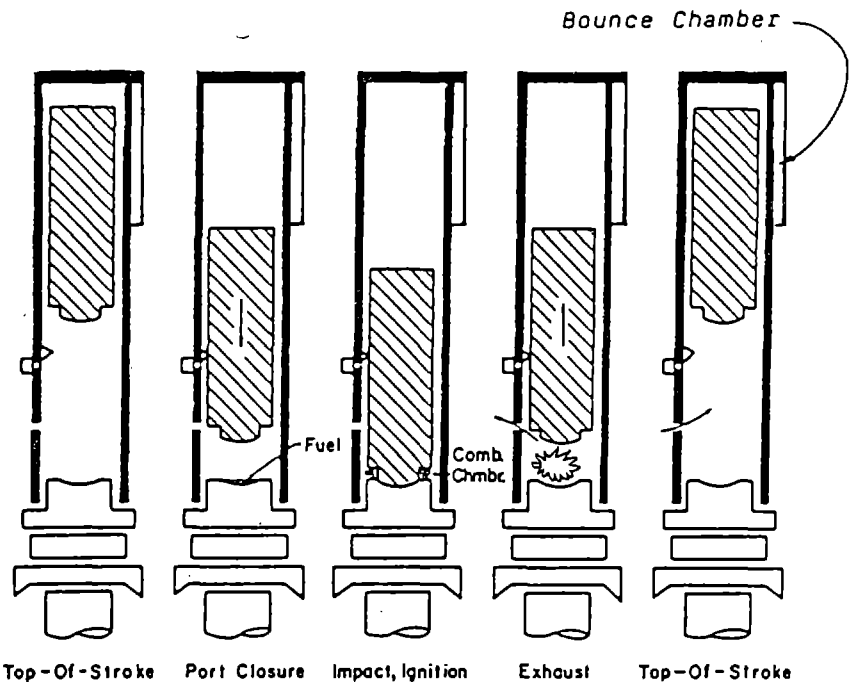

A) IDEALIZED OPERATIONAL CYCLE OF DIESEL PILE HAMMER (MODIFIED FROM REMPE AND DAVISSON, 1977)

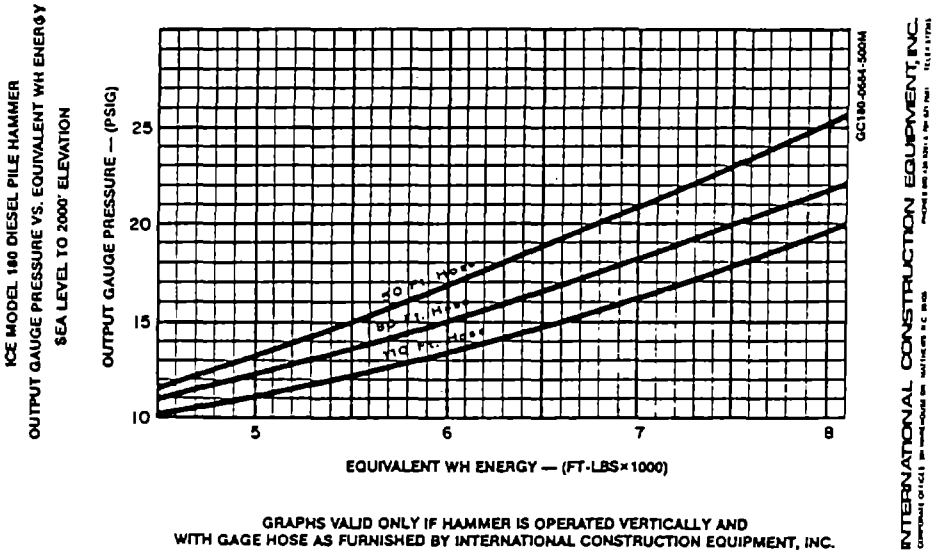

B) POTENTIAL ENERGY CALIBRATION FOR I.C.E. MODEL 180 DIESEL PILE HAMMER (FROM I.C.E. LITERATURE)

FIG. 29 OPERATIONAL AND POTENTIAL ENERGY CHARACTERISTICS OF DIESEL PILE HAMMER USED ON BECKER DRILL RIGS

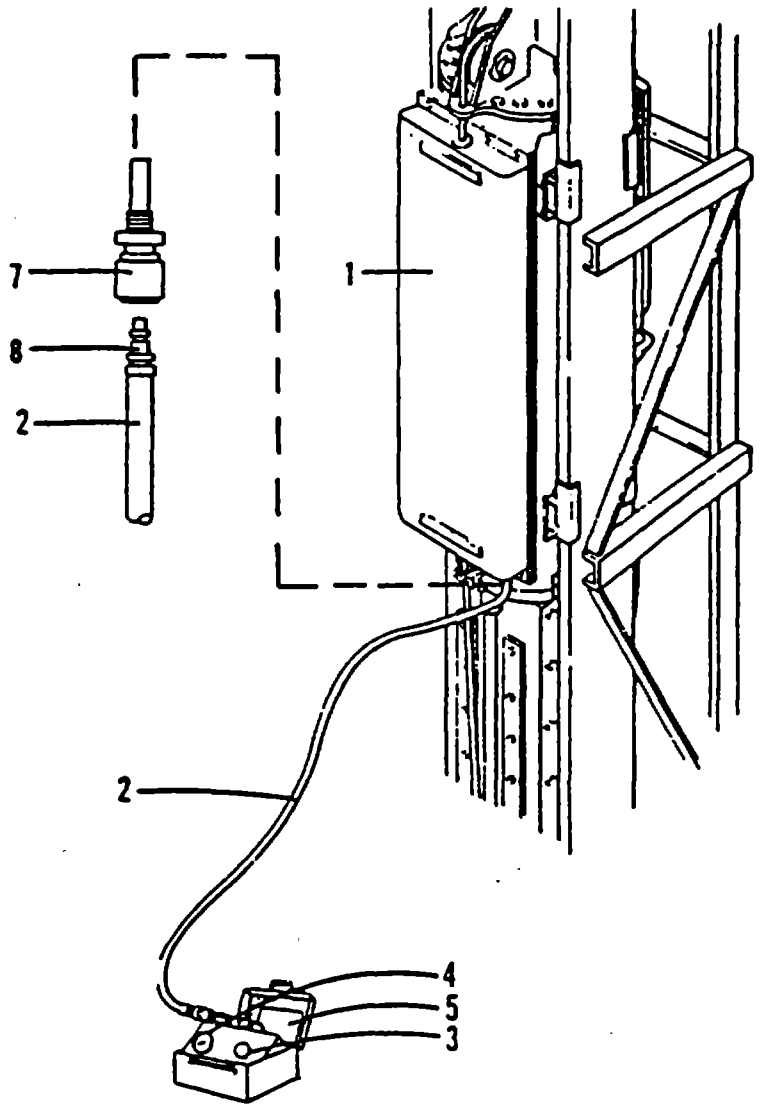

Output Energy Rating Instrument (Typical)

(1) Bounce Chamber
(2) Hose
(3) Push Button
(4) Gauge
(5) Graph
(6) Adaptor
(7) Socket
(8) Plug

FIG. 30 MONITORING GAGE FOR BOUNCE CHAMBER PRESSURE (adapted from ICE literature)

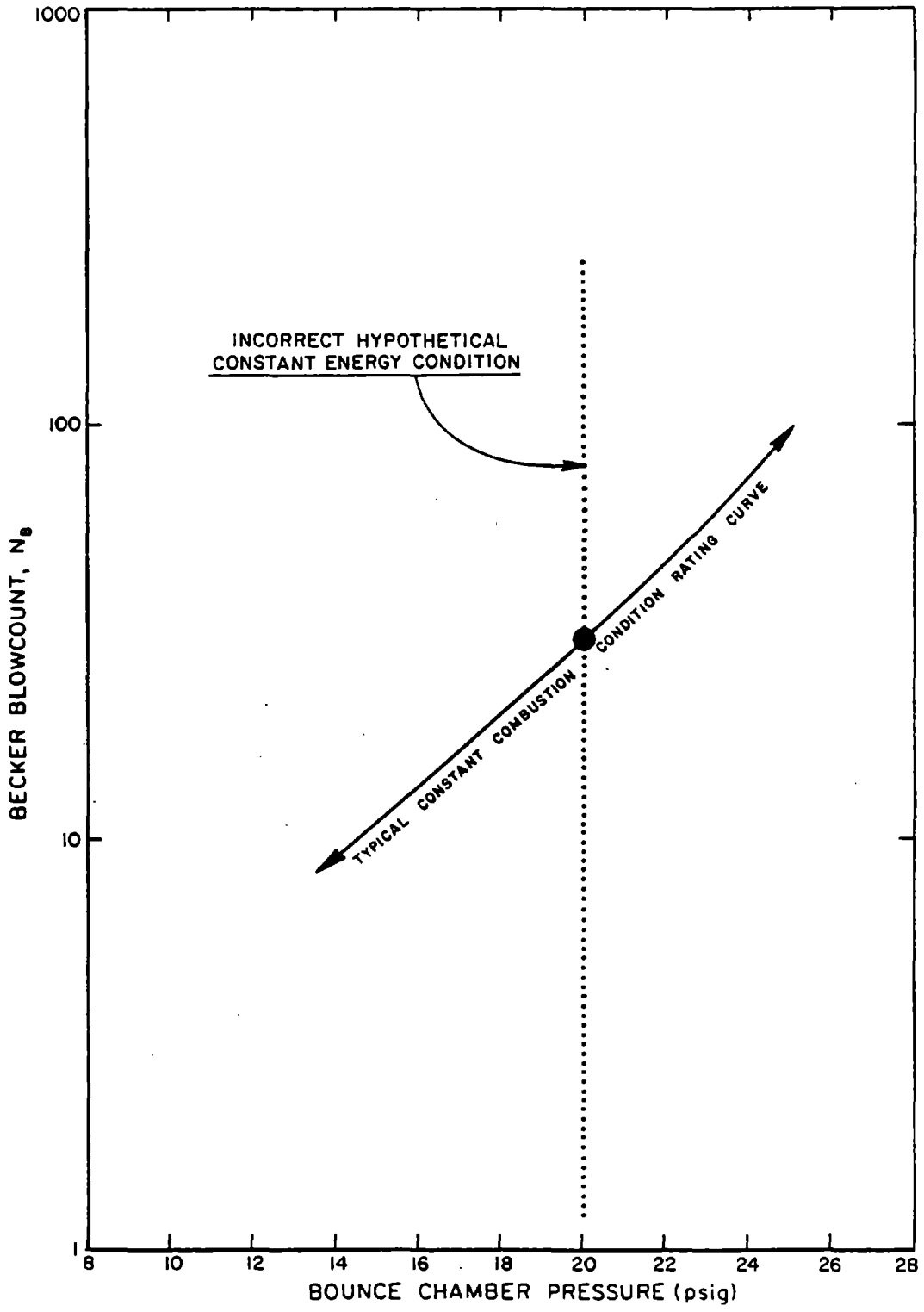

FIG. 31 IDEALIZATION OF RELATIONSHIP BETWEEN BECKER BLOWCOUNT AND BOUNCE CHAMBER PRESSURE

of 30. According to the correlation presented in Figure 29B, for a 50 ft length of pressure hose, a bounce pressure of 20 psig measured at sea level corresponds to a potential energy of about 6800 ft.-lb. If the energy level were constant, then the bounce pressure should stay at 20 psig regardless of blowcount and would be represented by the vertical dotted line in Figure 31. However, this does not occur because when the casing bit enters a softer material, the blowcount goes down and the amount of casing displacement per blow increases. With increasing casing displacement, a larger amount of energy from the expanding combustion gases is directed into the soil leaving less energy to send the ram up the cylinder for the next blow. With less energy on the next stroke, the ram would not compress the air in the bounce chamber to the same extent as on the previous stroke and the potential energy for the next stroke is thus reduced. If the blowcount continues to drop, the bounce chamber pressure and the potential energy of the ram continues to drop. Conversely, if the blowcount increases, then there is less casing displacement per blow and more of the combustion energy is directed upward in raising the ram. With the ram travelling upward with more energy, the air in the bounce chamber pressure compresses more and the potential energy for the following stroke is increased. Thus, even for absolutely constant combustion conditions (i.e. constant air-fuel mixtures) the potential energy of the ram does not remain constant. Figure 31 indicates a typical relationship between Becker blowcount and bounce chamber pressure (potential energy) for constant combustion conditions. The results shown in Figure 32 are actual blowcount and bounce chamber data points from tests performing at the Salinas test site under full throttle conditions in 1985. Although there is some scatter due to the fact that the gauge reading is only accurate to about the nearest half psi

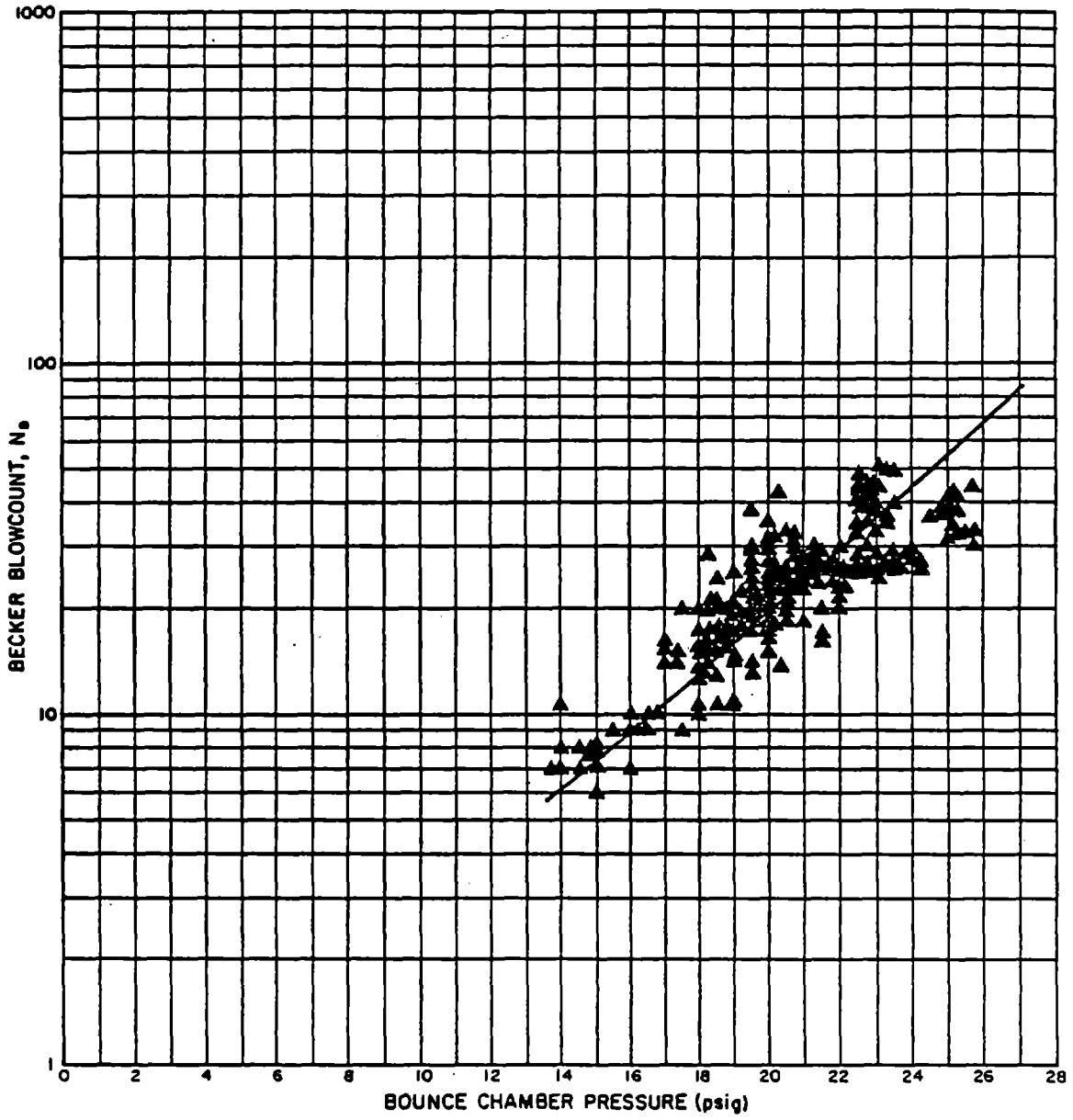

FIG. 32 RELATIONSHIP BETWEEN BECKER BLOWCOUNT AND BOUNCE CHAMBER PRESSURE FOR FULL THROTTLE COMBUSTION CONDITIONS AT THE SALINAS TEST SITE

and the fact that about 300 points are plotted, the data clearly shows the trend discussed above.

Effect of Blower and/or Reduced Throttle

If the Becker Hammer Drill always operated with relatively constant combustion, then all the blowcount and bounce chamber data should fall within the scatter of the data points in Figure 32 and the blowcounts could be used without further correction. Unfortunately, as mentioned previously, combustion conditions can and do vary significantly.

When the U.S. branch of Becker Drills changed from a 5.5-inch O.D. casing to a 6.6-inch O.D. casing as a more or less standard procedure, their operators found that it required a higher blowcount to drive the casing. To compensate for this, a rotary blower or supercharger was added to feed more air into the combustion chamber. This blower is connected to the intake port and it helps to clear the combustion chamber of exhaust gases. Better clearing in turn allows a higher throttle setting and more fuel to be used during the combustion process than would otherwise be possible. With a higher combustion energy, U.S. Becker operators are able to keep blowcounts with the larger 6.6-inch casing from getting uneconomically high. The Canadian Becker Hammer rigs, which still predominantly employ the smaller casing, do not generally use this blower.

To examine the effect of the blower, two 6.6-inch closed-bit soundings were performed at the Denver test site with the blower turned on. In the same area, two other 6.6-inch closed-bit soundings were performed with the blower turned off together with a corresponding reduction in throttle setting. Figure 33 shows the uncorrected Becker blowcounts for all four soundings plotted against depth. As can be observed, the soundings with the blower

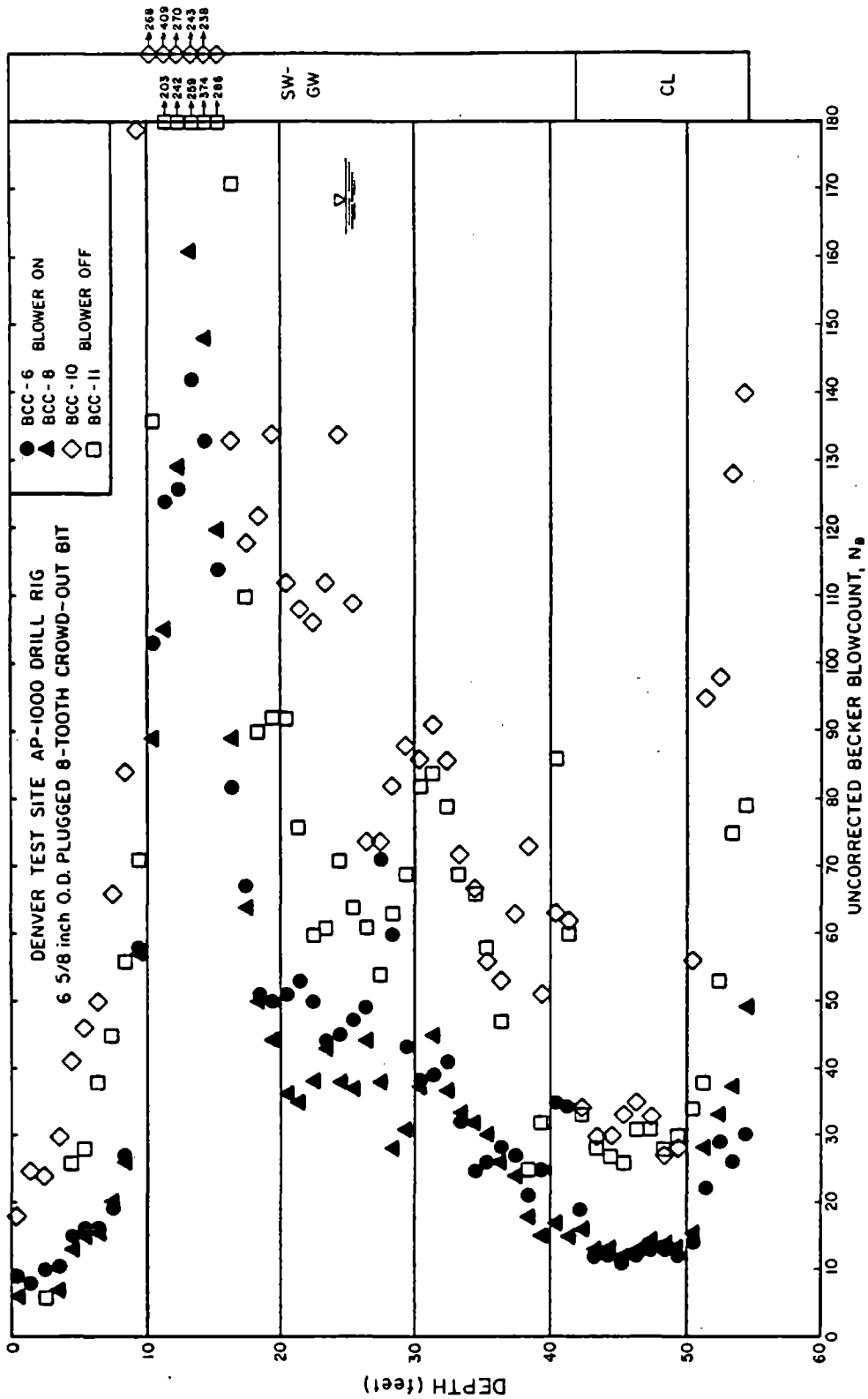

FIG. 33 EFFECT OF ROTARY BLOWER AND/OR REDUCED THROTTLE ON BECKER BLOWCOUNT AT DENVER TEST SITE

turned off produced blowcounts roughly twice those in soundings performed with the blower turned on.

The change in blowcounts results from a change in combustion conditions. Figure 34 compares the constant combustion rating curve data (blowcount vs. bounce chamber pressure) from the two soundings which used the blower with the data from the two soundings which did not use the blower. The two conditions produce very different rating curves, with the "blower off" condition giving a rating curve to the left of the curve for the "blower on" condition. This is consistent with the blower producing a lower blowcount (i.e. higher combustion energy).

Figures 35 through 40 present most of the same data only grouped in 4- to 6-foot depth increments. In general, a lowering of the bounce chamber pressure by about 4 to 7 psi was enough to double the blowcounts. However, this is inconsistent with the potential energy curves shown in Figure 29B. According to this figure, a drop in pressure of 6 psi, say from 18 to 12 psig, would produce only about a 26% reduction (4680 ft-lb./6310 ft-lb.) in blowcount. Thus, although the changes in bounce chamber pressure were consistent with the trend of the blowcount change, the potential energy charts supplied by ICE (Figure 29B) were inadequate for predicting the magnitude of the effect of potential energy on the blowcounts.

Similar studies were performed at the Mackay test site. Two 6.6-inch closed-bit soundings performed with the blower on were compared to three similar soundings performed with the blower off and/or with the throttle reduced. Figure 41 shows the uncorrected blowcounts for all five soundings plotted against depth. Again, the soundings with the blower turned off produced blowcounts significantly higher than those in soundings performed with either the blower turned on and/or with a reduced throttle setting.

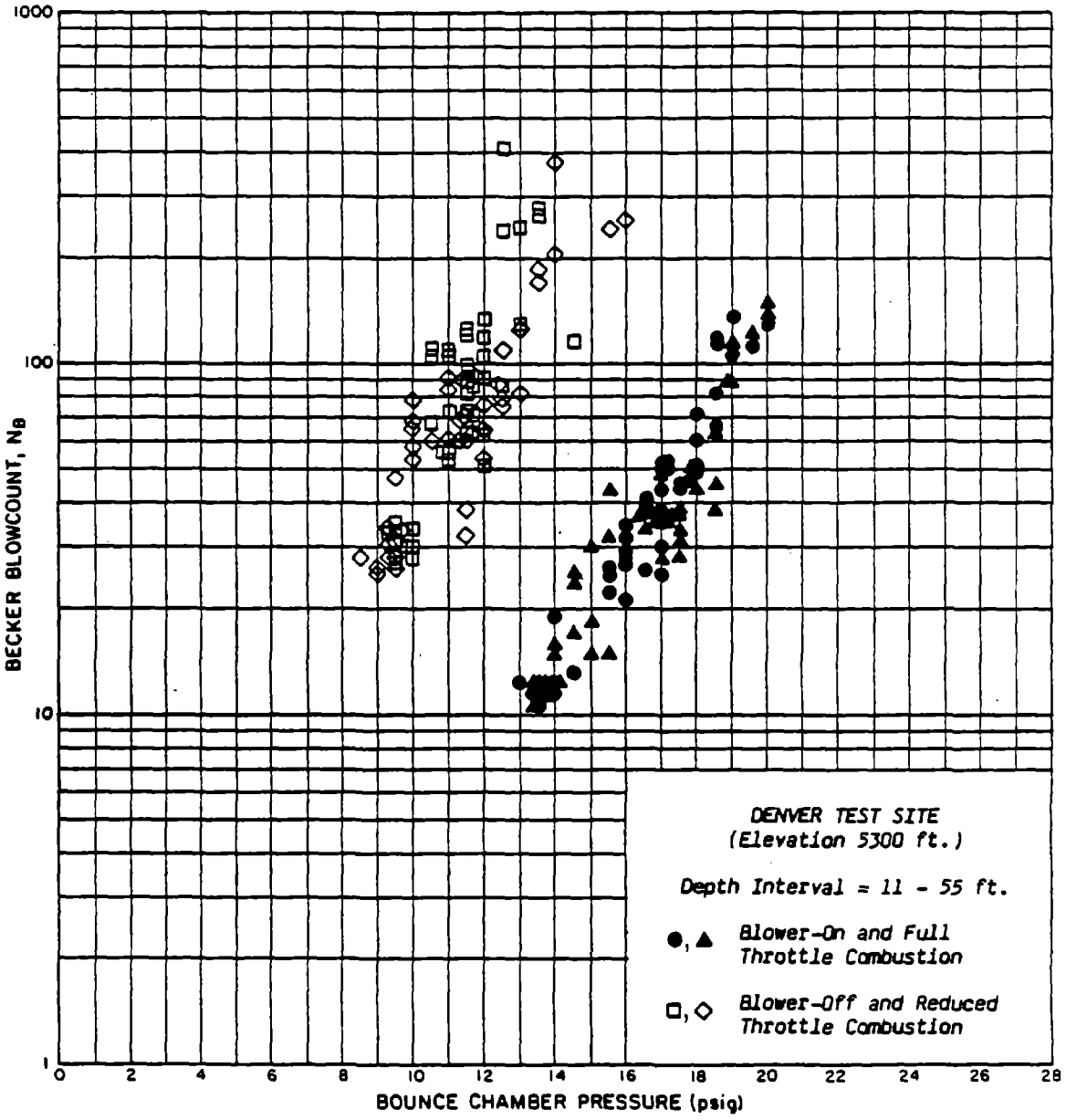

FIG. 34 CONSTANT COMBUSTION RATING CURVES FOR FULL AND REDUCED THROTTLE CONDITIONS AT DENVER TEST SITE

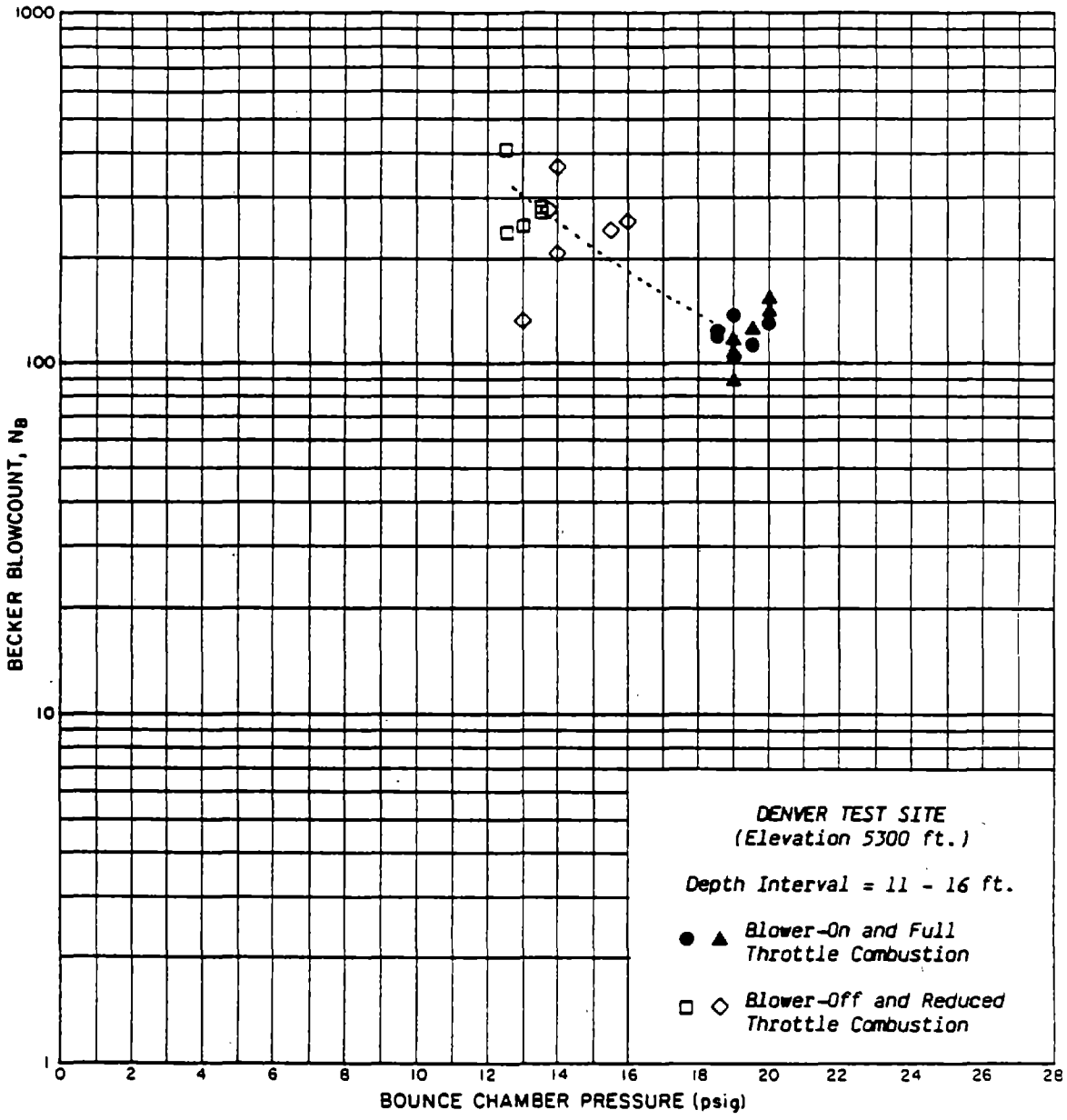

FIG. 35 EFFECT OF ENERGY REDUCTION ON THE BECKER BLOWCOUNT - BOUNCE CHAMBER PRESSURE RELATIONSHIP FOR DENVER TEST SITE (Depth Interval = 11-16 feet)

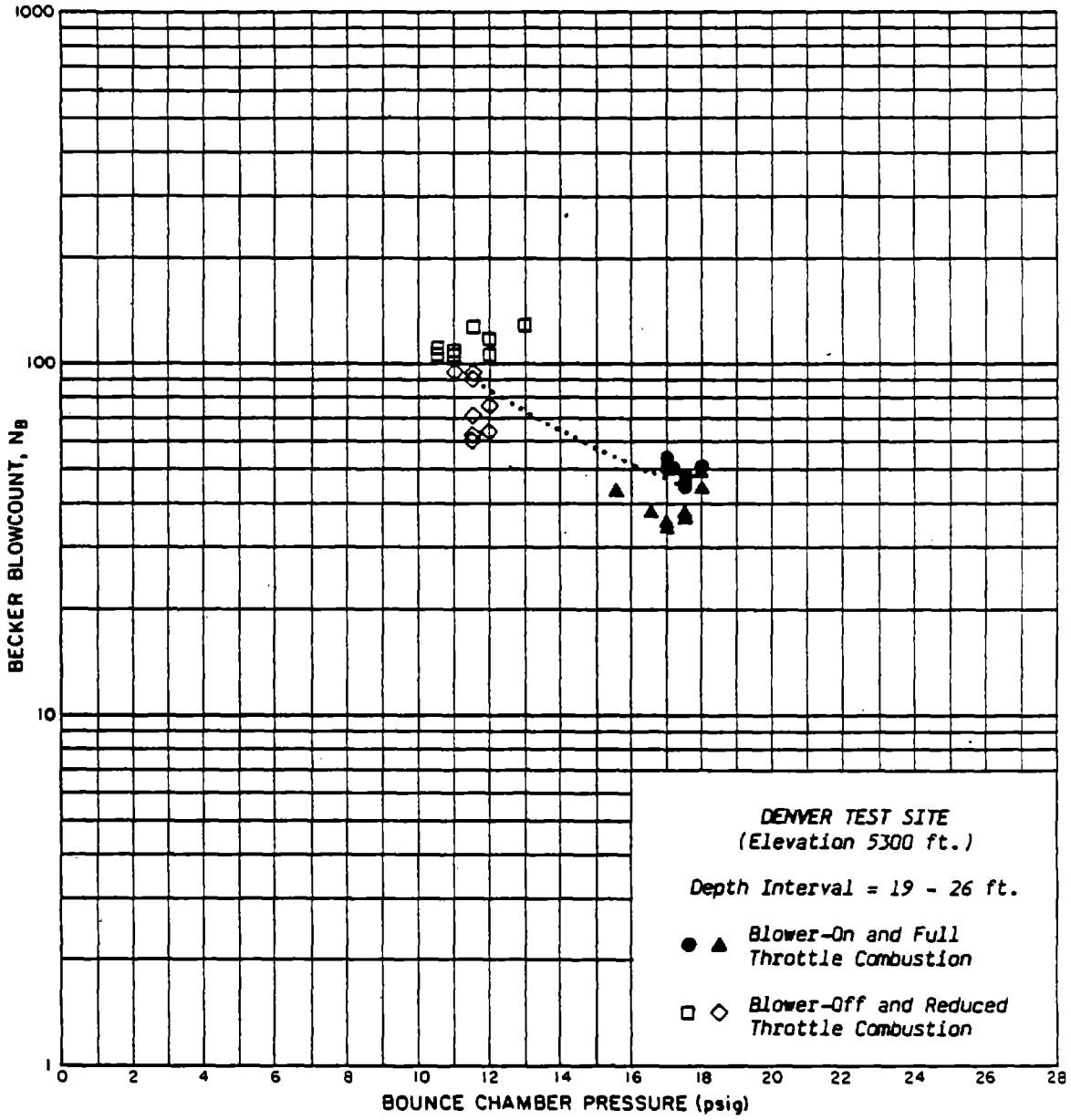

FIG. 36 EFFECT OF ENERGY REDUCTION ON THE BECKER BLOWCOUNT - BOUNCE CHAMBER PRESSURE RELATIONSHIP FOR DENVER TEST SITE (Depth Interval = 19-26 feet)

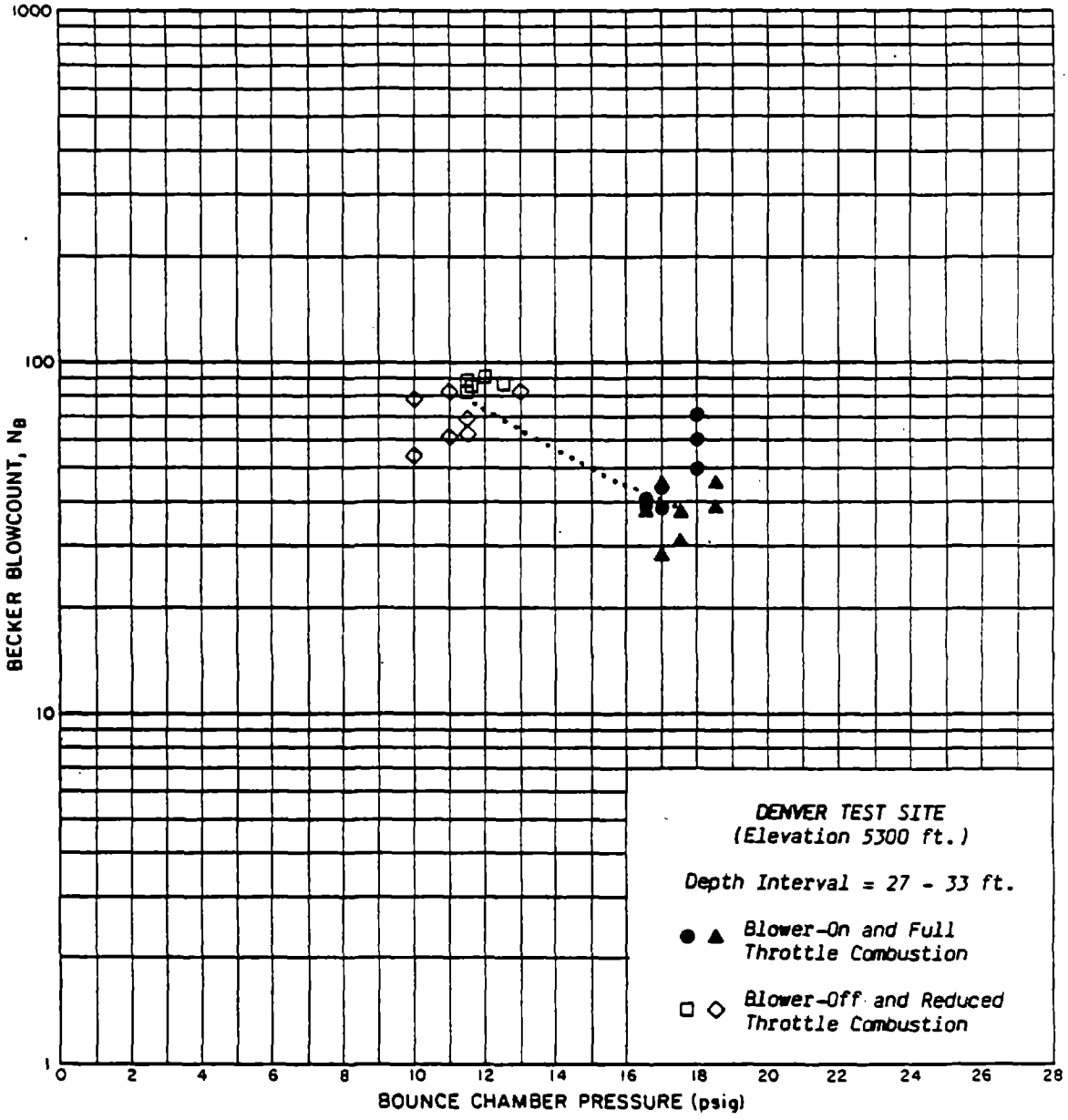

FIG. 37 EFFECT OF ENERGY REDUCTION ON THE BECKER BLOWCOUNT - BOUNCE CHAMBER PRESSURE RELATIONSHIP FOR DENVER TEST SITE (Depth Interval = 27-33 feet)

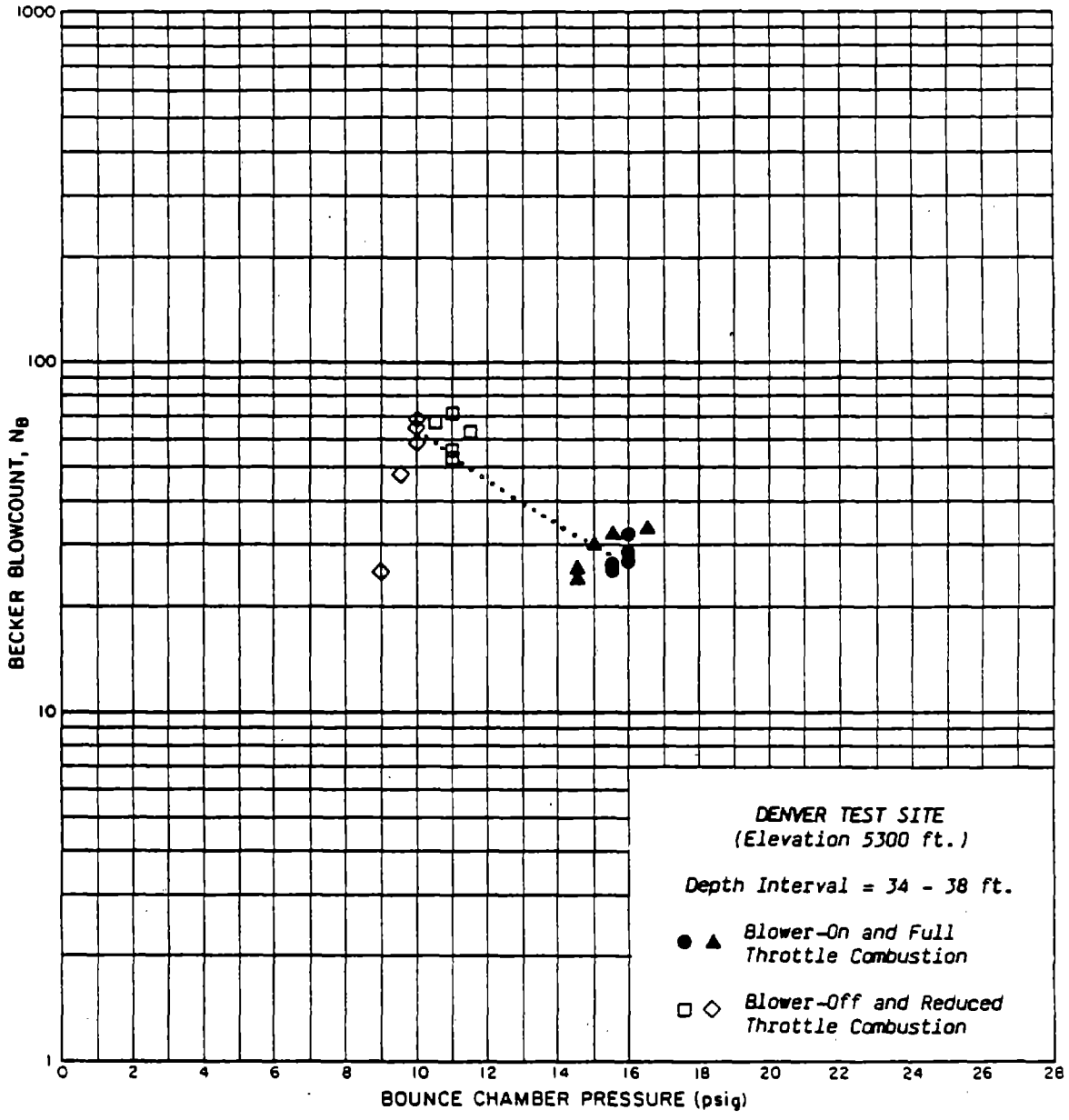

FIG. 38 EFFECT OF ENERGY REDUCTION ON THE BECKER BLOWCOUNT - BOUNCE CHAMBER PRESSURE RELATIONSHIP FOR DENVER TEST SITE (Depth Interval = 34-38 feet)

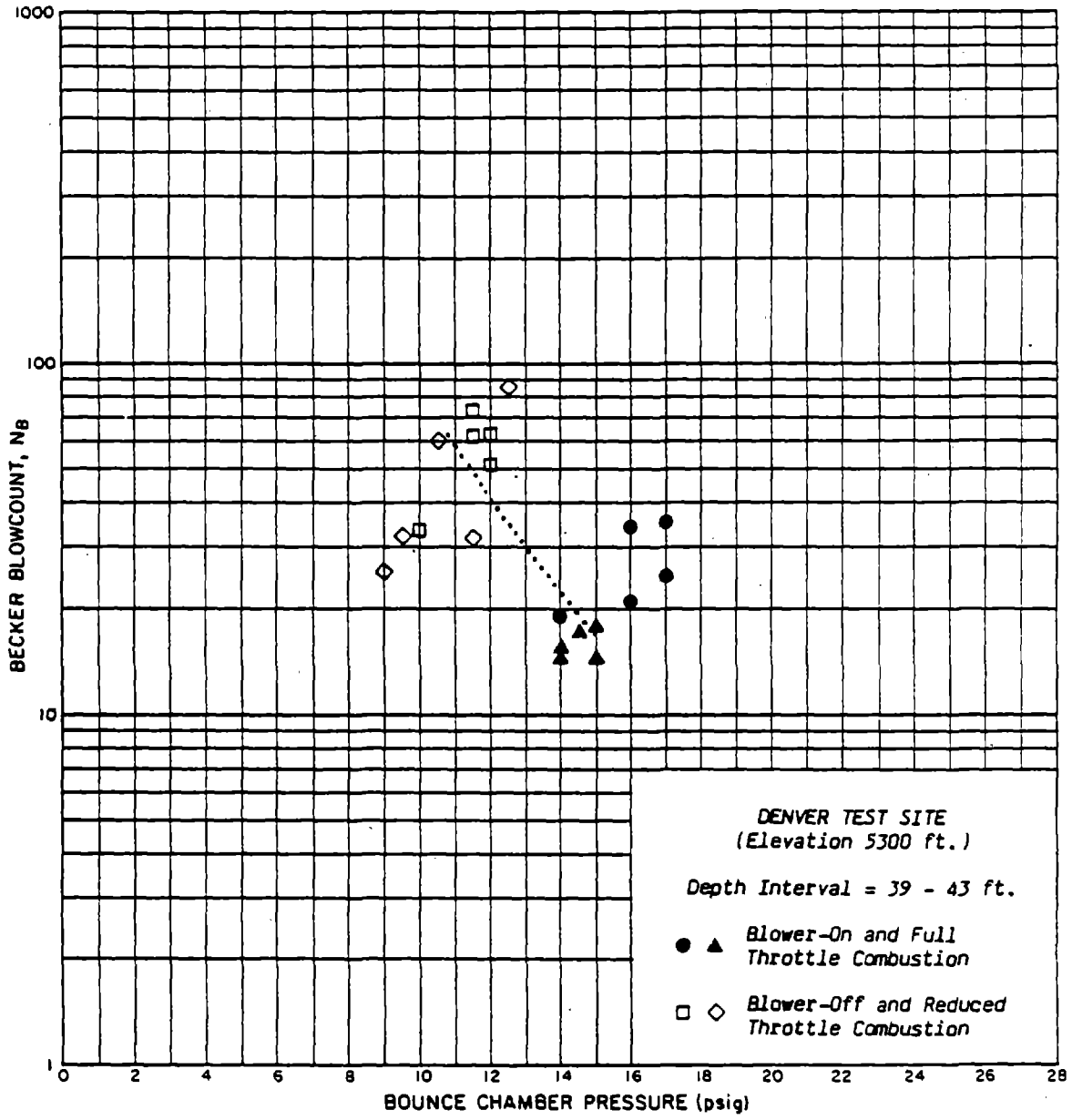

FIG. 39 EFFECT OF ENERGY REDUCTION ON THE BECKER BLOWCOUNT - BOUNCE CHAMBER PRESSURE RELATIONSHIP FOR DENVER TEST SITE (Depth Interval = 39-43 feet)

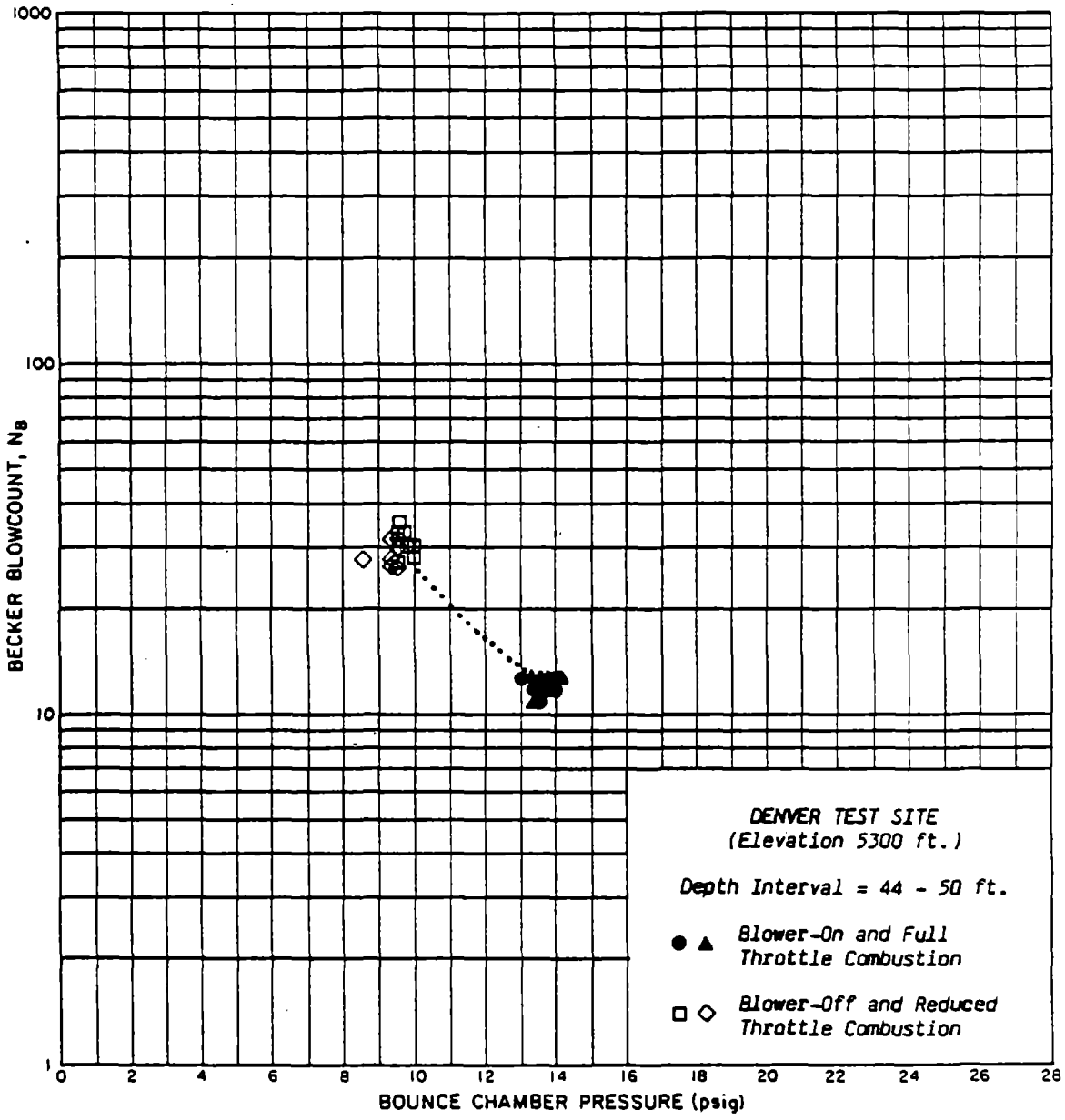

FIG. 40 EFFECT OF ENERGY REDUCTION ON THE BECKER BLOWCOUNT - BOUNCE CHAMBER PRESSURE RELATIONSHIP FOR DENVER TEST SITE (Depth Interval = 44-50 feet)

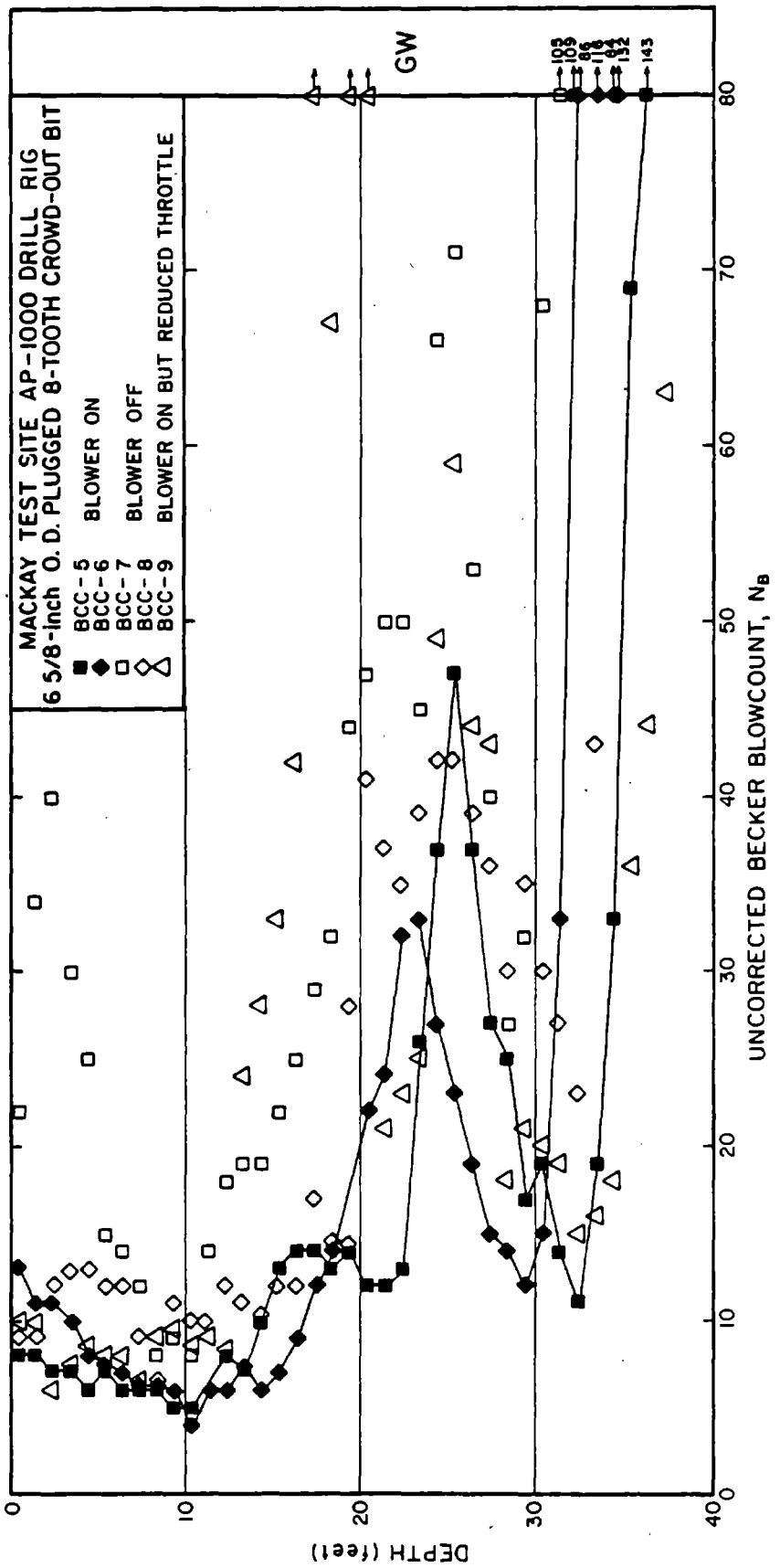

FIG. 41 EFFECT OF ROTARY BLOWER AND/OR REDUCED THROTTLE ON BECKER BLOWCOUNT AT MACKAY TEST SITE

Figure 42 presents the constant combustion rating curves for both conditions. Figures 43 through 45 present the data for three depth intervals having the least scatter. In a manner similar to that observed at Denver, a reduction in bounce chamber pressure of only about 3 psi was sufficient to double the blowcount. Although the bounce pressures in these figures were generally less than 10 psig and beyond the limits of the chart provided by ICE (Figure 29B), the results are clearly inconsistent with the curves on the chart.

The most discouraging experience in attempting to use the ICE chart for correcting blowcount values occurred in relation to data obtained at the Salinas test site. During the second series of explorations at this site in August 1985, three 6.6-inch closed-bit soundings were performed with the blower on and more or less full throttle. For four other 6.6-inch closed-bit soundings, the operator was directed to reduce the throttle setting to obtain varying bounce chamber pressures. Figure 46 shows that the reduced throttle settings greatly increased the Becker blowcounts above those obtained with full throttle. The constant combustion rating curve obtained for the three full-throttle soundings was previously presented in Figure 32. Figures 47 through 51 present data obtained with the reduced throttle settings for five depth intervals. As may be observed, the results in these five figures trace paths for increases in blowcount as a function of bounce chamber pressure decreases (energy drops). These blowcount paths generally curve more sharply upward after about an 8 psi drop. For example, Figure 47 shows the blowcounts recorded in the depth interval of 29 to 34 feet. The three full-throttle soundings produced average blowcounts of about 24 at a bounce chamber pressure of roughly 20 psig. By operating the throttle so that the bounce chamber pressure dropped to 10 psig, the blowcounts increased to over 1000, an increase of about 4000 percent. By contrast, the ICE chart would indicate only

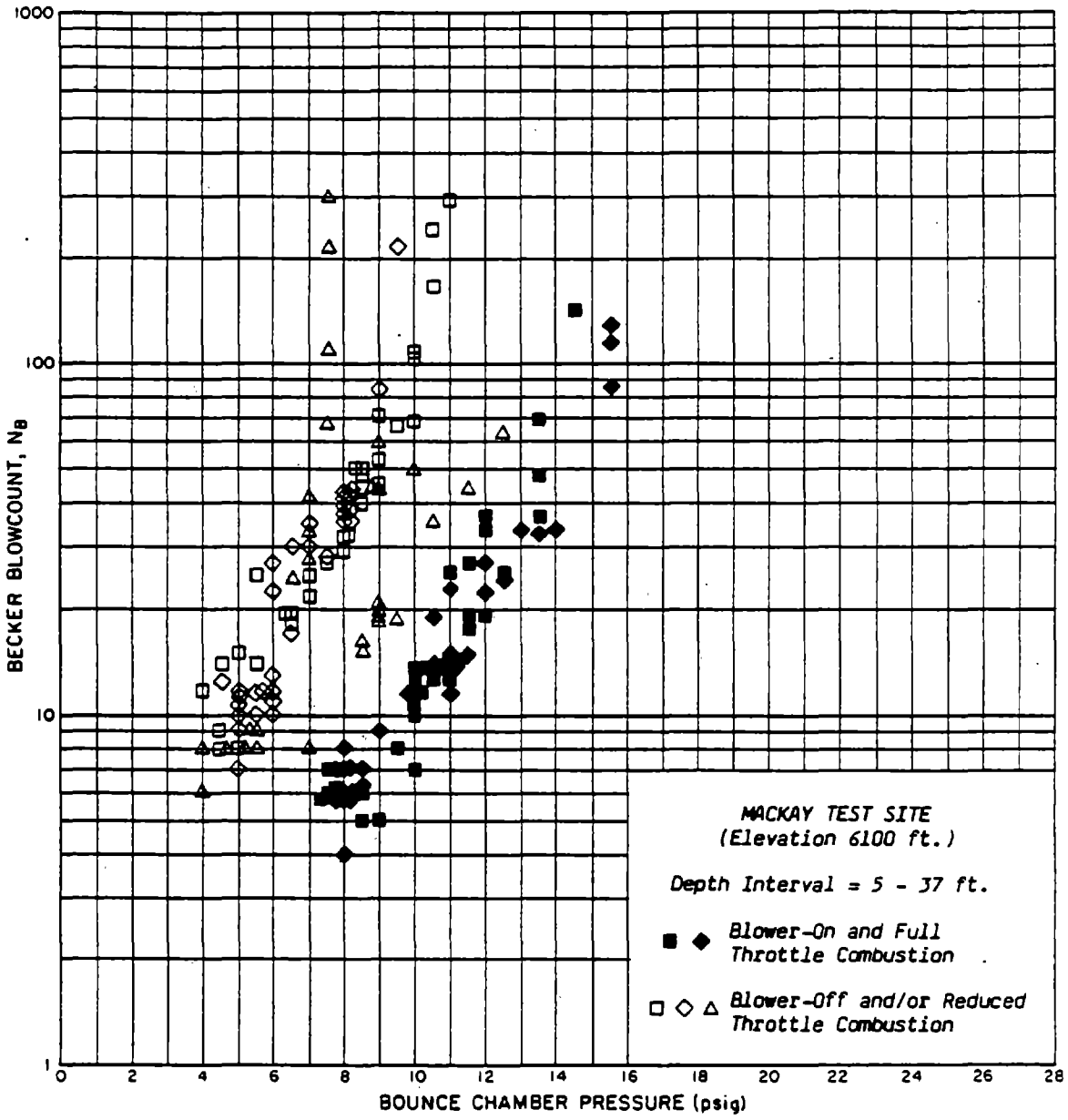

FIG. 42 CONSTANT COMBUSTION RATING CURVES FOR FULL AND REDUCED THROTTLE CONDITIONS AT MACKAY TEST SITE

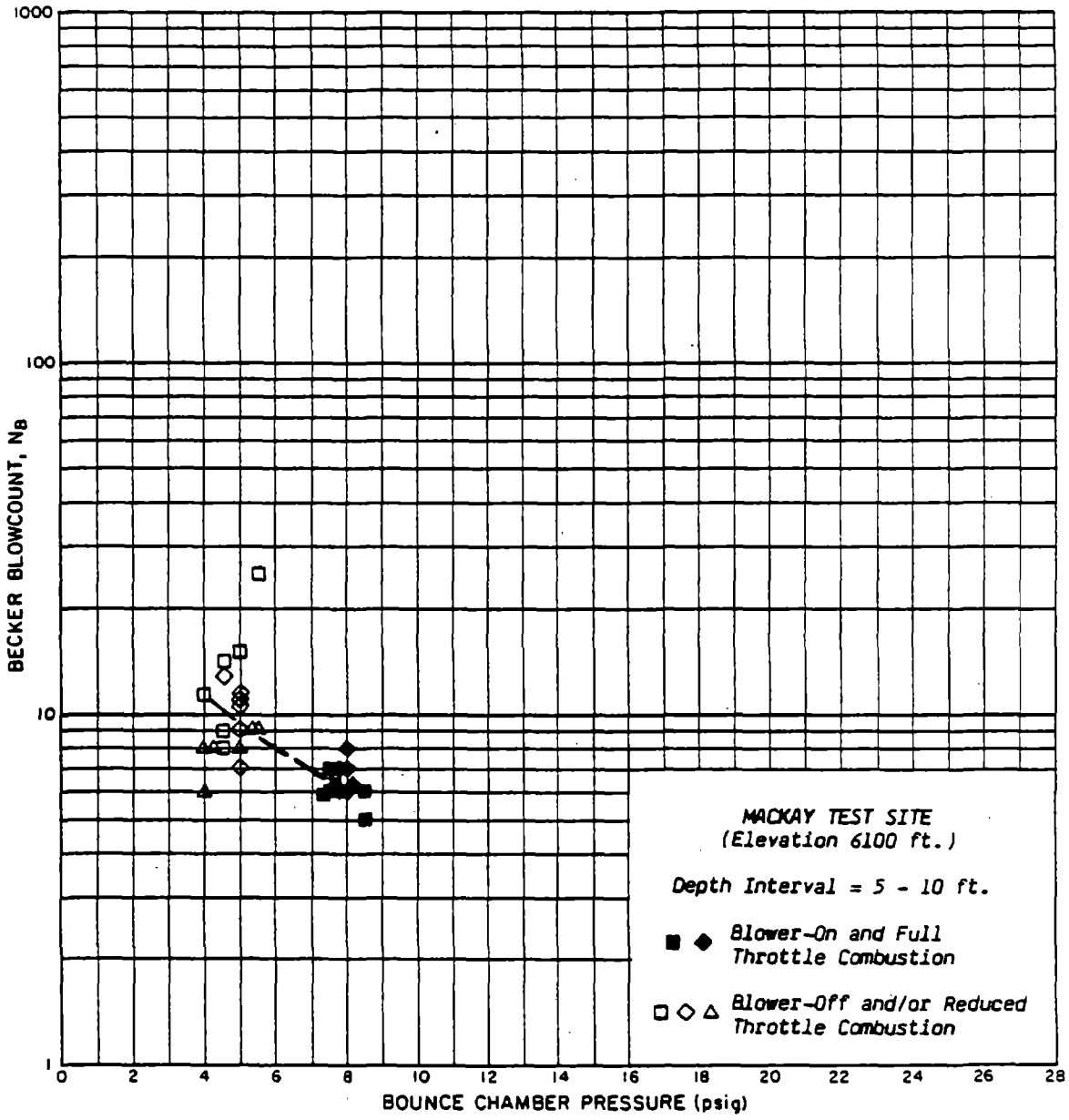

FIG. 43 EFFECT OF ENERGY REDUCTION ON THE BECKER BLOWCOUNT - BOUNCE CHAMBER PRESSURE RELATIONSHIP FOR MACKAY TEST SITE (Depth Interval = 5-10 feet)

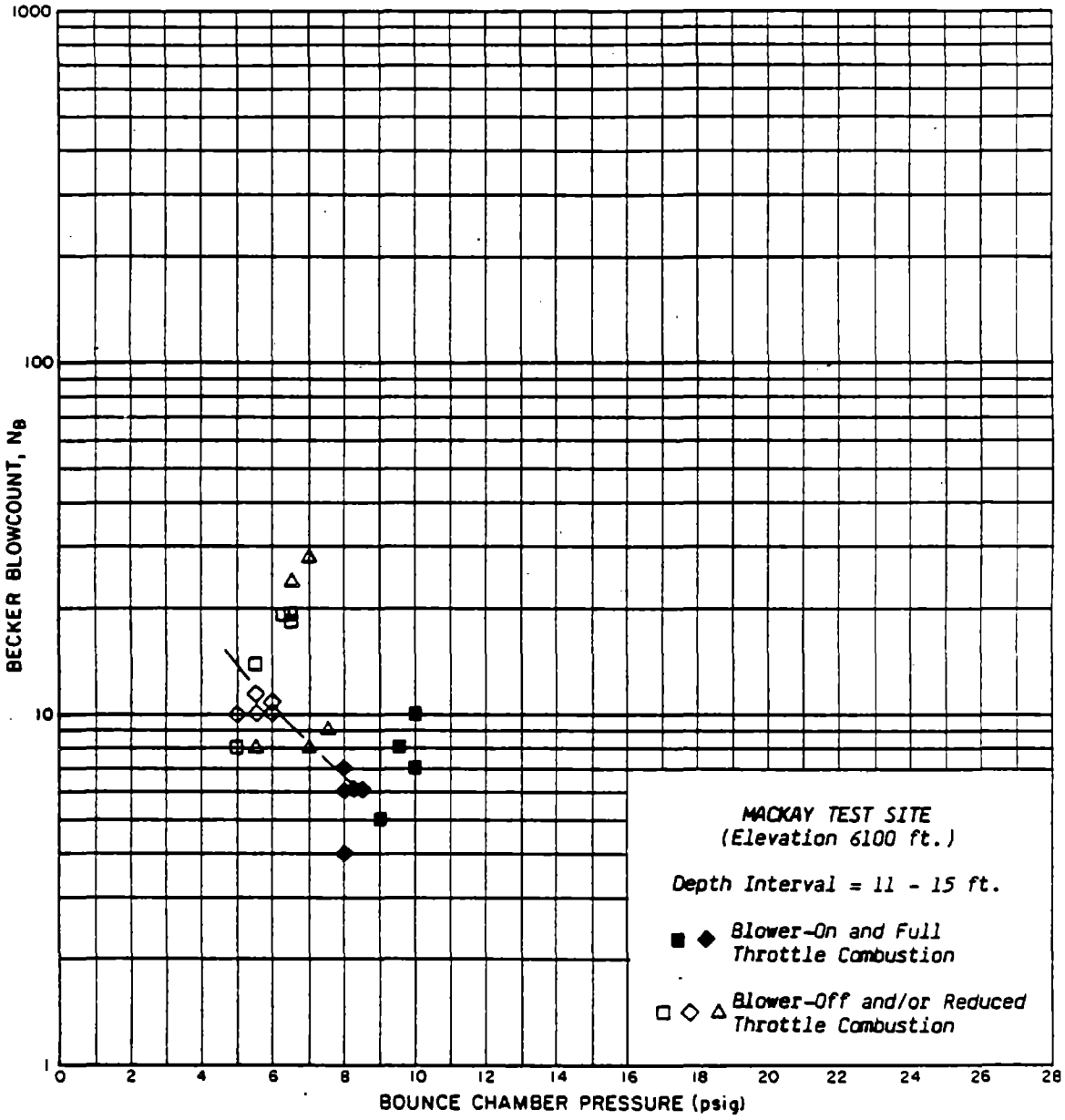

FIG. 44 EFFECT OF ENERGY REDUCTION ON THE BECKER BLOWCOUNT - BOUNCE CHAMBER PRESSURE RELATIONSHIP FOR MACKAY TEST SITE (Depth Interval = 11-15 feet)

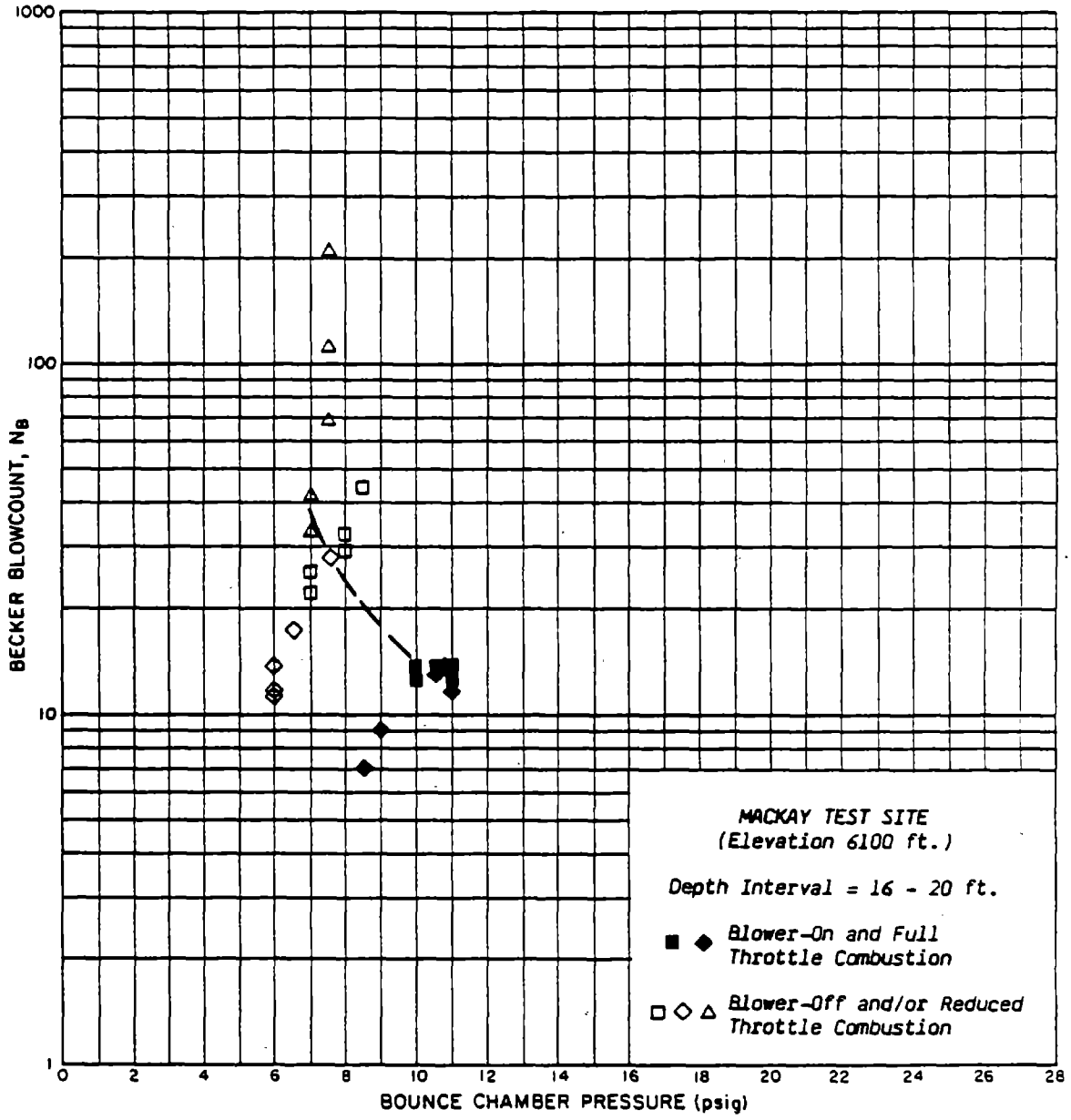

FIG. 45 EFFECT OF ENERGY REDUCTION ON THE BECKER BLOWCOUNT - BOUNCE CHAMBER PRESSURE RELATIONSHIP FOR MACKAY TEST SITE (Depth Interval = 16-20 feet)

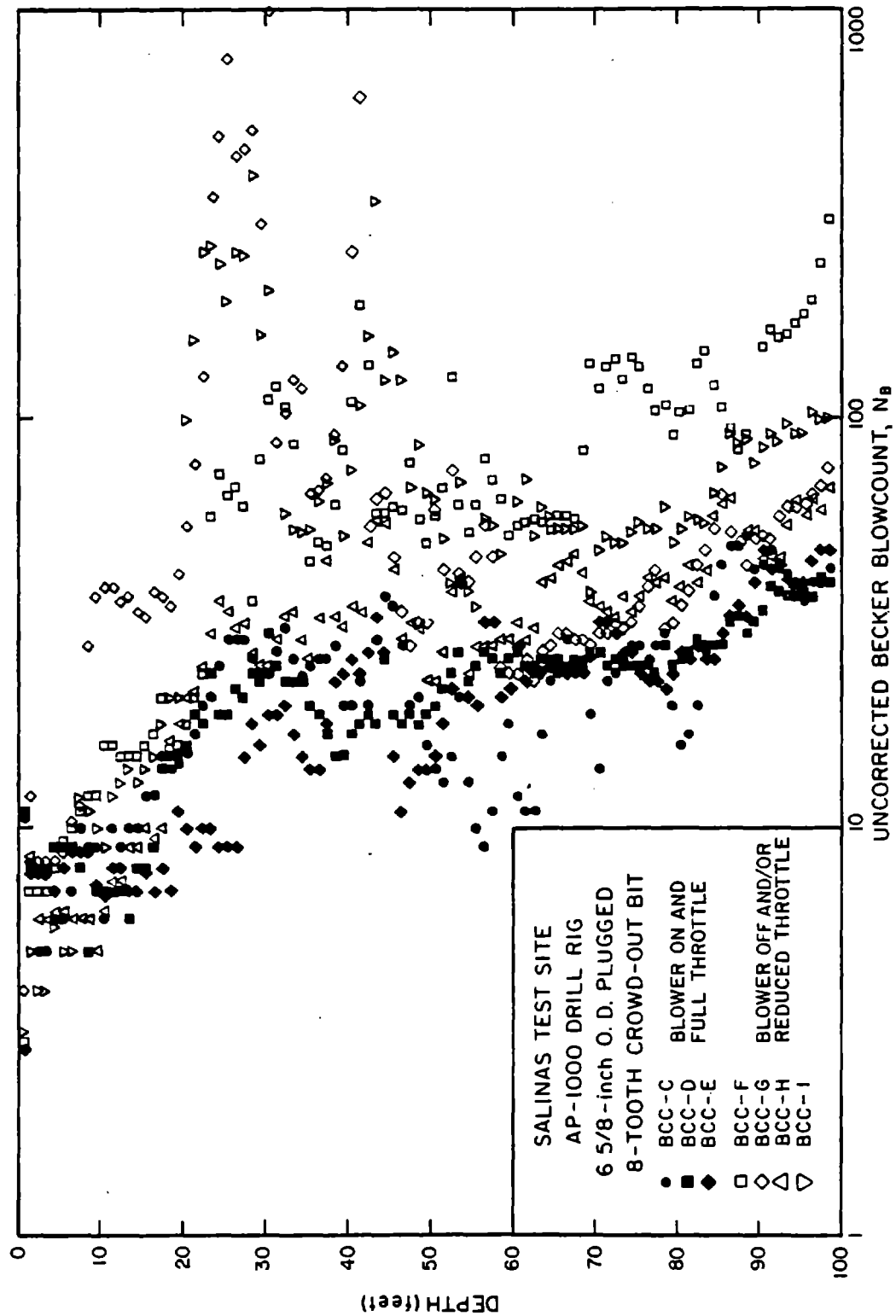

FIG. 46 EFFECT OF BLOWER ELIMINATION AND/OR REDUCED THROTTLE ON BECKER BLOWCOUNT AT SALINAS TEST SITE

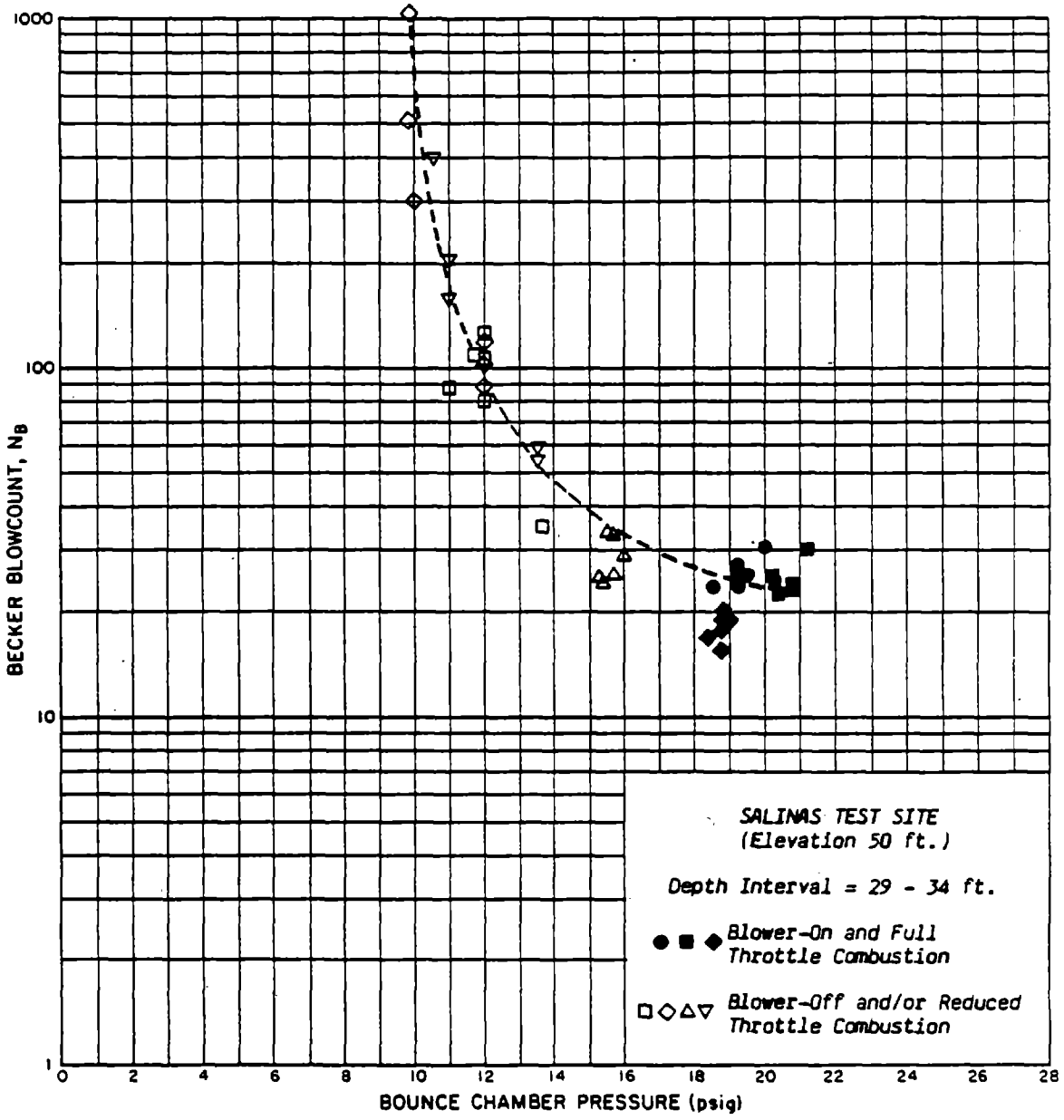

FIG. 47 EFFECT OF ENERGY REDUCTION ON THE BECKER BLOWCOUNT - BOUNCE CHAMBER PRESSURE RELATIONSHIP FOR SALINAS TEST SITE (Depth Interval = 29-34 feet)

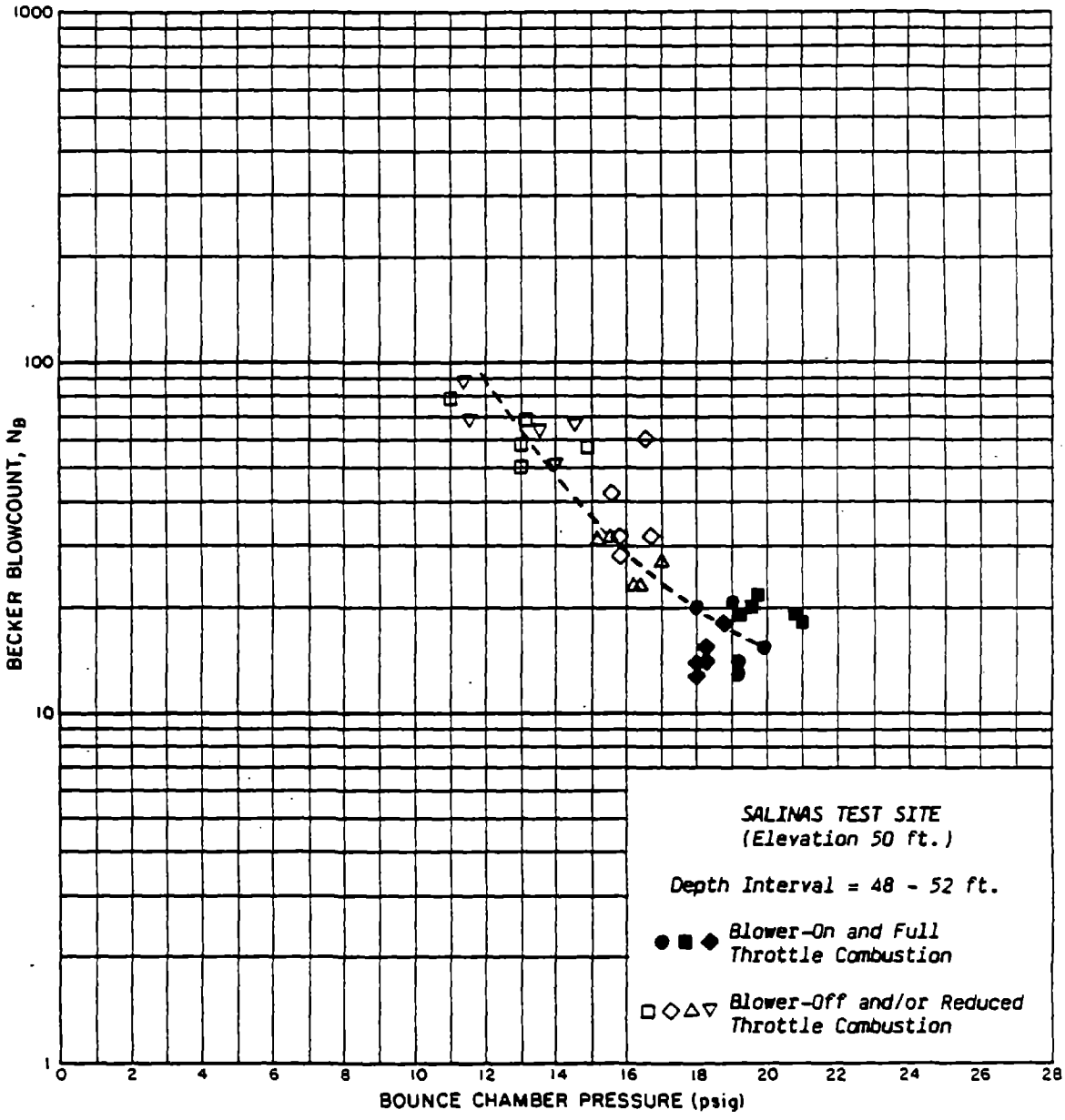

FIG. 48 EFFECT OF ENERGY REDUCTION ON THE BECKER BLOWCOUNT - BOUNCE CHAMBER PRESSURE RELATIONSHIP FOR SALINAS TEST SITE (Depth Interval = 48-52 feet)

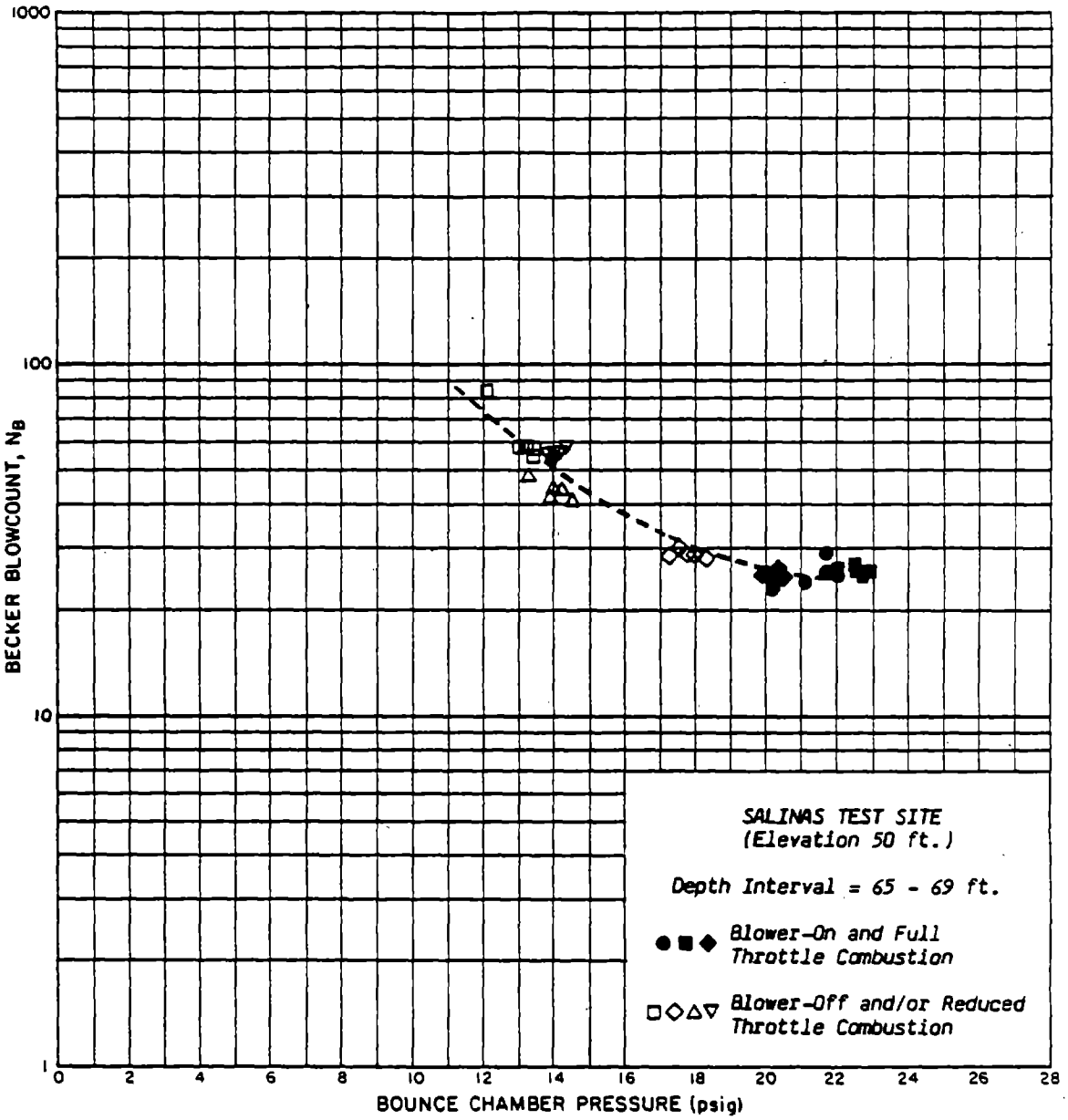

FIG. 49 EFFECT OF ENERGY REDUCTION ON THE BECKER BLOWCOUNT - BOUNCE CHAMBER PRESSURE RELATIONSHIP FOR SALINAS TEST SITE (Depth Interval = 65-69 feet)

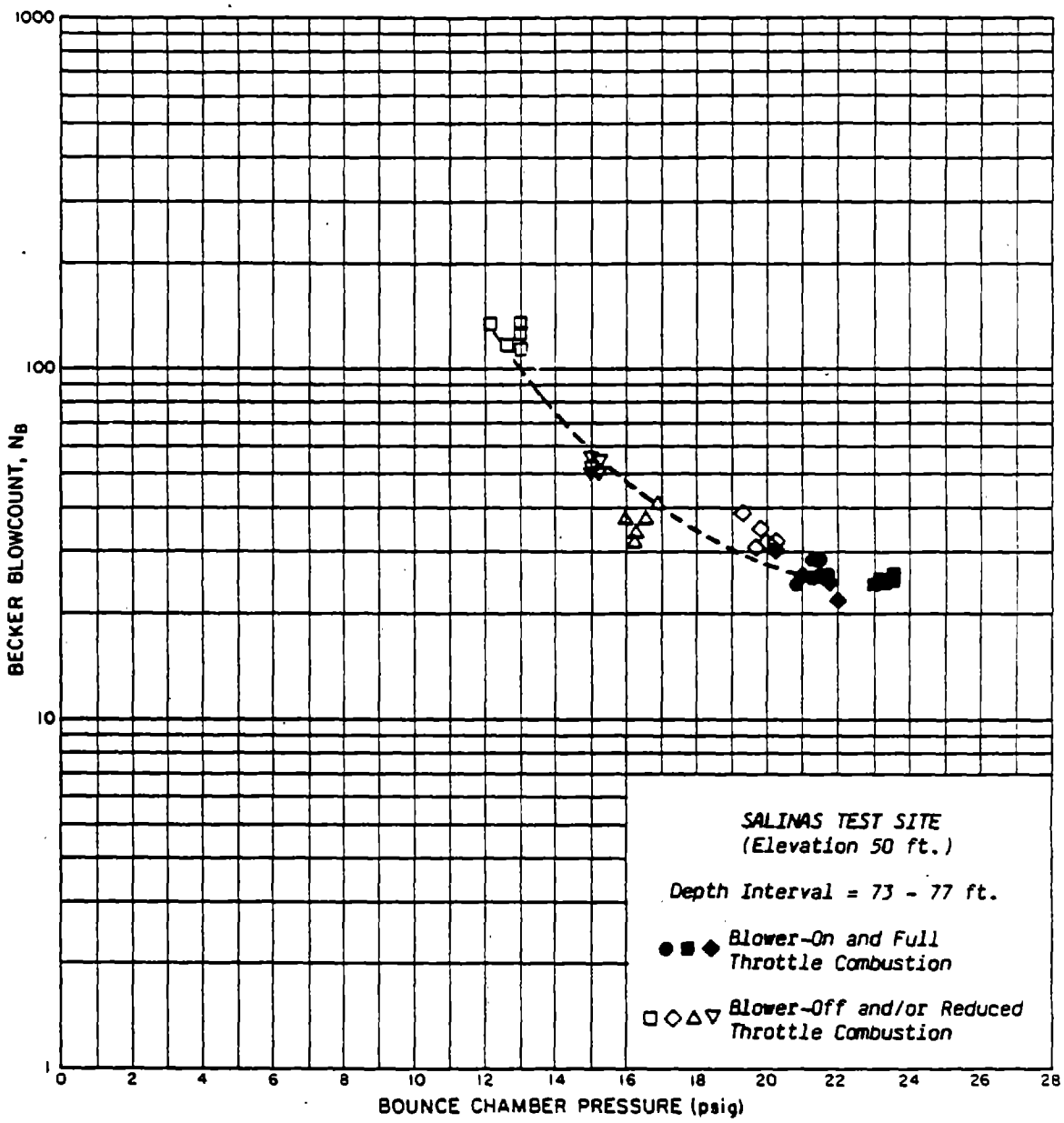

FIG. 50 EFFECT OF ENERGY REDUCTION ON THE BECKER BLOWCOUNT - BOUNCE CHAMBER PRESSURE RELATIONSHIP FOR SALINAS TEST SITE (Depth Interval = 73-77 feet)

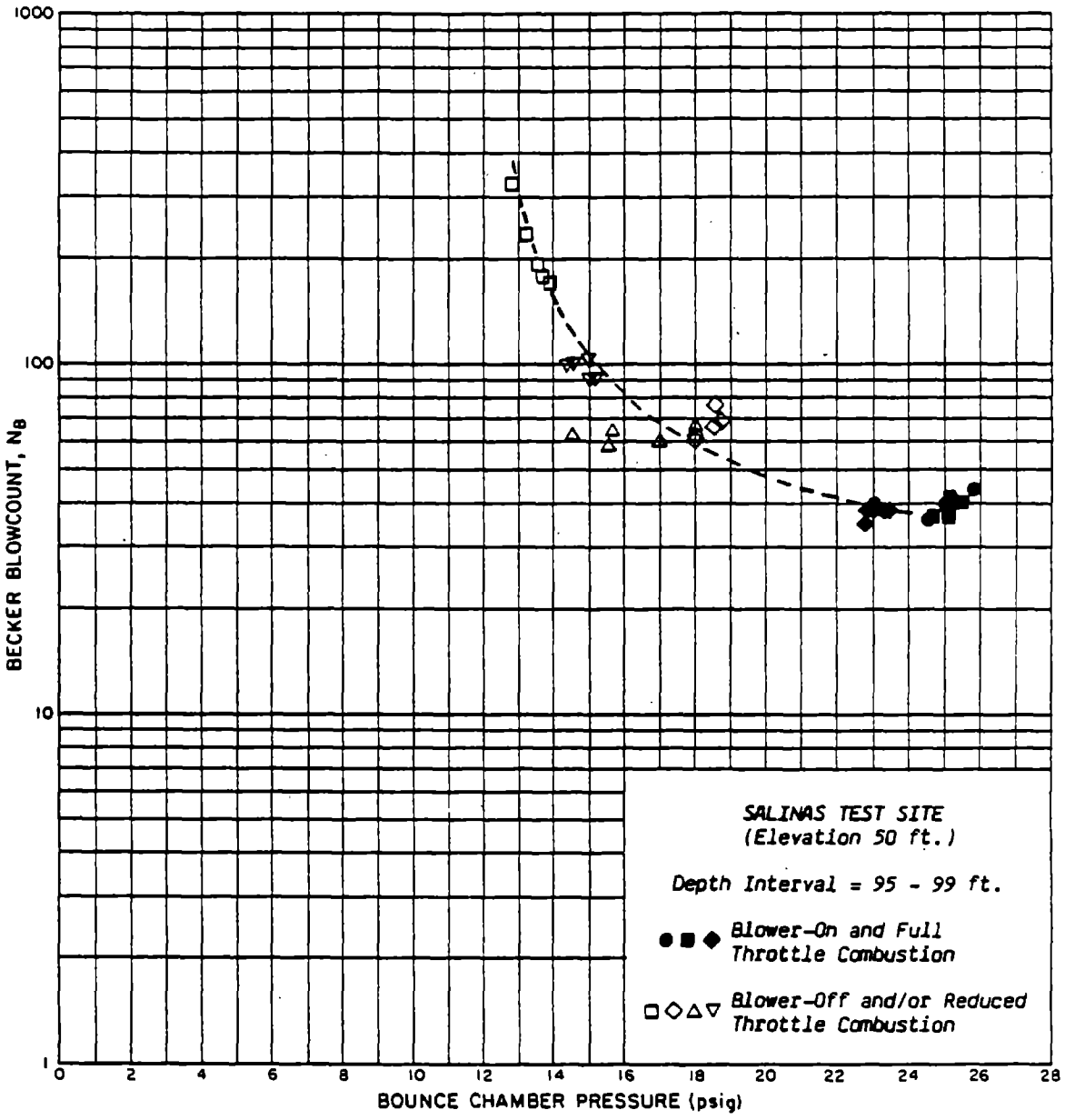

FIG. 51 EFFECT OF ENERGY REDUCTION ON THE BECKER BLOWCOUNT - BOUNCE CHAMBER PRESSURE RELATIONSHIP FOR SALINAS TEST SITE (Depth Interval = 95-99 feet)

about a 40 percent reduction in potential energy (4060 ft.-lb./6810 ft.-lb.). Such lack of agreement raises serious questions concerning the applicability and validity of the potential energy chart shown in Figure 29B, especially as a basis for correcting the blowcount for different combustion conditions.

Evaluation of Energy Effects

During each cycle of the hammer, the load developed in the casing is composed of three elements:

1. A Precompression Force
2. An Impact Force
3. An Explosive Force

The precompression force is a gas force caused by the compression of air and fuel in the combustion chamber as the ram travels downward towards the anvil. The impact force results from the impact of the ram on the anvil. The explosive force comes from the combustion of the fuel and the expansion of resulting gases. An idealized representation of the force developed in a long casing during each stroke, developed by Rempe and Davisson (1977) is illustrated in Figure 52. During each stroke, the force is zero until the ram closes the combustion chamber ports on its downward path. As the ram travels further downward, the force due to gas compression gradually increases. The force increases sharply at impact and then decreases gradually during gas expansion. When the ram travels far enough upwards to open the combustion chamber ports, the force in the casing is again reduced to zero. The force-time curve can be integrated to get the net energy delivered to the casing. This net energy should be some percentage of the available potential energy of the ram and the combustion energy. However it should be recognized that in the sequence of load development effects described above, there is probably a

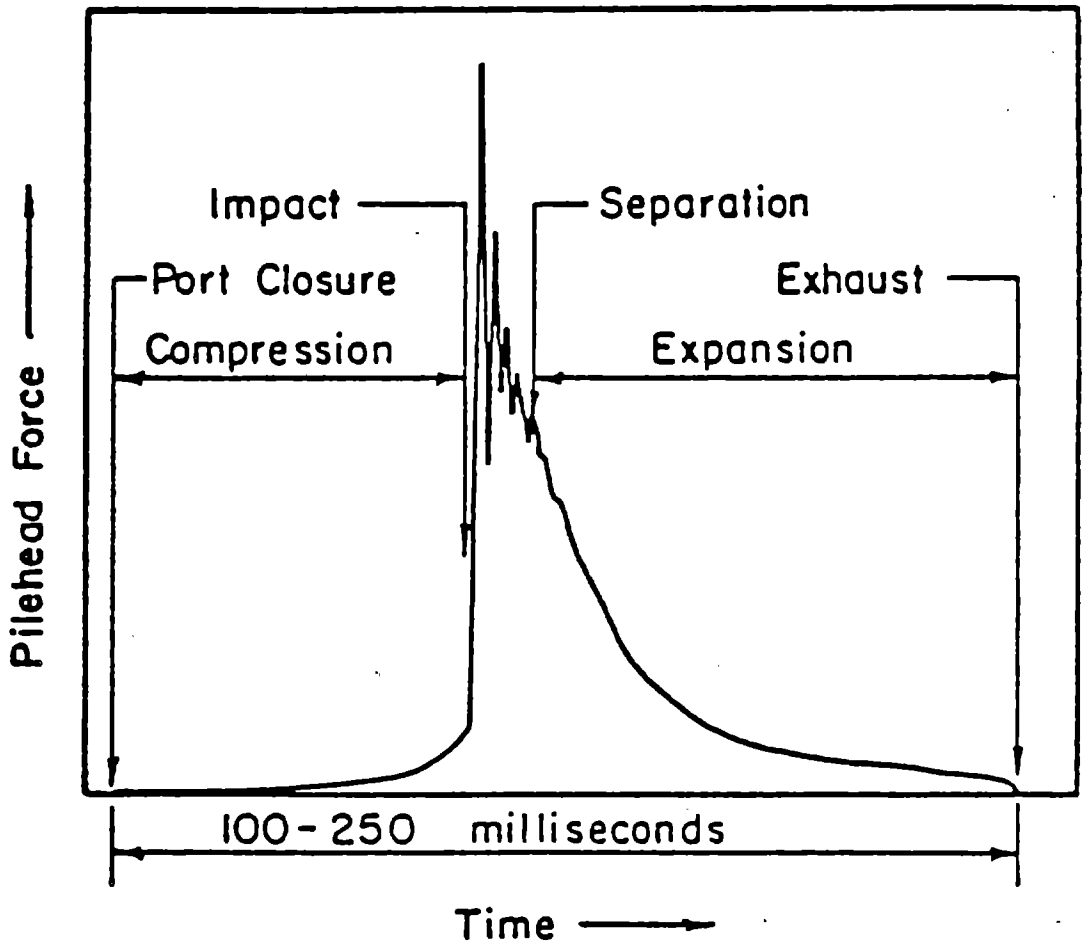

FIG. 52 IDEALIZED FORCE TIME-HISTORY EXPERIENCED IN A LONG CASING (from Rempe and Davisson, 1977)

severe kinetic energy loss when the air and fuel are compressed in the combustion chamber prior to impact of the ram on the casing.

The potential energy charts developed by ICE and shown in Figure 29B were based on the assumption that the total potential energy is the sum of the potential energy stored in the bounce chamber and the potential energy of the ram determined by the product of its weight and its height of fall from the top of its stroke (WH). This sum (represented by an equivalent stroke) is the total potential energy of the ram. However, just as the air in the bounce chamber pressure acts as a spring storing extra potential energy, the action of the ram travelling downward and compressing the air and fuel in the combustion chamber acts as a cushion which slows down the ram so that the kinetic energy at impact is severely reduced. It was pointed out by Tony Last, ICE representative, that the amount of energy lost in this way may be only a function of the atmospheric pressure and the dimensions of the combustion chamber (Ref. 16). Thus, for a particular atmospheric pressure and diesel hammer type, the energy loss due to cushioning effects would be essentially constant and could be estimated using the same procedures used to evaluate the energy stored in the bounce chamber (See Appendix). For the atmospheric pressure at sea level (14.7 psia) and the ICE 180 diesel hammer, the energy lost by compression of gases in the combustion chamber is found to be approximately 3810 ft-lb. This energy loss is a substantial portion of the potential energy and it leads to the actual kinetic energy of the ram at impact (i.e. potential energy minus compression energy loss) being significantly less than the potential energy of the ram at the top of its stroke.

The implications of this energy loss are illustrated in Table 3 where the kinetic energy of ram impact is presented for a range of bounce chamber pressures. For a bounce chamber pressure of 20 psig, the theoretical

Table 3: Potential and Impact Kinetic Energies for Sea Level

Bounce Chamber Pressure (psig)	Potential Energy (ft-lb)	Energy Loss (ft-lb)	Ram Impact Kinetic Energy (ft-lb)
10	4060	3810	250
11	4370	3810	560
12	4680	3810	870
13	4970	3810	1160
14	5250	3810	1440
15	5530	3810	1720
16	5800	3810	1990
17	6060	3810	2250
18	6320	3810	2510
19	6560	3810	2750
20	6810	3810	3000
21	7050	3810	3240
22	7280	3810	3470
23	7500	3810	3690
24	7730	3810	3920
25	7940	3810	4130
26	8160	3810	4350
27	8360	3810	4550
28	8580	3810	4770

potential energy is 6810 ft-lb but the impact kinetic energy is probably only about 3000 ft-lb. For a bounce chamber pressure of 10 psig, the theoretical potential energy is 4060 ft-lb but the net kinetic energy is probably only about 250 ft-lb. The ratio of potential energies is 1.67; but the ratio of the impact kinetic energies is 12. A comparison of the impact kinetic energy ratios would help explain why the blowcount increases so markedly with only moderate decreases in bounce chamber pressure. Figure 53 shows the same data presented previously for the 29 to 34-foot depth interval at the Salinas Test Site, illustrating the very large increase in blowcount which results from energy decreases. Also shown is a line representing the increase predicted by using the ratio of net kinetic energies. The agreement between the test data and the prediction is relatively good. Comparisons for other depth intervals give similarly good agreement.

Since the impact kinetic energy appears to control the resulting blowcount, it would appear that the precompression and explosive forces do not play important roles in the direct driving of the casing. This is not totally inconsistent since the precompression force is probably insufficient to drive the casing into the soil. However, the explosive force cannot be considered a minor force. A possible explanation for its apparently small effects, suggested by Fuller (1983), is that most of the explosive energy is directed towards raising the ram for its next stroke. If this is so, then the explosive force would have a negligible influence on the casing penetration during any given cycle.

Effect of Elevation on Energy and Bounce Chamber Pressure

Operators of the Becker drill rigs have long believed that higher elevations reduce the amount of energy developed by the diesel hammers. This belief was fostered partly because oxygen levels are known to be lower at

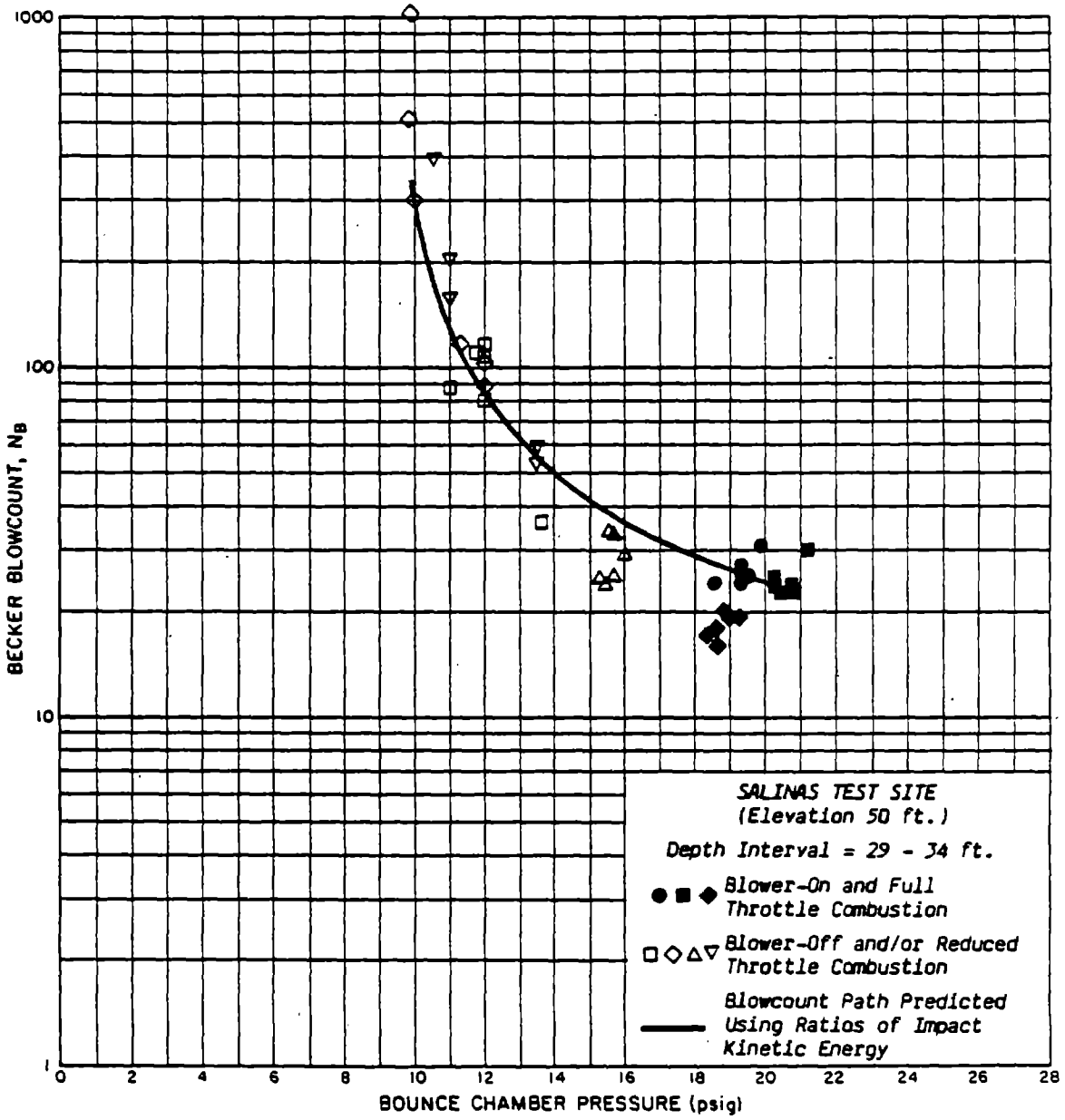

FIG. 53 COMPARISON OF ACTUAL BLOWCOUNT INCREASES WITH PREDICTIONS BASED ON RATIOS OF IMPACT KINETIC ENERGY FOR SALINAS TEST SITE (Depth Interval = 29-34 feet)

higher elevations. In addition, the operators have noted that the bounce chamber pressures appear to be lower at higher elevations. For example, in dense soils at 6000 feet elevation, the bounce chamber pressures rarely exceeded 20 psig. However, at sea level, bounce chamber pressures often reached 28 psig in dense soils. This behavior can also be observed in Figure 54 by examining the full throttle constant combustion rating curves for the Salinas (Elev. 50 feet), Denver (Elev. 5300 feet), and Mackay (Elev. 6100 feet) Test Sites. This figure suggests that an increase in elevation moves the rating curve to the left (i.e. causes a decrease in energy).

There is a correction required, however, in using the bounce chamber pressure as an indicator of energy for different elevations. This correction is needed because the atmospheric pressure is not the same at all elevations. For example, at sea level, the atmospheric pressure is usually around 14.7 psig. At an elevation of 6000 feet, the atmospheric pressure is around 11.7 psig. This affects the calculations for potential energy, energy lost during combustion chamber compression, and the resulting impact kinetic energy. Table 4 shows the various energies calculated for an elevation of 6000 feet. Figure 54 shows the impact kinetic energy as a function of bounce chamber pressure for both elevations. For the same bounce chamber pressure, the net kinetic energy at 6000 feet is in fact, significantly greater than that at sea level. For example, the net kinetic energy at a bounce chamber pressure of 10 psig at sea level is only about 16 percent (250/1600) of the energy developed for the same bounce pressure at the 6000-foot elevation.

To correct for the effect of different atmospheric pressures on the net kinetic energy, it appears that the best approach is simply to make an adjustment to the bounce chamber pressure value. For example, if the blowcount and bounce chamber pressure relationships developed at sea level are adopted as a

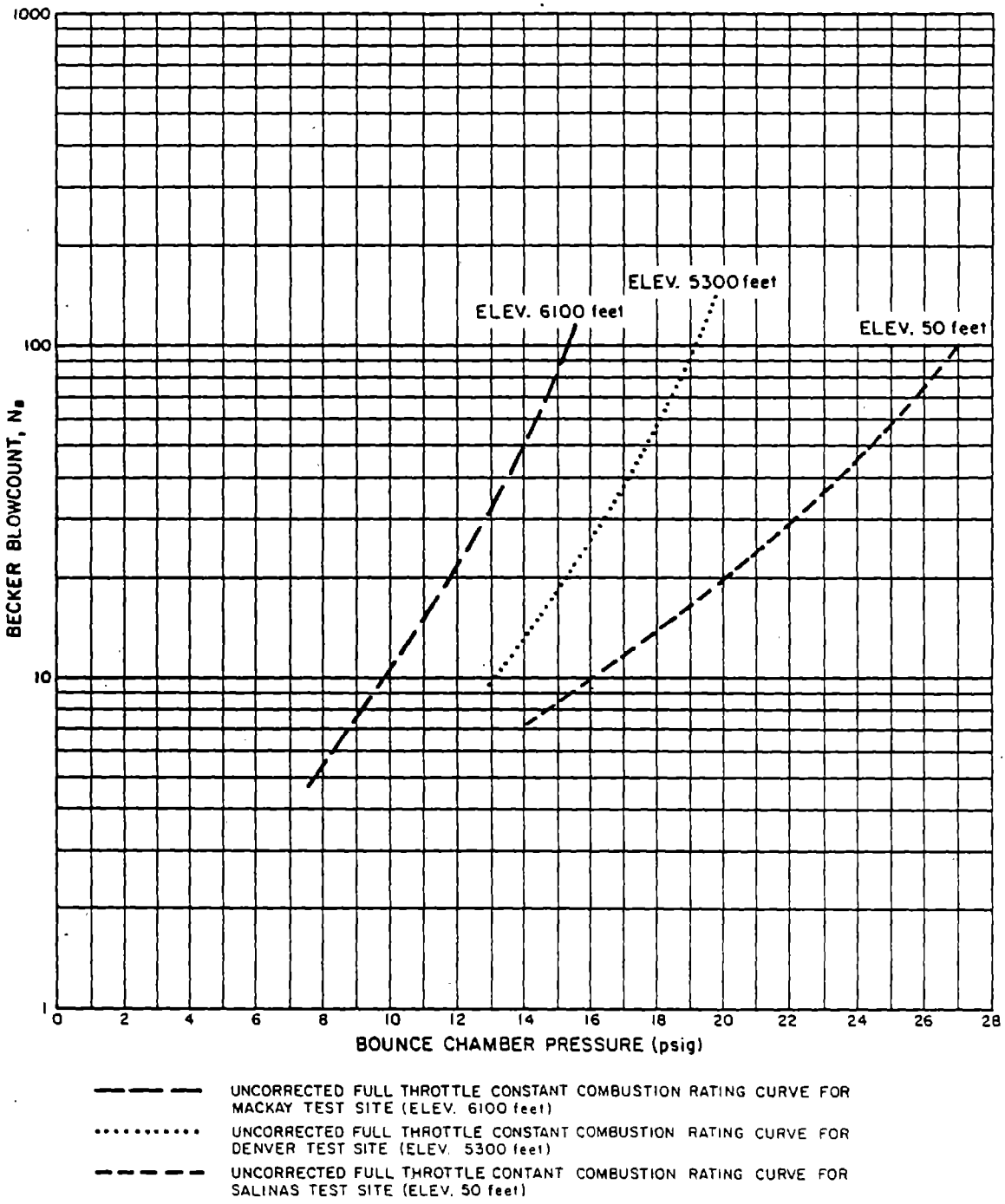

FIG. 54 UNCORRECTED FULL THROTTLE COMBUSTION RATING CURVES FOR SALINAS, DENVER, AND MACKAY TEST SITES

Table 4: Potential and Impact Kinetic Energies for Elev. 6000'

Bounce Chamber Pressure (psig)	Potential Energy (ft-lb)	Energy Loss (ft-lb)	Ram Impact Kinetic Energy (ft-lb)
6	3150	3030	120
7	3560	3030	530
8	3950	3030	920
9	4290	3030	1260
10	4630	3030	1600
11	4960	3030	1930
12	5270	3030	2240
13	5570	3030	2540
14	5870	3030	2840
15	6150	3030	3120
16	6420	3030	3390
17	6690	3030	3660
18	6940	3030	3910
19	7190	3030	4160
20	7430	3030	4400
21	7670	3030	4640
22	7900	3030	4870
23	8120	3030	5090
24	8340	3030	5310

standard, then bounce chamber pressures obtained at higher elevations would need to be adjusted upward by some amount to represent the appropriate kinetic energy level. For an elevation of 6000 feet, this adjustment would range from about 3.7 at a bounce pressure of 6 psig to about 6.2 for a bounce chamber pressure of 20 psig (See Figure 55).

Shown again in Figure 56 is the constant combustion rating curve for full throttle combustion developed at the Salinas Test Site (El. 50). Also shown are the full throttle rating curves for the Denver and Mackay Test Sites after being corrected to sea level conditions as described above. The corrections used were those shown in Figure 55 for conditions at 6000 feet elevation. Application of this correction brings the rating curve for the Denver Test Site (Elevation 5300 feet) into excellent agreement with the rating curve determined for the Salinas site. Although the combustion rating curve for the Mackay Test Site remains significantly higher than the others, it is moved much closer to the Salinas curve after correction. Whether the remaining difference between the Mackay and the Denver and Salinas curves is due to the reduced partial pressure of oxygen at Mackay, or possibly to the use of lower grade fuel at that site remains unknown. However, it is possible to conclude that changes in elevation do not change the rating curve as much as previously thought.

Adoption of a Calibration Combustion Rating Curve

Under ideal circumstances and conditions, the best way to calibrate energy effects would be to measure transmitted energies within the casing steel. Consideration was given to attempting such measurements using accelerometers, strain gauges, etc., but this approach was finally rejected for the following reasons:

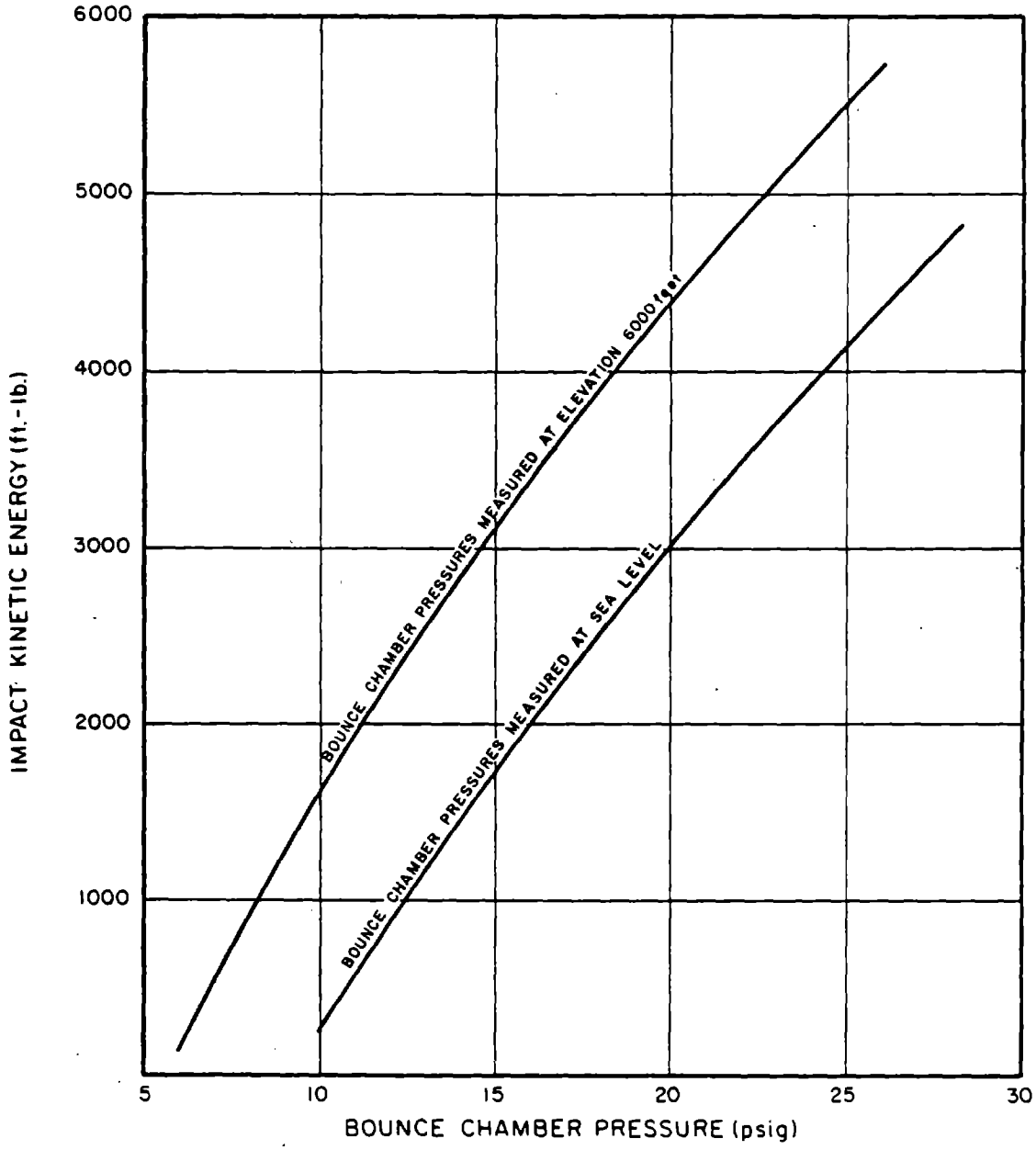

FIG. 55 ESTIMATED KINETIC ENERGY OF RAM AT ANVIL IMPACT

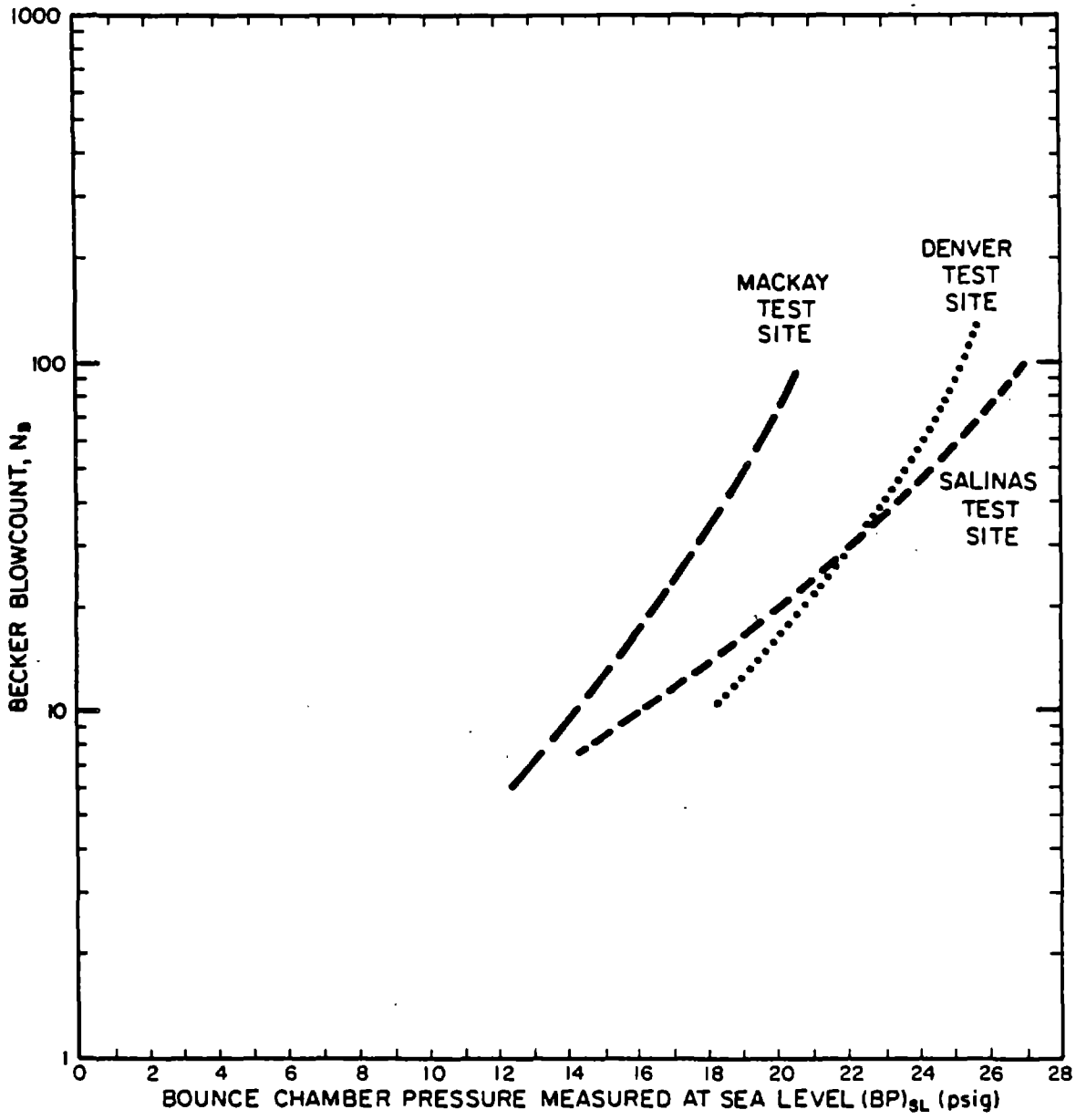

FIG. 56 FULL THROTTLE COMBUSTION RATING CURVES FOR SALINAS, DENVER, AND MACKAY TEST SITES CORRECTED TO SEA LEVEL ATMOSPHERIC PRESSURE

1. Employing sophisticated transducers requires specialized equipment and experience. It also requires assumptions and simplifications in order to evaluate energy levels.
2. There is some doubt that the equipment and theories would be able to adequately account for the effects of the inner casing floating within the outer casing.
3. Using sophisticated transducers would slow down the drilling process and reduce some of the economic attraction of the Becker process.
4. The wide variety of pile hammers and pile sizes used in the pile-driving industry is not present with the Becker equipment. The Becker equipment uses only one kind of hammer, only one or two types of "pile" sizes and impedances, and only one kind of hammer cushion. Thus variations from one site to another should not be very large so long as a standard procedure is followed.
5. Using the bounce chamber pressure gauge together with field data regarding the effect of combustion effects on blowcount was considered to be an adequate way of handling energy effects. Thus, although the exact magnitude of the energy transmitted down the casing may not be known, it is possible to monitor the impact energy and then predict the effect on the measured blowcounts.

Figure 57 shows an idealization of different constant combustion rating curves and the blowcount paths for constant depths in the same material that range across the rating curves. As has been shown previously, several different combustion rating curves can exist for the same hammer operating at the same site, depending on the throttle settings. With different combustion conditions, the resulting blowcount can be radically different. Therefore, in

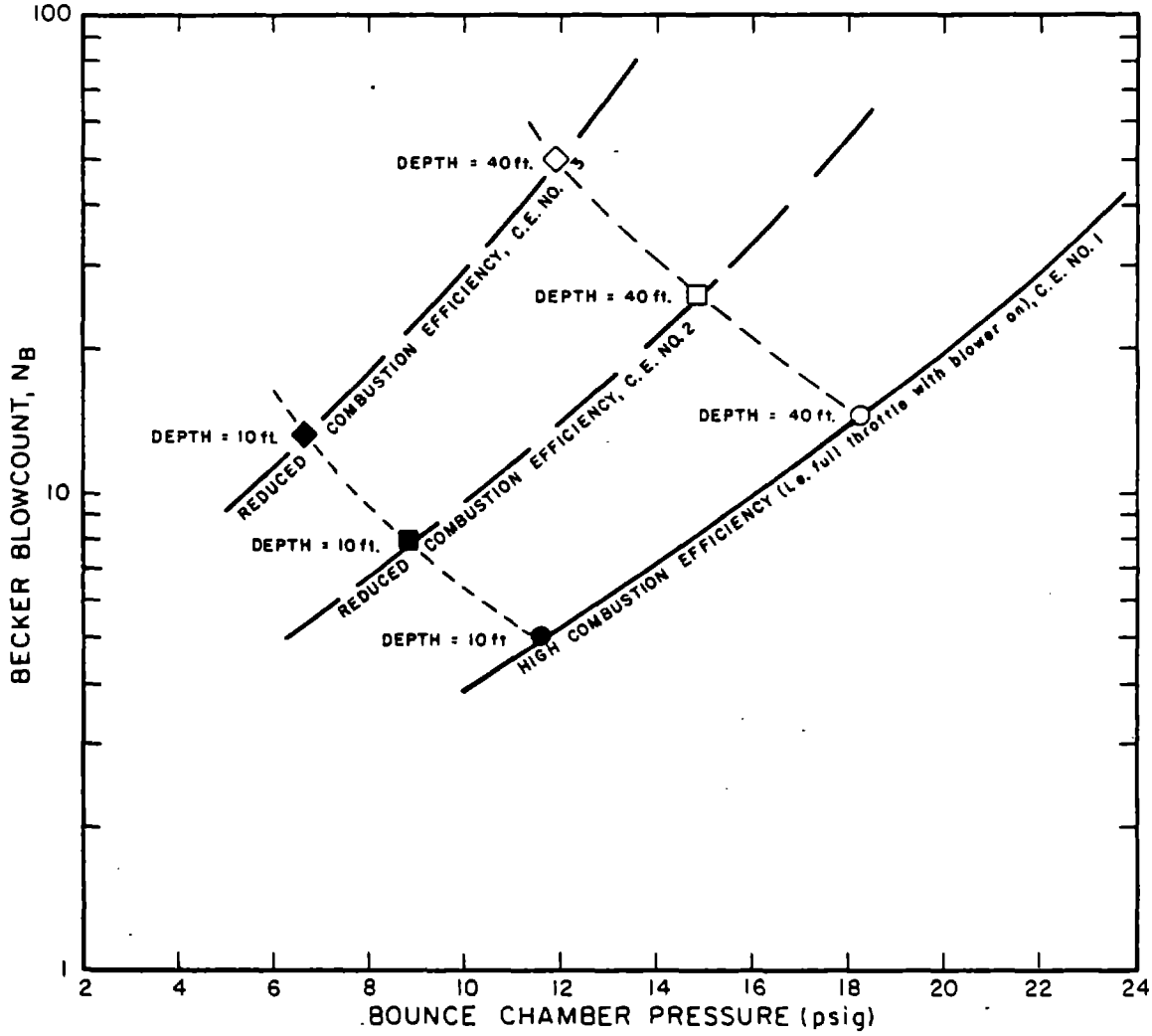

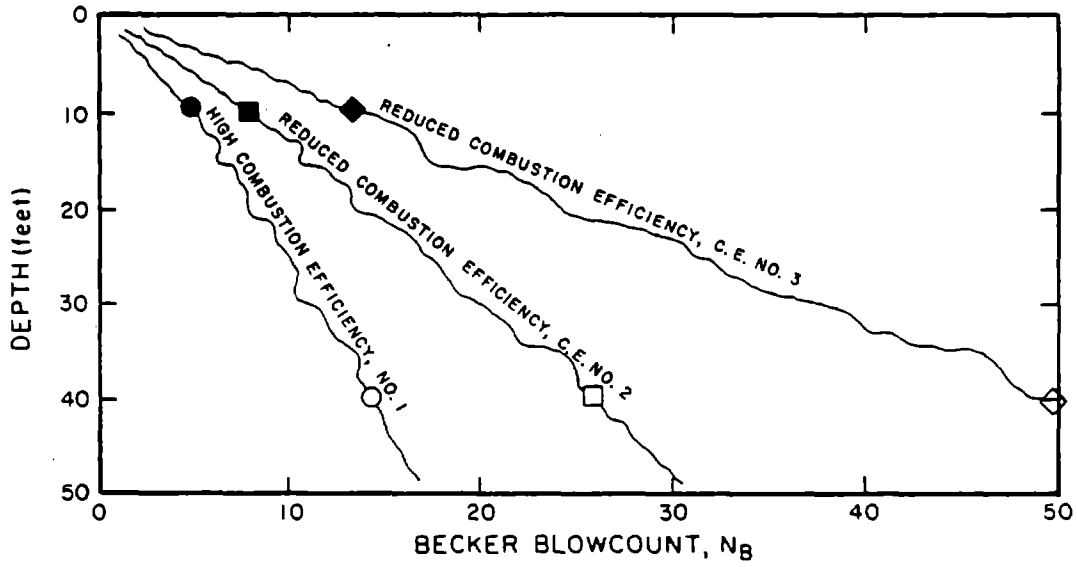

FIG. 57 IDEALIZATION OF HOW DIESEL HAMMER COMBUSTION EFFICIENCY AFFECTS BECKER BLOWCOUNTS

order to use the Becker Penetration Test as an indicator of soil properties, it is necessary to adopt one combustion rating curve as a standard and develop corrections for combustion curves that are different from that standard. The constant combustion rating curve adopted in this research program is that for full throttle combustion developed at the Salinas Test Site (Figure 32). This curve was chosen because it represents the highest energy (i.e. the lowest blowcount curve) observed in any of the field tests and corrections to this curve will result in correcting blowcounts in only one direction (i.e. reducing blowcounts to allow for lower energies employed under other conditions. Blowcounts which fall on this calibration curve, or which have been corrected to fall on this curve, will here-after be designated as corrected Becker blowcounts and will be given the symbol N_{BC}.

The development of correction curves for lower energy combustion conditions made use of both field measurements and calculations based on determinations of kinetic impact energy. Figure 58 shows the blowcount paths measured in the field for different combustion conditions at different sites. These curves were previously presented in Figures 35-40, 43-45, and 47-51, but in Figure 58 they have been corrected for elevation where necessary. Also shown in Figure 58 are blowcount paths based on ratios of impact kinetic energy. The agreement between the two sets of data is relatively good and from these data, the correction curves shown in 59 were drawn and adopted for use in this study.

To use the correction curves, it is simply necessary to locate each uncorrected test result on the chart shown in Figure 59, using both the uncorrected blowcount and the bounce chamber pressure, and then follow the correction curves down to the standard rating curve AA, to obtain the corrected Becker blowcount, N_{BC}. For example, if the uncorrected blowcount was

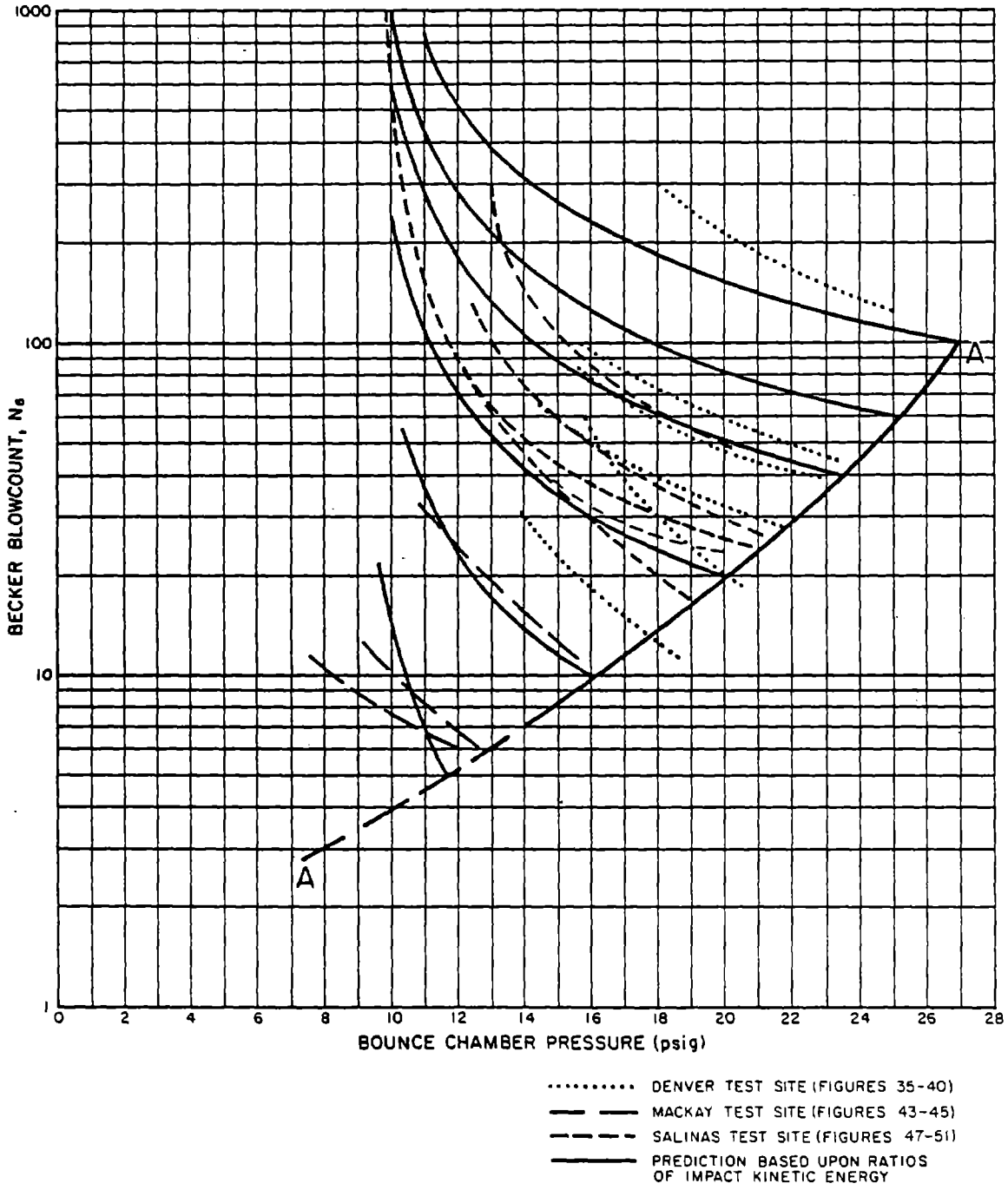

FIG. 58 PATHS OF BECKER BLOWCOUNT INCREASES FOR DECREASING HAMMER ENERGY BASED ON FIELD DATA AND RATIOS OF IMPACT KINETIC ENERGY

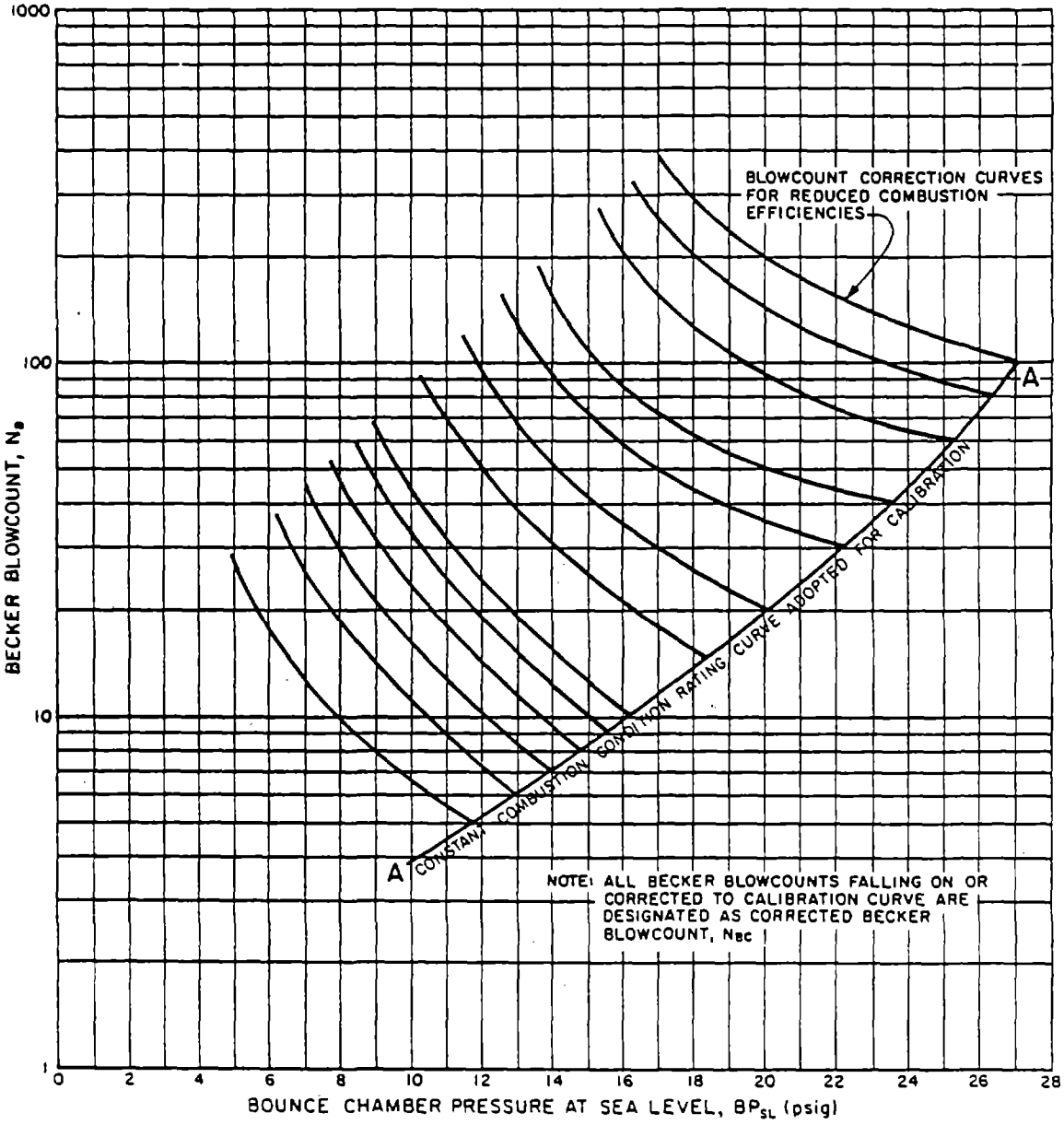

FIG. 59 CORRECTION CURVES ADOPTED TO CORRECT BECKER BLOWCOUNTS TO CONSTANT COMBUSTION CURVE ADOPTED FOR CALIBRATION

43 and it was obtained at sea level with a bounce chamber pressure of 18 psig, then the corrected Becker blowcount would be 30, as shown in Figure 60. If the bounce chamber pressure requires a correction to sea level, that correction should first be made and then the corrected blowcount determined as before. For instance, if the uncorrected Becker blowcount was 24 and it was obtained at al elevation of 6000 feet with a bounce chamber pressure of 12.5 psig, the bounce chamber pressure is first corrected to sea level conditions by adding 5 psig (See Figure 55). Using an uncorrected blowcount of 24 and a corrected bounce chamber pressure of 17.5 psig then yields a corrected Becker blowcount of 18 (Figure 60).

Effect of Drill Rig Type on Becker Blowcount

Becker Drills, Inc. employs principally two types of drill rigs to perform the Becker Penetration Test. The older rig is designated the B-180 drill rig (it is also known as the HAV-180 rig) and a newer model, developed in the mid-70's, which is designated the AP-1000 drill rig. Both rigs employ the same model of diesel hammer, an ICE Model 180. The main difference between the drill rigs is that the mast of the newer AP-1000 rig is more elaborate and the way the hammer is hung onto the mast is more complicated. On the older B-180 rigs, the hammer is mounted on wear blocks and follows the casing by weight alone. There are cables mounted to the top of the hammer frame for raising the hammer with hydraulic rams, but none for pulling down on the hammer frame. On the newer AP-1000 rigs, there are cables connected to both the top and the bottom of the hammer frame. These cables are connected to hydraulic rams and, in addition to being able to raise the ram back up the mast, they allow the hammer to be pulled down onto the casing during driving. This "pull-down" static force is used mainly during the driving of

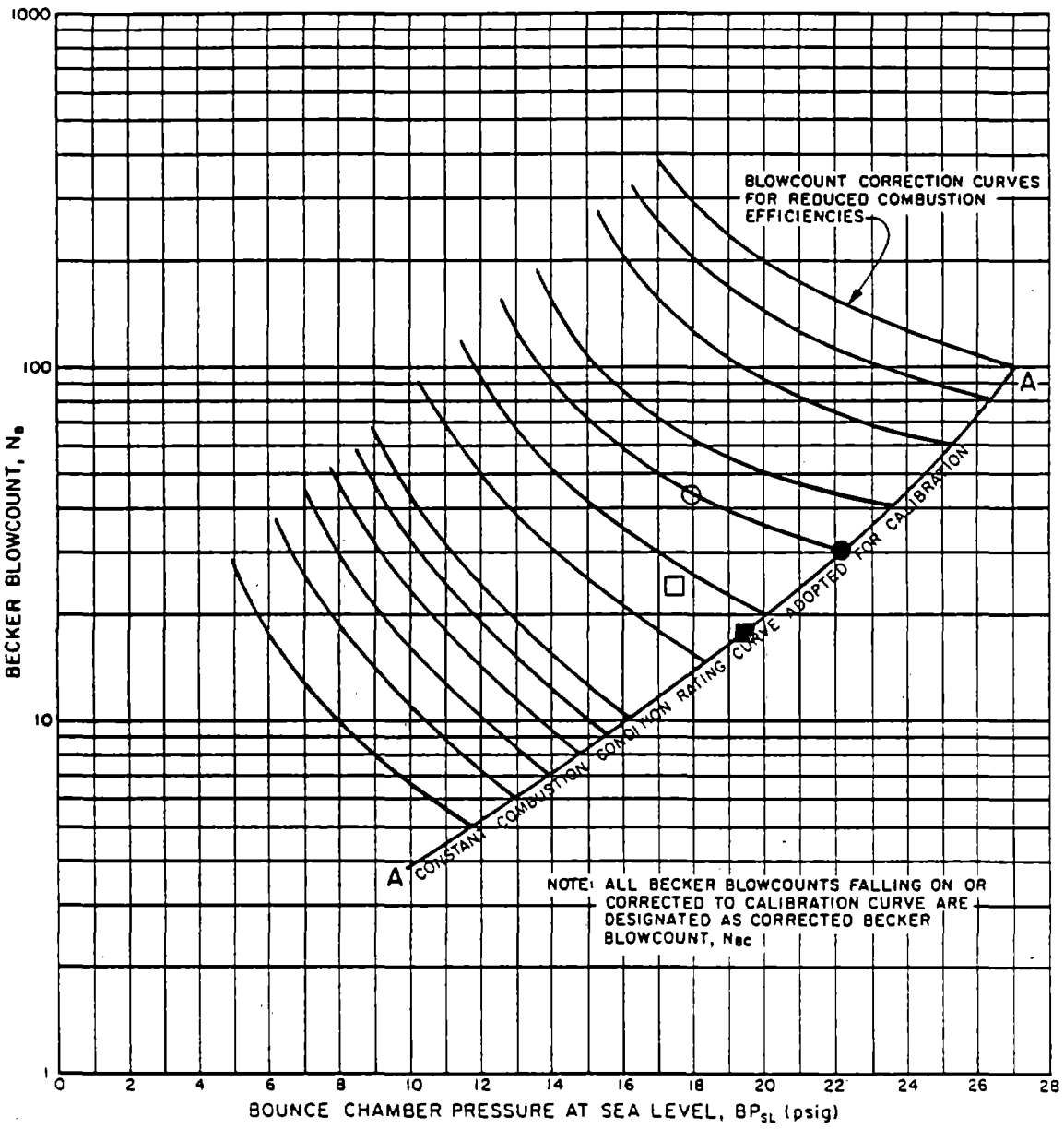

FIG. 60 EXAMPLES ILLUSTRATING THE USE OF CORRECTION CURVES TO CORRECT BECKER BLOWCOUNTS

particularly stiff material with, say, more than 200 blows per foot, in order to reduce the number of blows during driving.

Most of the Becker Penetration Testing carried out in this investigation were performed with an AP-1000 drill rig (Rig. No. 57). Even though the pull-down option was never used during these studies, it was decided to investigate whether the use of the other type of rig, a B-180, would produce a different result. Consequently, the soundings performed at the San Diego Test Site were performed with a B-180 drill rig (Rig No. 11). The results from this site were compared to those obtained at the Salinas and Thermalito sites where the AP-1000 rig was used. At all three sites, good quality SPT results were available. Surprisingly, the Becker blowcounts at the San Diego site appeared relatively low when compared to the results from the other two sites. The older B-180 rig appeared to give Becker blowcounts that were only about one half of the values that would be indicated for the same SPT blowcounts from the Salinas and Thermalito sites. The result indicated that the B-180 rig was almost twice as efficient at transmitting hammer energy as was the AP-1000 rig.

To further investigate the effect of different drill rigs on Becker blowcounts, 2 pairs of soundings were performed at the Denver Test Site. One pair of soundings was performed using the same AP-1000 rig (Rig. No. 57) as that was used at the Salinas and Thermalito Test Sites. Another pair of soundings, performed in close proximity to the first pair, was carried out using a B-180 drill rig (Rig. No. 55), a different rig than the one used at San Diego). Figure 61 shows a photograph of the two different rigs used at the Denver Site. The resulting uncorrected Becker blowcounts are presented in Figure 62. As may be observed, the AP-1000 rig gave uncorrected Becker blow-counts that were consistently 60 percent higher than those obtained with the

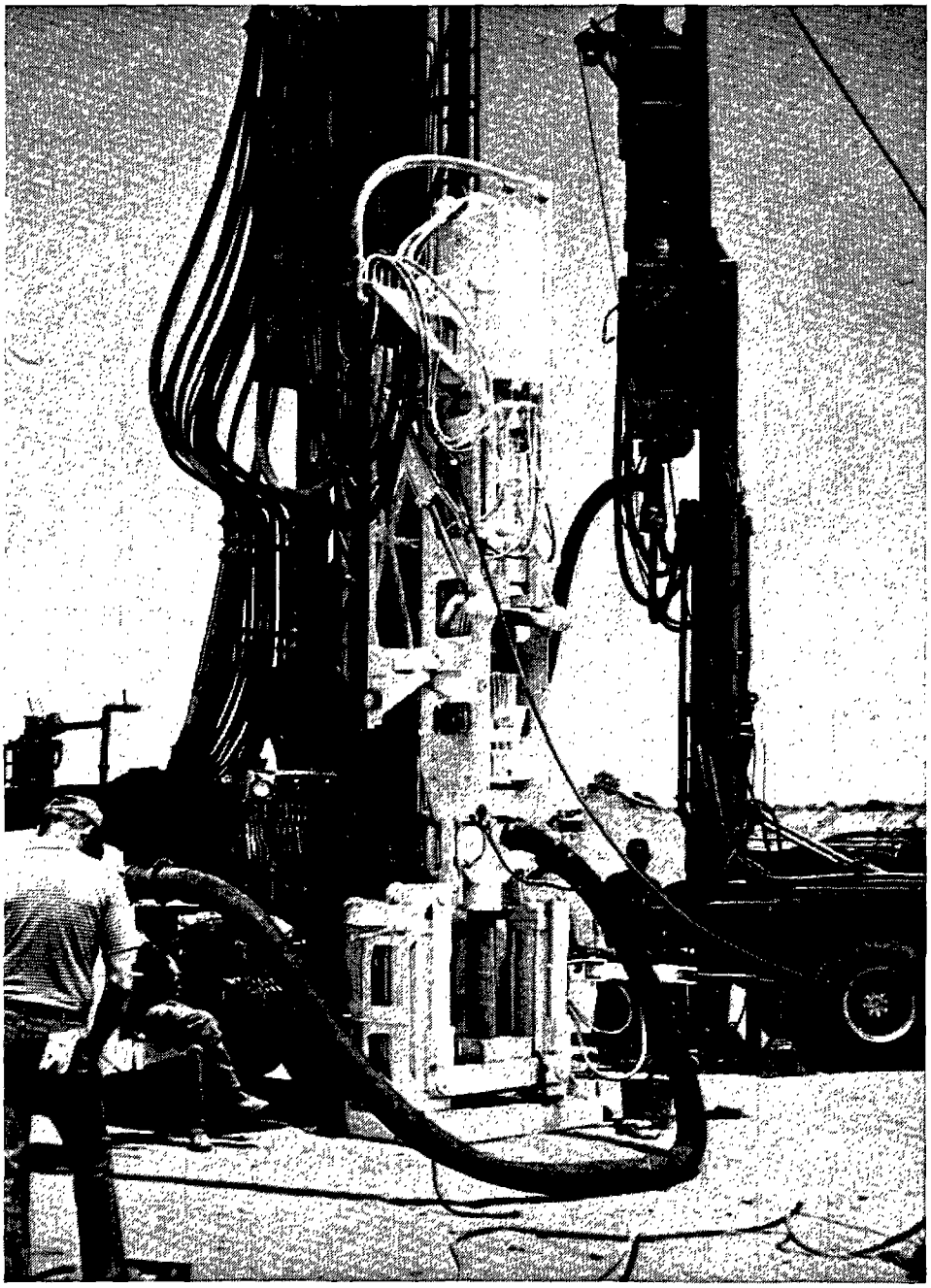

FIG. 61 PHOTOGRAPH ILLUSTRATING THE MORE COMPLICATED MAST OF THE AP-1000 DRILL RIG (LEFT) COMPARED TO THAT OF THE B-180 DRILL RIG (RIGHT)

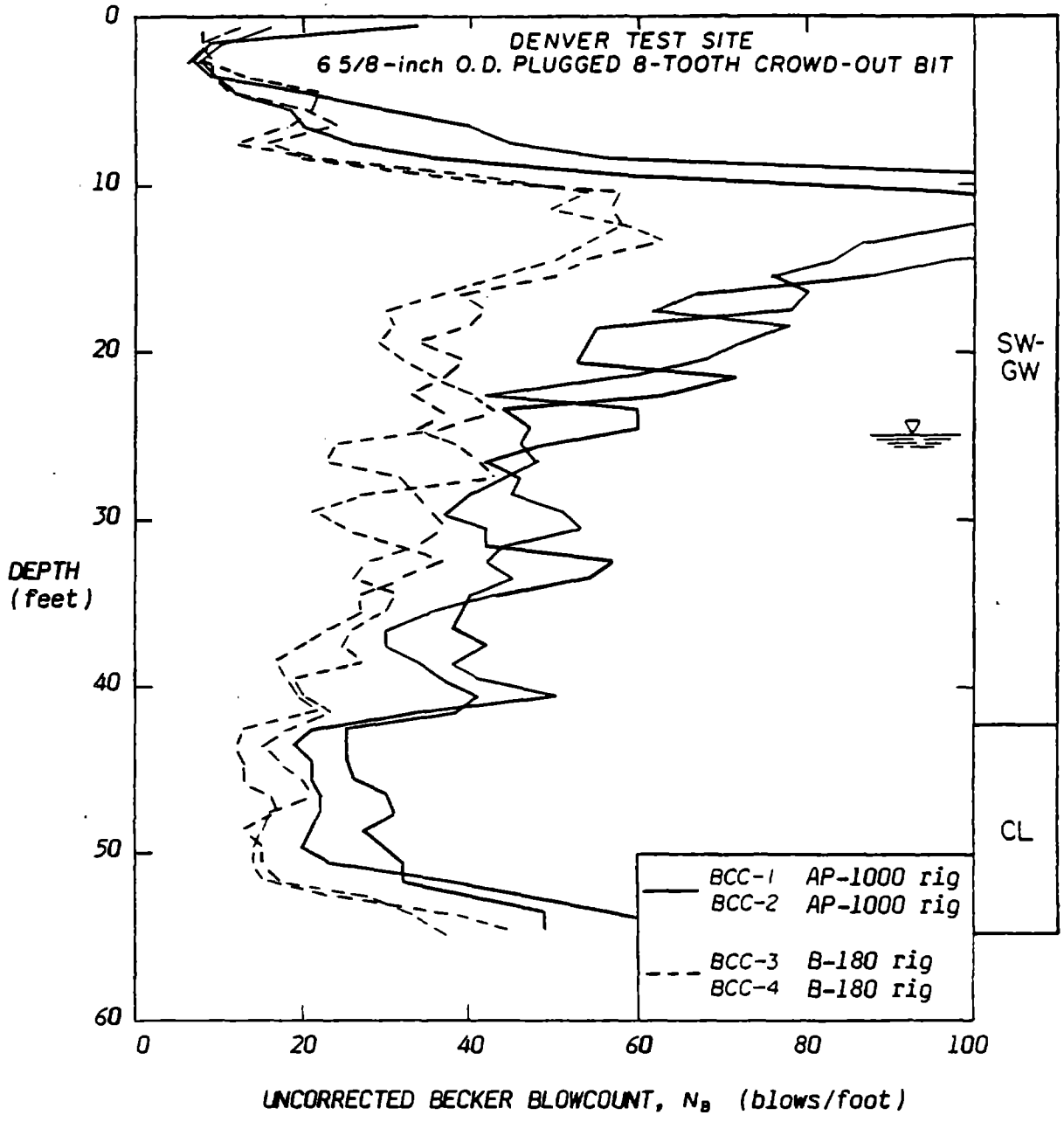

FIG. 62 COMPARISONS OF UNCORRECTED BECKER BLOWCOUNTS OBTAINED WITH DIFFERENT DRILL RIGS AT THE DENVER TEST SITE

B-180 rig. These results are similar in form to those obtained at the San Diego, Salinas, and Thermalito Test Sites described above.

Figure 62 indicates that the B-180 is roughly 60 percent more efficient in transmitting hammer energy than is the AP-1000 rig. However, the efficiency difference refers only to uncorrected blowcounts. An additional factor needs to be considered because the B-180, giving a lower blowcount, is operating at a lower bounce chamber pressure and, therefore with a lower energy (see previous discussion). This effect can be accounted for by correcting the bounce chamber pressures to sea level and using Figure 59 to obtain corrected Becker blowcounts, N_{BC}. After making these corrections, the data can be plotted in the form shown in Figure 63. In this figure, the mean corrected Becker blowcount values for each pair of soundings are plotted against each other for each foot of penetration between depths of 11 and 55 feet. Figure 63 shows that after correcting for hammer energies, the AP-1000 drill rig generally gives a blowcount about 50 percent higher than the B-180 drill rig.

The reason why the older B-180 drill rig is roughly 50 percent more efficient in transmitting hammer energy is not totally clear. Both the B-180 and the AP-1000 rigs employ the same type of diesel hammer. The only possibility that is readily apparent is that the more complicated cable and hydraulic ram arrangement on the AP-1000 rig prevents the hammer from following the casing during driving as well as the cable system on the B-180 rig. Figure 64 shows a photograph of the cable and hydraulic support system for the AP-1000 rig. It seems likely that this cable system is absorbing a significant portion of the hammer energy. Support for this theory comes from direct observation of the two rigs in action. During driving with the B-180 rig, there is relatively little bounce or oscillation of the hammer frame as the hammer

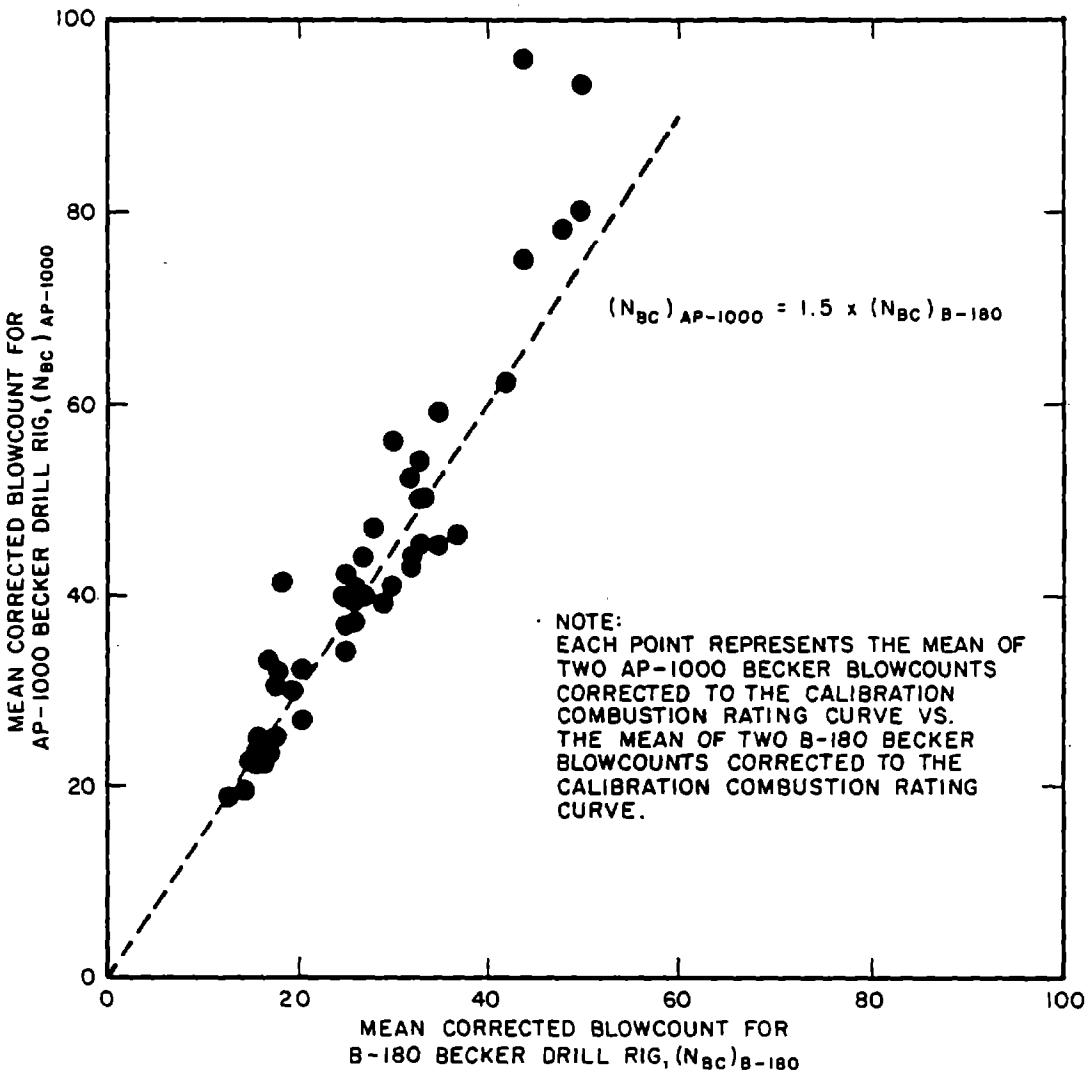

FIG. 63 EFFECT OF DRILL RIG ON CORRECTED BECKER BLOWCOUNT

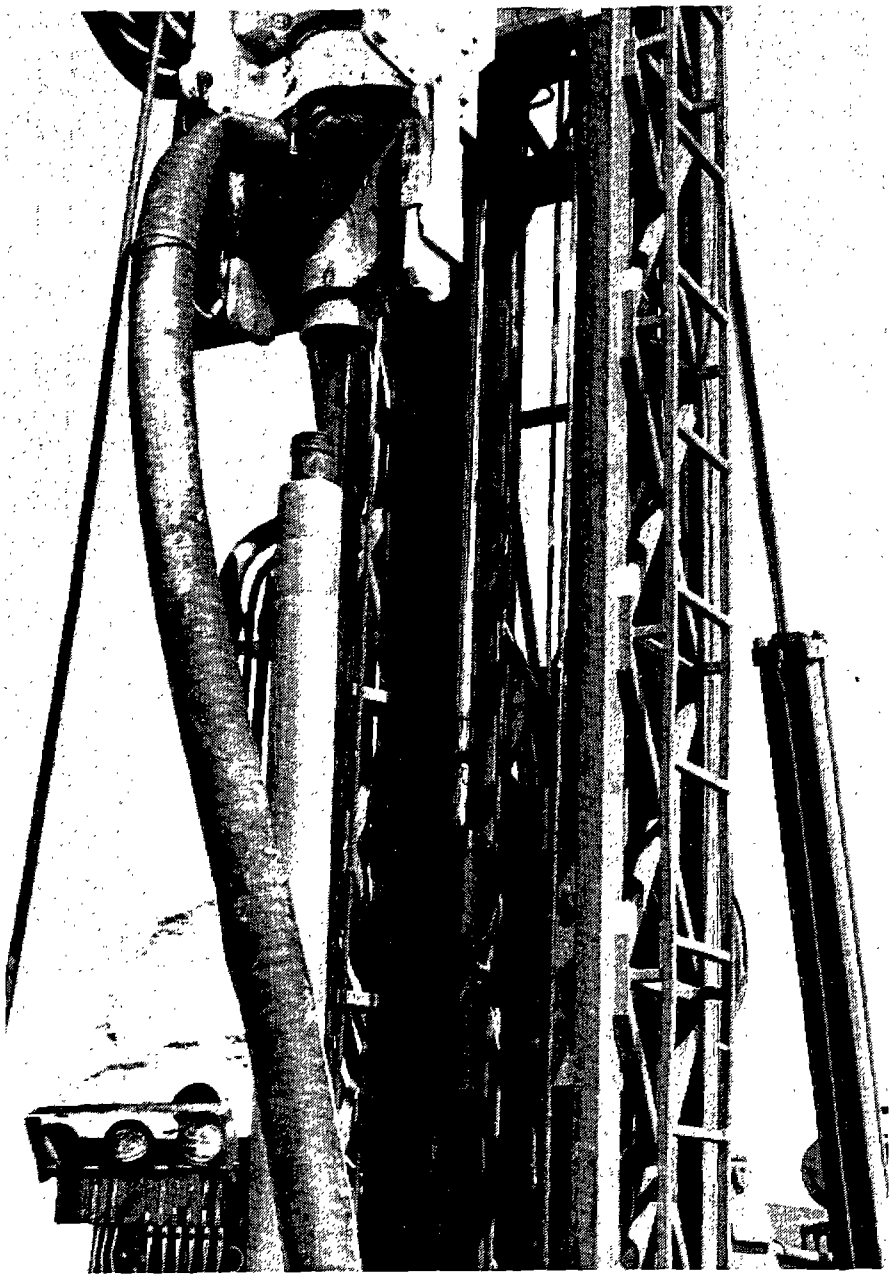

FIG. 64 PHOTOGRAPH SHOWING THE HYDRAULIC AND CABLE SUPPORT SYSTEM FOR THE DIESEL HAMMER ON THE AP-1000 DRILL RIG MAST

moves down the mast. However, during driving with the AP-1000 rig, the hammer frame bounces up and down on its cables, thus indicating that the cables are indeed absorbing some of the energy.

Effect of Casing Size on Becker Blowcount

As previously discussed, the Becker casings most widely used for penetration testing are available in two sizes. The casing used predominantly in Canada has a 5.5-inch O.D. whereas the casing used predominantly in the United States has a 6.6-inch O.D. To explore the effect of casing diameter, a pair of 6.6-inch plugged bit soundings were performed in the same proximity as were a pair of 5.5-inch plugged-bit soundings at the Denver Test Site. A comparison of the uncorrected Becker blowcounts obtained with the different bit sizes is presented in Figure 26. This figure indicates that a plugged 5.5-inch crowd-out bit gave a blowcount that was roughly 60 percent of that produced by a plugged 6.6-inch crowd-out bit. However, as with the data involving different drill rig types, the 60 percent ratio does not include the effect of differing bounce chamber pressures and energies. Because the smaller casing gives a lower blowcount, it is operating at a lower bounce chamber pressure and, therefore lower energy. As with the effect for different drill rig types, this difference can be accounted for by correcting the bounce chamber pressures to sea level and using Figure 59 to obtain corrected Becker blowcounts. After obtaining corrected Becker blowcounts, the data can be plotted in the form shown in Figure 65. In this figure, the mean values of corrected Becker blowcount for each pair of soundings are plotted against each other for each foot of penetration between depths of 11 and 55 feet. Figure 65 shows that after making the adjustment for different bounce chamber pressures, the 6.6-inch casing generally gives a blowcount about 3 times higher than the smaller 5.5-inch casing. This is a rather large

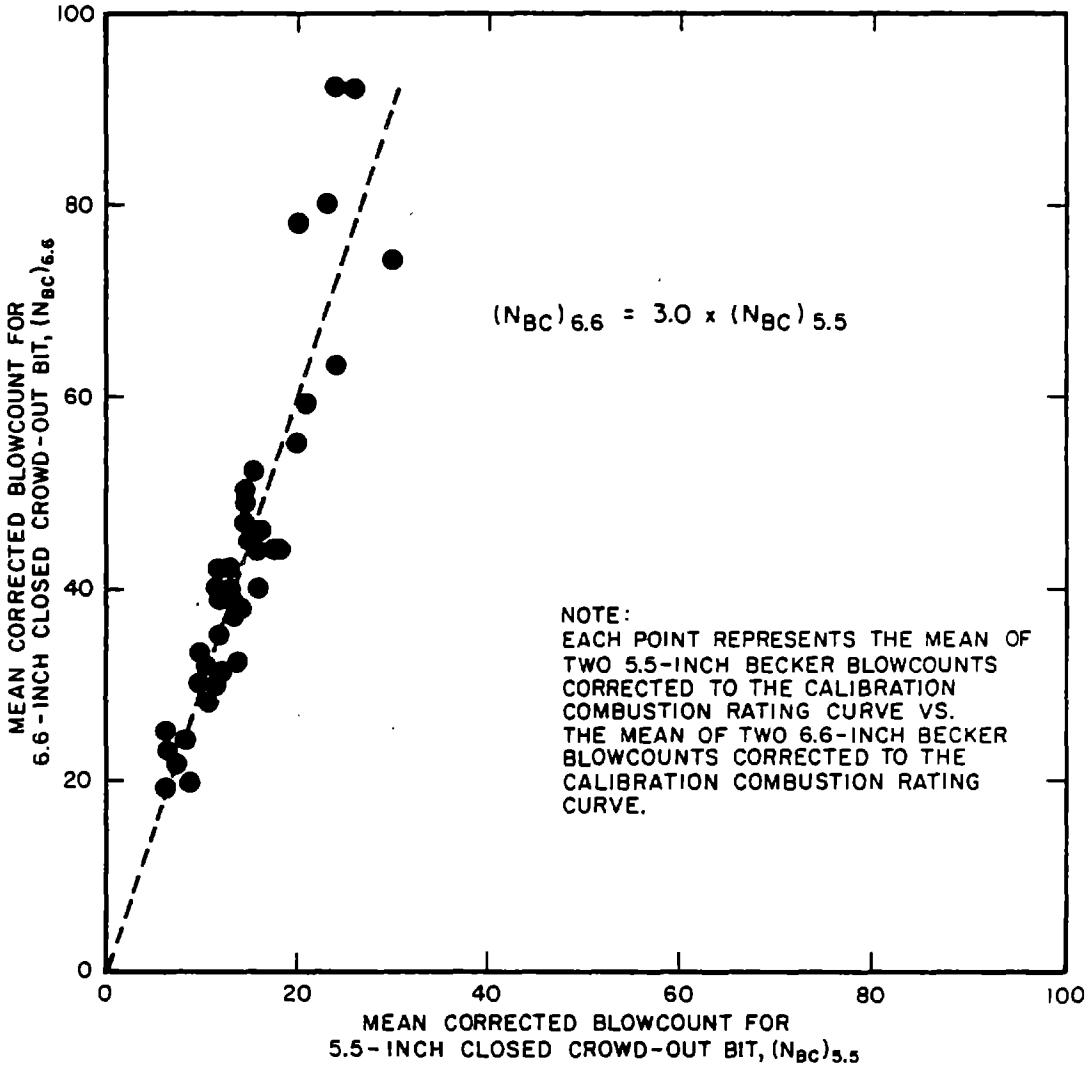

FIG. 65 EFFECT OF BIT DIAMETER ON CORRECTED BECKER BLOWCOUNT

correction, especially when the uncorrected results indicated only about a 60 percent increase. The large correction comes about because the bounce chamber pressures for the two sets of data were very different. This suggests that constant combustion rating curves are very different for different casing and bit sizes despite combustion conditions being the same.

Effect of Casing Friction on Becker Blowcount

Conventional methodologies for pile design involve the determination of resistances for both the bearing at the pile tip and for friction along the embedded length of the pile. Even for cohesionless soils, the resistance attributed to friction along the pile length is often calculated to be a significant proportion of the total supporting capacity of the pile. If these components of static pile capacity were applicable during driving, then the applicability of the Becker Penetration Test would be severely limited. Fortunately, it appears that friction along a pile shaft may well drop to minimum levels during driving, especially in looser sands and gravels (e.g. Terzaghi, 1943; Peck et al., 1974). Some recent support for this concept is also provided by test data reported by Mitchell (1985), who presented data on the static resistance of 6-inch diameter casings vibrated into deep sand deposits as well as the cone penetration resistance for the deposits. Comparisons show that the relationship between the total static casing resistance and the conventional cone penetration resistance (tip resistance) does not change significantly with depth, thus indicating that casing friction had minimal effects on the total casing resistance.

To examine the effect of casing friction on the Becker blowcounts, a special redriving test was performed at the Mackay Test Site. After completion of a 6.6-inch plugged-bit sounding, BCC-1, at a terminal depth of 43 feet, the casing was raised 5 feet up to the 38-foot depth level and redriven.

The original uncorrected blowcounts in this 5 ft depth range exceeded 200 blows per foot. However, as shown in Figure 66, the redriven blowcounts dropped to zero (i.e. the casing and hammer settled under its own weight) for a distance of more than 3 feet.

The above data would indicate that casing friction has only a minor effect on Becker penetration resistance. The reason for this behavior may be due to the disruption of the particle fabric during the undoubtedly severe straining around the bit during penetration. Studies by Mitchell et al. (1985) have shown that SPT and CPT resistance temporarily drops in sand after densification by blasting despite the fact that the sand has significantly increased in density. Another possibility may be that the gravel particles arch around the casing and that this effect reduces the normal stress on the casing. However, apparently low skin friction was also observed in the silty sands at the San Diego Test Site. As shown in Figure 20, the two open-bit soundings at this site developed relatively low and unrepresentative blowcounts below 30 feet. Sounding BOC-A actually developed blowcounts of zero below 33 feet. However, a zero blowcount would not be possible if skin friction were a significant factor because the casing must slide through the upper 30 feet of silty sand no matter what the resistance at the tip. The upper 30 feet consisted of sand of moderate density and there was no apparent heave of soil into the bit through this interval. Despite going through this material, the results from BOC-A indicate that the effect of casing friction was very small.

It should not be concluded, however, that the friction on the casing is zero just because there is a zero blowcount. It is important to note that the diesel hammer weighs over 4500 pounds and that each 10-foot length of casing weighs an additional 500 pounds. Nevertheless, the basic conclusion from the

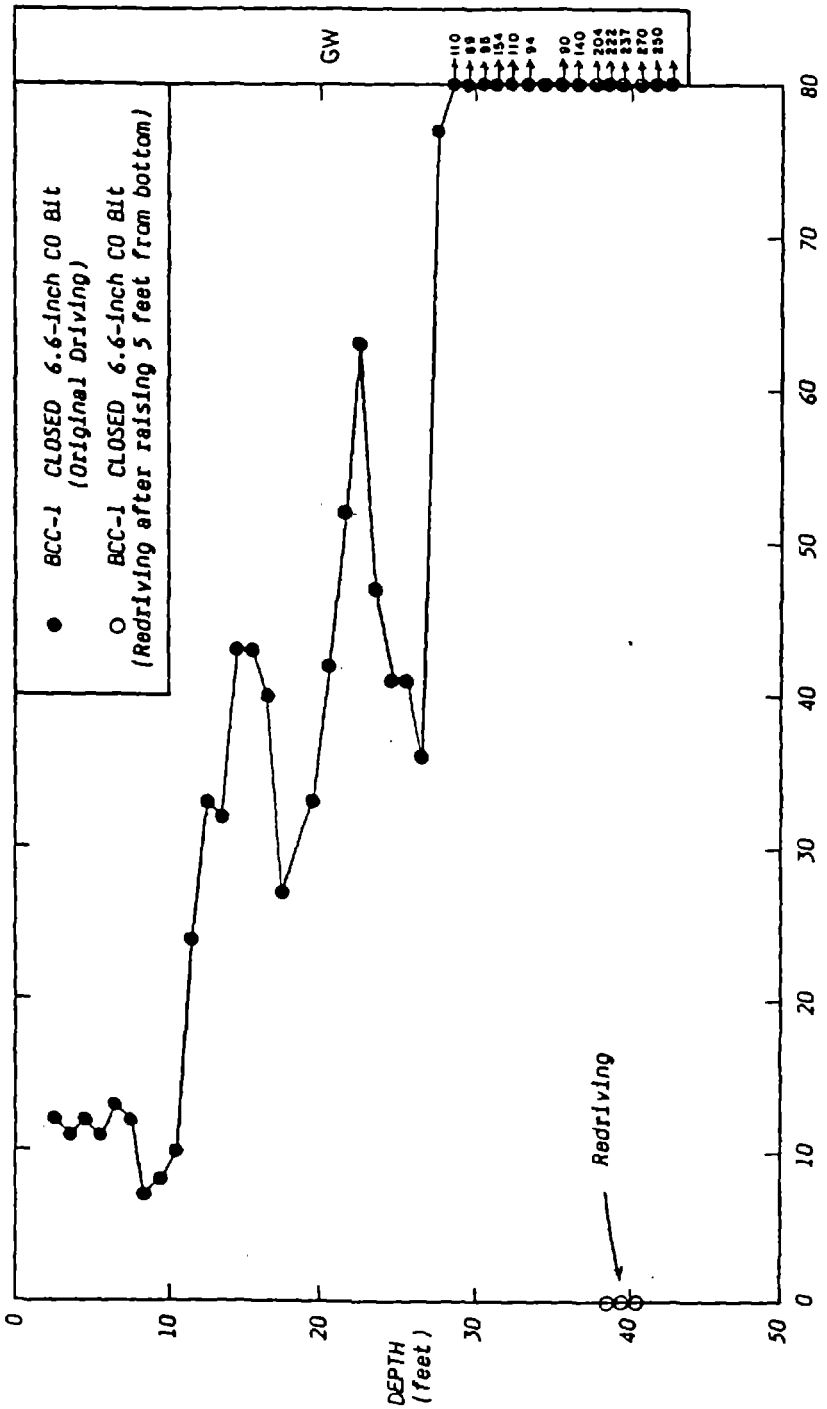

FIG. 66 UNCORRECTED BECKER BLOWCOUNTS FROM INITIAL AND REDRIVING TEST AT MACKAY TEST SITE

above data is that, at least for cohesionless soils, casing friction has a minimal effect on the Becker blowcount values.

Chapter 4

DEVELOPMENT OF A CORRELATION BETWEEN BECKER AND SPT BLOWCOUNTS

In the preceding chapter, it has been shown how different drilling procedures and equipment can affect the Becker blowcounts. As summarized in Table 5, the Becker blowcount can be changed significantly depending on how the test is performed. This does not mean, however, that the test cannot give meaningful results. Rather, it indicates the need to perform the test carefully in a manner which will eliminate most of the potential variability. Table 6 lists the equipment and procedure recommended for obtaining standard values of corrected Becker blowcounts.

The principal purpose of performing all the investigations concerning the Becker Penetration Test was to obtain a useful correlation between Becker blowcounts and SPT blowcounts in soils where both tests give meaningful results. As described previously, the sites where good quality SPT tests existed in sands and silts were the Salinas, Thermalito, and San Diego Test Sites. The development of the desired correlation between SPT N-values and Becker blowcount values at these sites involved three steps:

1. At each of the three sites, the uncorrected SPT blowcounts were corrected to N_{60} blowcounts. The correction factors used to perform this test were described previously.
2. The second step consisted of correcting the uncorrected Becker blowcounts to N_{BC} blowcounts. The procedure to perform this task is outlined in Table 6. (Note: Both N_{60} and N_{BC} data obtained at less than 10-foot depths were multiplied by a correction factor of 0.75 to account for energy losses in the short length of drill rods or casing.

Table 5: Influences of Procedures and Equipment on Becker Blowcounts

VARIABLE	INFLUENCE	INVESTIGATION
I. DRILL RIG		
A. AP-1000 (new style)	$(N_{BC})_{AP\text{-}1000} = 1.5 \times (N_{BC})_{B\text{-}180}$	1. San Diego Test Site
B. B-180 (old style)		2. Denver Test Site
II. BLOWER OR SUPERCHARGER	$(N_B)_{blower} = (0.4 \text{ to } 0.8) \times (N_B)_{no\ blower}$	1. Denver Test Site
		2. Mackay Test Site
		3. Salinas Test Site
III. THROTTLE SETTING	Infinitely variable	1. Mackay Test Site
		2. Salinas Test Site
IV. CASING DIAMETER		
A. 5.5-inch O.D.	$(N_{BC})_{6.6} = 3.0 \times (N_{BC})_{5.5}$	1. Denver Test Site
B. 6.6-inch O.D.		
V. BIT PLUG		
A. Plugged Crowd-out bit	Anywhere between 0 and infinity	1. San Diego, Salinas, & Thermalito Test Sites
B. Open Crowd-out bit	(depends upon soil type)	2. Denver Test Site
		3. Mackay Test Site

Table 6: Recommended Procedure for Obtaining Becker Blowcounts

EQUIPMENT

Drill Rig: AP-1000

Diesel Pile Hammer: ICE 180

Throttle Setting: Full throttle with blower on

Casing Diameter: 6.6-inch O.D.

Drill Bit: Closed 6.6-inch O.D., 8-tooth Crowd-out

PROCEDURE

1. *Measure Becker blowcounts and bounce pressures.*
2. *Correct bounce pressures measured at high elevations to equivalent bounce pressures at sea level.*
3. *Use corrected bounce pressure and Becker blowcount together with calibration chart (Figure 59) to obtain the corrected Becker blowcount, N_{BC}.*

and, tentatively,

4. *If Becker blowcounts were obtained using a B-180 Drill rig, first use Figure 59 to obtain corrected Becker blowcounts, N_{BC}. Then multiply the corrected blowcounts by 1.5 to obtain equivalent AP-1000 rig corrected Becker blowcounts.*
5. *If Becker blowcounts were obtained using the 5.5-inch O.D. casing, first use Figure 59 to obtain corrected Becker blowcounts, N_{BC}. Then multiply the corrected blowcounts by 3.0 to obtain equivalent 6.6-inch O.D. corrected Becker blowcounts.*

3. The final step consisted of averaging both sets of corrected data across depth intervals varying between 1 and 7 feet. The selection of each interval size was based on the uniformity of blowcount data along the depth profile at each site.

The results of the development process for the Becker-SPT correlation are summarized in Table 7 and plotted in Figure 67. Although there is some scatter, the amount of scatter is significantly less than that found in previous correlations. In addition, the data from the different sites agree relatively well with each other.

The correlation curve shown in Figure 67 is based on a judged best fit of the data. The trend of the curve suggests a roughly 1:1 ratio for corrected blowcounts of less than about 20. This is consistent with some of the previous correlations shown previously in Figure 10. However, for corrected SPT blowcounts above about 20, the correlation curve bends downward. This later trend is significantly different from that indicated by most of the previous correlations. Since the new correlation is the only one which incorporates procedures and corrections to reduce the potentially large variability of the Becker Penetration Test procedures, it seems reasonable to conclude that it is a distinct improvement over those presented previously and can be used with a good degree of confidence for evaluating the engineering properties of coarse-grained cohesionless soils.

Table 7: Summary of Data Used to Develop Corrected Becker-SPT Blowcount Correlation

Site	Depth (feet)	Corrected Becker Blowcount, N_{BC} Range	Mean	Corrected SPT Blowcount, N_{60} Range	Mean	Soil Type
	4 - 6	2.5 - 3.5	3.	3. - 4.5	3.5	ML
	7 - 9	3. - 4.5	3.5	3. - 4.5	3.5	ML
	10 - 12	3.5 - 8.	5.5	1.5 - 7.5	5.	ML
	13 - 15	4.5 - 8.	6.5	7.5 - 7.5	6.5	ML
	16 - 18	6. - 13.	8.	7.5 - 16.	11.5	SM
SALINAS, CA	19 - 21	9. - 16.	12.	11. - 13.5	12.	SP-SM
	22 - 24	9.5 - 23.	15.5	7.5 - 13.5	11.5	SP-SM
	25 - 27	9.5 - 26.	18.	6.5 - 17.5	12.5	SP-SM
	28 - 30	14. - 26.	20.5	12. - 15.	14.	SP-SM
	31 - 33	18. - 29.	22.5	13.5 - 20.	18.	SP-SM
	34 - 37	13.5 - 23.	19.5	13.5 - 21.5	17.5	SP-SM
	11 - 12	19. - 28.	23.5	9. - 54.5	26.5	SP-SM
	14 - 16	13. - 36.	26.	15.5 - 28.5	22.	SP-SM
	18 - 19	18. - 30.	25.5	14.5 - 38.5	24.5	SP-SM
THERMALITO, CA	21 - 23	25. - 36.	30.5	17. - 28.5	22.	SP-SM
	25 - 26	30. - 37.	34.5	20. - 38.5	25.	SP-SM
	28 - 29	43. - 56.	50.	24.5 - 70.	36.5	SP-SM
	3 - 5	7.5 - 9.5	8.	18.5 - 19.5	19.	SP-SM
	6 - 7	8.5 - 8.5	8.5	11. - 15.5	13.	SP-SM
	8 - 11	9.5 - 11.	10.	11. - 12.5	11.5	SM
	12	8.5	8.5	7.5	7.5	SM
	13 - 14	8. - 8.5	8.5	1. - 1.	1.	SM
SAN DIEGO, CA	15 - 19	13. - 13.5	13.	17.5 - 25.	20.	SM
	20 - 25	12. - 26.5	18.	24.5 - 28.5	26.5	SM
	26 - 31	48. - 66.5	57.	36.5 - 42.5	39.5	SM
	32 - 38	59. - 90.	72.5	39.5 - 57.5	50.5	SM
	39 - 44	76. - 96.	82.5	50. - 93.	72.	SM
	45 - 49	74.5 -108.5	102.	64. -103.5	74.5	SM

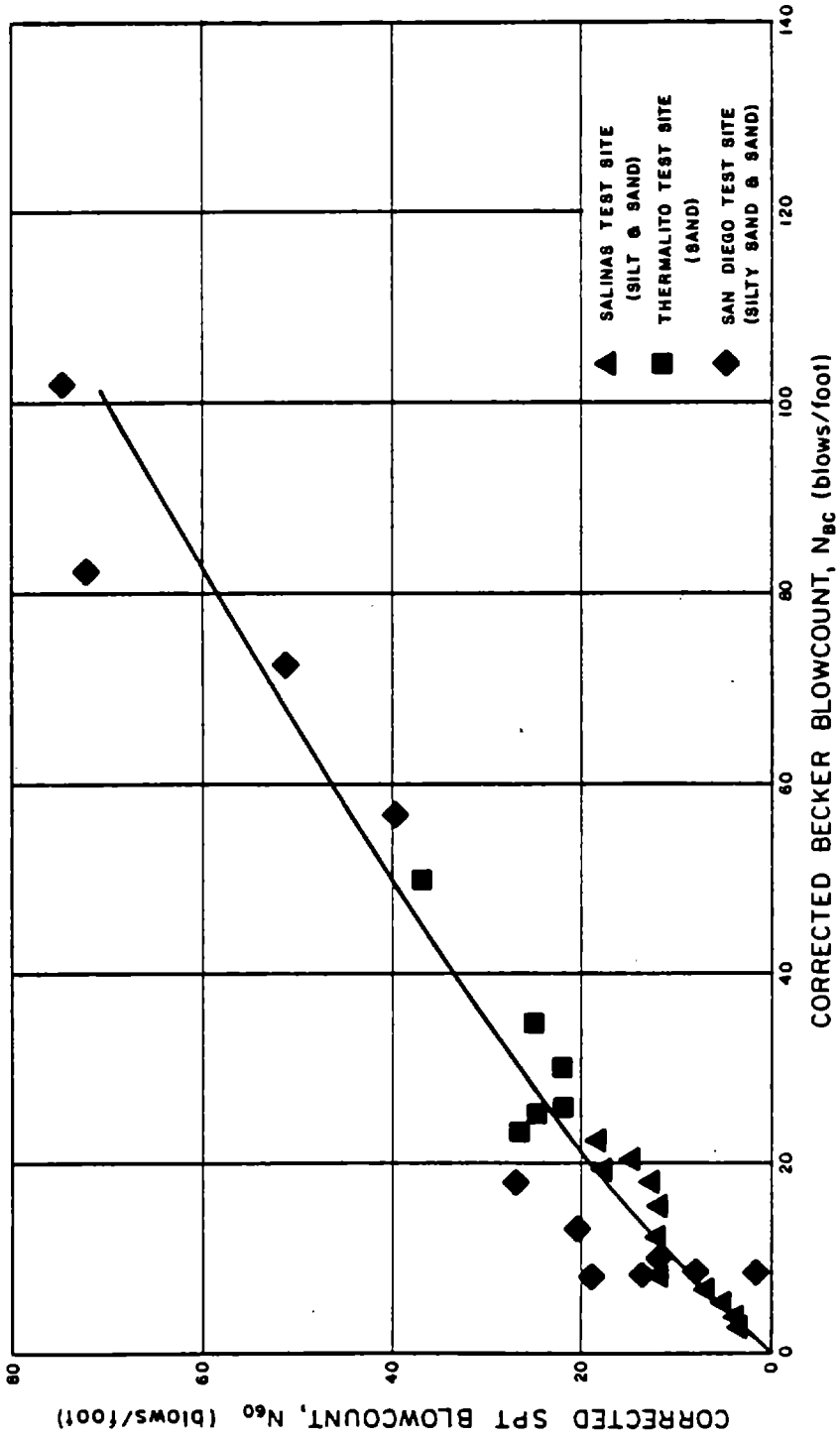

FIG. 67 CORRELATION BETWEEN CORRECTED BECKER AND SPT BLOWCOUNTS

REFERENCES

1. Andrus, R. D., Youd, T. L., and Carter, R. R. (1986), "Geotechnical Evaluation of a Liquefaction Induced Lateral Spread, Thousand Springs Valley Idaho", Proceedings of the Twenty-Second Annual Symposium on Engineering Geology and Soils Engineering, Boise, ID, February 24-26, 1984.

2. Becker Drills, Inc., Literature and file data, Denver, Colorado.

3. California Department of Water Resources (1983), "Thermalito Afterbay Dam Seismic Evaluation," Final Draft Report and supplemental file data.

4. Coulter, H. W. and Migliaccio, R. R. (1966), "Effects of the Earthquake of March 27, 1964 at Valdez, Alaska," U. S. Geological Survey Professional Paper 542-C, U. S. Department of the Interior.

5. Decker, M. D., Holtz, R. D. and Kovacs, W. D., "Energy Transfer of SPT Hammers," in preparation.

6. Ertec Western, Inc. (1981) "Evaluation of the Cone Penetrometer for Liquefaction Hazard Assessment," Report to the U.S. Geological Survey.

7. Ertec Western, Inc. (1984), "Cone Penetrometer Test: Pore Pressure Measurements and SPT Hammer Energy Calibration for Liquefaction Hazard Assessment," Report to the U.S. Geological Survey.

8. Fuller, Frank M. (1983), Engineering of Pile Installations, McGraw-Hill, Inc., New York.

9. Geotechnical Consultants, Inc. (1981), "Geotechnical Evaluation of Alluvium, Santa Felicia Dam, Ventura County, California," Report to the United Water Conservation District, October.

10. Geotechnical Consultants, Inc. (1983), "Geotechnical Investigation for Vern Freeman Diversion Structure, Santa Clara River near Saticoy, Ventura County, California," Report to the United Water Conservation District, November.

11. Harder, Jr., Leslie F. (1986), "Use of Penetration Tests to Determine the Liquefaction Potential of Soils During Earthquake Shaking," Dissertation submitted in partial fulfillment for Doctor of Philosophy Degree, University of California, Berkeley, (In preparation).

12. Harder, Jr., Leslie F. (1986), "Evaluation of Becker Penetration Tests Performed at the Mormon Island Dike, Folsom Dam," Report prepared for the Waterways Experiment Station, U.S. Army Corps of Engineers (In preparation).

13. International Construction Equipment, Inc., Calibration charts for diesel hammer energies.

14. Ishihara, Kenji (1985), "Stability of Natural Deposits During Earthquakes," Proceedings of the Eleventh International Conference on Soil Mechanics and Foundation Engineering, San Francisco, California, 1985.

15. Jones, Walter V. and Christensen, Curt (1982), "Performance of Heavily-Loaded Shallow Foundations Supported on Gravels," Paper presented at the 1982 ASCE National Convention, New Orleans, Louisiana, October 25-29, 1982.

16. Last, Tony (1985), International Construction Equipment, Inc., Personal communication.

17. Liang, Nancy (1983), "An Examination of the Standard Penetration Test with Comparisons to Other In Situ Tests," Senior Thesis, University of British Columbia, April.

18. Mitchell, James K. (1986), "Practical Problems From Surprising Soil Behavior," The Twentieth Karl Terzaghi Lecture, Journal of the Geotechnical Engineering Division, ASCE, Vol. 112, No. 3, March.

19. Northern Engineering and Testing, Inc., File data for Job Nos. 68-16, 68-17, 68-19, and 68-204.

20. Peck, Ralph, Hanson, W. E., and Thornburn, T. H. (1974), Foundation Engineering, Second Edition, Wiley, New York.

21. Rempe, D. M. and Davisson, M. T. (1977), "Performance of Diesel Pile Hammers," Proceedings of the Ninth International Conference of Soil Mechanics and Foundation Engineering, Tokyo, Japan, 1977.

22. Seed, H. Bolton, Tokimatsu, K., Harder, L. F., and Chung, Riley M. (1985), "Influence of SPT Procedures in Soil Liquefaction Resistance Evaluations," Journal of the Geotechnical Engineering Division, ASCE, Vol. 111, No. 12, December.

23. Sergent, Hauskings and Beckwith (1973), "An Investigation of the Load Carrying Capacity of Drilled Cast-In-Place Concrete Piles Bearing On Coarse Granular Soils and Cemented Alluvial Fan Deposits," Report to the Arizona Highway Department, Phoenix, Arizona.

24. Terzaghi, K. (1943), Theoretical Soil Mechanics, John Wiley and Sons, New York.

25. Wang, Wenshao (1984), "Earthquake Damages to Earth Dams and Levees in Relation to Soil Liquefaction," Proceedings of the International Conference on Case Histories in Geotechnical Engineering, 1984.

26. Youd, T. L., Harp, E. L., Keefer, D. K., and Wilson, R. C. (1985), "The Borah Peak, Idaho Earthquake of October 28, 1983--liquefaction," Earthquake Spectra, Earthquake Engineering Research Institute, Vol. 2, No. 1, November.

APPENDIX

DERIVATIONS OF RELATIONSHIPS BETWEEN DIESEL HAMMER ENERGY AND BOUNCE CHAMBER PRESSURE

General

This appendix presents the derivations of potential energy stored in the bounce chamber, total potential energy, and kinetic energy of ram impact. The derived energies are correlated to the peak pressure measured in the bounce chamber and are based on the laws of thermodynamics. The derived equations for potential energies were used by International Construction Equipment, Inc. (ICE) to produce the energy correlation charts shown in Figure 29b. Details of the derivations were provided by Tony Last, ICE representative.

Derivation of Potential Energy Stored in Bounce Chamber

A diesel pile hammer is basically a single cylinder diesel engine. For the ICE Model 180, the top of the cylinder is closed off and, during the upward travel of the ram, air is trapped above the ram in the upper half of the cylinder (compression cylinder) and in an adjoining bounce chamber. This trapped air is compressed by the ram and acts as a spring on the ram. Much of the potential energy of the ram comes from the stroke energy (ram weight times stroke distance). However, the trapped air above the ram also provides a substantial portion of the potential energy.

To calculate the potential energy stored in the compressed air above the ram, the following gas law for polytropic expansion and compression was used:

$$PV^n = \text{constant} \qquad \text{(A.1)}$$

where P = absolute pressure

V = volume

n = exponent

Shown in Figure A.1 is a curve which represents the application of this pressure-volume relationship during the upstroke of the ram. Just as the ram closes the atmospheric ports of the compression cylinder on its upstroke, the initial absolute pressure, P_1, is equal to atmospheric pressure. The volume of air above the ram in the compression cylinder and bounce chamber at atmospheric port closure is denoted as V_1. For the ICE Model 180 hammer, this volume is equal to 6773 cubic inches. As the ram continues upward, the volume of air is compressed and the pressure is increased. At the top of the stroke, the trapped volume reaches a minimum value of V_2 and the compressed air pressure reaches a maximum value of P_2. Using appropriate fittings and a gage, this peak pressure, P_2, can be monitored during driving and is denoted as the bounce chamber pressure.

During the downstroke of the ram, potential energy in the trapped air performs work on the ram by expanding back along the curve shown in Figure A.1 until the initial conditions are restored. The increment of work is represented by:

$$\text{Increment of work} = F \cdot ds = P \cdot A \cdot ds = P \cdot dv \qquad (A.2)$$

where F = Force acting on ram

A = Ram area

P = Pressure acting on ram

dS = Increment of ram travel along the cylinder

dV = Increment of volume change in the cylinder

The total gross work performed on the ram by the expansion of the trapped air, ignoring mechanical friction, then becomes:

$$\text{Total gross work, } E_G = \int_{V_2}^{V_1} P \cdot dV \qquad (A.3)$$

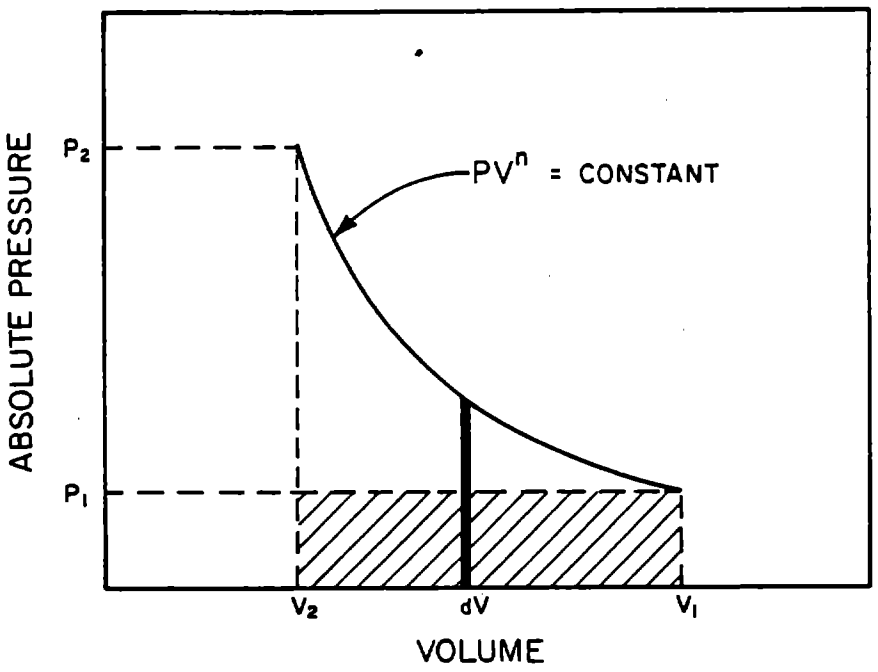

P_1 = *Initial absolute pressure above ram in compression cylinder and bounce chamber before ram begins its upstroke.*
= *absolute atmospheric pressure.*

P_2 = *Peak absolute pressure above ram in compression cylinder and bounce chamber at top of ram stroke. Measured by pressure gage.*

V_1 = *Total trapped air volume above ram in compression cylinder and bounce chamber at atmospheric vent closure.*
= *6773 cu. in. for ICE Model 180 diesel hammer.*

V_2 = *Volume of compressed air above ram in compression cylinder and bounce chamber at top of ram stroke.*

n = *Exponent = 1.4 for adiabatic conditions.*

FIG. A.1 PRESSURE-VOLUME RELATIONSHIP USED FOR DERIVING POTENTIAL ENERGY STORED IN BOUNCE CHAMBER

This total gross work is equivalent to the area beneath the curve shown in Figure A.1. To solve the above equation, it should be noted, from Equation A.1, that PV^n = constant and therefore:

$$PV^n = \text{constant} = P_1V_1{}^n$$

and

$$P = \frac{P_1V_1{}^n}{V^n}$$

Thus

$$E_G = \int_{V_2}^{V_1} P \cdot dV = \int_{V_2}^{V_1} \frac{P_1V_1{}^n}{V^n}\, dV = P_1V_1{}^n \int_{V_2}^{V_1} V^{-n}\, dV$$

$$= P_1V_1{}^n \left[\frac{V^{1-n}}{1-n}\right]_{V_2}^{V_1} = P_1V_1{}^n \left(\frac{V_1{}^{1-n}}{1-n}\right) - P_1V_1{}^n \left(\frac{V_2{}^{1-n}}{1-n}\right)$$

$$= \frac{P_1V_1}{1-n} - \frac{P_2V_2{}^nV_2{}^{1-n}}{1-n}$$

$$= \frac{P_1V_1 - P_2V_2}{1-n} \qquad (A.4)$$

To obtain the useful work, E_{BC}, stored in the compression cylinder and bounce chamber, one must subtract the work performed by the atmosphere on the ram, E_A. This work is represented by the cross-hatched area shown in Figure A.1 and equals $P_1(V_1 - V_2)$.

Thus, the useful work that is stored in the compression cylinder and bounce chamber becomes:

$$E_{BC} = E_G - E_A = \frac{P_1V_1 - P_2V_2}{1-n} - P_1(V_1 - V_2) \qquad (A.5)$$

In this equation, parameters P_1 and V_1 are known quantities before the test and P_2 is simply the pressure measured in the bounce chamber. The parameter, V_2, is calculated using equation A.1:

$$P_2V_2^n = \text{constant} = P_1V_1^n$$

$$V_2 = \sqrt[n]{\frac{P_1V_1^n}{P_2}} \tag{A.6}$$

The value of the exponent, n, is equal to 1.4 for the adiabatic (no heat transfer) compression and expansion of air. Although the action within the compression cylinder is not strictly adiabatic because of the potential for heat transfer between the air and the metallic surfaces of the cylinder and ram, the cycle is so rapid that little time exists for heat transfer and the process approaches adiabatic conditions. Thus, for volumes expressed in cubic inches, pressures in psia, and energy expressed in ft-lb., equation A.5 becomes:

$$E_{BC} = \frac{P_1V_1 - P_2V_2}{12(1 - 1.4)} - \frac{P_1(V_1 - V_2)}{12}$$

$$= \frac{P_2V_2 - P_1V_1}{4.8} - \frac{P_1(V_1 - V_2)}{12} \tag{A.7}$$

Calculation of Total Potential Energy

As previously described, the total potential energy is composed of (1) the energy stored in the air compressed above the ram, E_{BC}, and (2) the stroke energy, E_{WH}, of the ram. To obtain the stroke energy, it is necessary to determine the product of the weight of the ram and the maximum upward travel or stroke of the ram. For the ICE Model 180, the ram weighs 1724 pounds. To determine the stroke of the ram, the volume change of the air trapped above the ram is simply divided by the area of the ram. For the ICE Model 180, the area of the ram is 95.0 square inches. Thus:

$$\text{Compression Cylinder Ram Stroke} = \frac{\text{Volume Change of Trapped Air}}{\text{Ram Area}}$$

$$= \frac{V_1 - V_2 \text{ cu. in.}}{95.0 \text{ sq. in.}} \tag{A.8}$$

Because the ram does not close off the atmospheric ports in the upper cylinder until after 1 inch of upward travel after striking the anvil, the total ram stroke equals the stroke calculated from the compression cylinder volume change plus 1 inch. Thus:

$$\text{Total Ram Stroke, } H = \frac{(V_1 - V_2) \text{ cu. in.}}{95.0 \text{ sq. in.}} + 1 \text{ inch} \qquad (A.9)$$

The stroke energy of the ram then becomes:

$$E_{WH} = W\,H = \frac{1724 \text{ lb.}}{12} \cdot \left[\frac{(V_1 - V_2) \text{ cu. in.}}{95.0 \text{ sq. in.}} + 1 \text{ inch} \right] \text{ft.-lb.} \qquad (A.10)$$

The total potential energy values calculated by ICE for their energy vs. bounce chamber curves (Figure 29b) are the sum of E_{BC} and E_{WH}. To demonstrate the use of the above equations, an example is shown in Figure A.2 for the case where an ICE Model 180 hammer is operating at sea level and a bounce pressure reading of 20 psig is recorded. For such a case the total potential energy of the ram, E_{PE}, is 6804 ft-lb.

Impact Kinetic Energy

The above calculations show how the total potential energy of the ram is determined. However, not all of this potential energy is converted into the kinetic energy of the falling ram. As the ram falls towards the anvil and compresses the fuel-air mixture in the combustion chamber, some of the potential energy is lost as a result of the work required to compress the fuel-air mixture. The magnitude of this lost work can be calculated using equation A.7:

$$\text{Work Done in Compression} = E_C = \frac{P_2V_2 - P_1V_1}{4.8} - \frac{P_1(V_1 - V_2)}{12}$$

EXAMPLE: ICE Model 180 Diesel Pile Hammer Operating at Sea Level

Bounce Chamber Pressure = 20 psig

P_1 = 14.7 psia

V_1 = 6773 cu. in.

P_2 = 20 psig + 14.7 psi = 34.7 psia

Equation A.6 $V_2 = 1.4\sqrt{\frac{P_1V_1}{P_2}^{1.4}} = 1.4\sqrt{\frac{(14.7)(6773)}{34.7}^{1.4}} = \underline{3667 \text{ cu. in.}}$

Potential Energy Stored in Bounce Chamber:

Equation A.7 $E_{BC} = \frac{(P_2V_2 - P_1V_1)}{4.8} - \frac{P_1(V_1 - V_2)}{12}$

$E_{BC} = \frac{34.7(3667) - 14.7(6773)}{4.8} - \frac{14.7(6773 - 3667)}{12} = \underline{1962 \text{ ft.-lb.}}$

Maximum Stroke of Ram:

Equation A.9 $H = \frac{V_1 - V_2}{\text{Ram Area}} + 1 \text{ inch} = \frac{(6773 - 3667)\text{cu. in.}}{95.0 \text{ sq. in.}} + 1 \text{ inch} = \underline{33.7 \text{ in.}}$

Potential Stroke of Ram:

Equation A.10 $E_{WH} = W \times H = 1724 \text{ lb} \cdot 33.7 \text{ in./12 in./ft.} = \underline{4842 \text{ ft.-lb.}}$

Total Potential Energy of Ram

Total Potential Energy = Bounce Chamber Potential Energy + Ram Stroke Potential Energy

$E_{PE} = E_{BC} + E_{WH}$

E_{PE} = 1962 + 4842 ft. lb.

$E_{PE} = \underline{6804 \text{ ft. lb.}}$

FIG. A.2 EXAMPLE CALCULATION OF POTENTIAL ENERGY OF DIESEL PILE HAMMER RAM

where P_1 = Absolute atmospheric pressure (psia)

V_1 = Volume of air trapped beneath the ram after the ram closes the intake and exhaust ports in the lower cylinder (for ICE Model 180, V_1 = 777 cu. in.)

V_2 = Volume of air trapped in the combustion chamber as the ram strikes the anvil (for ICE Model 180, V_2 = 51.0 cu. in.)

P_2 = Absolute compression pressure = $P_1\left(\frac{V_1}{V_2}\right)^{1.4}$

For sea level conditions:

$$P_2 = 14.7 \text{ psia}\left(\frac{777}{51}\right)^{1.4} = 666 \text{ psia}$$

Thus:

$$E_C = \frac{P_2V_2 - P_1V_1}{4.8} - \frac{P_1(V_1 - V_2)}{12}$$

$$= \frac{(666)(51) - 14.7(777)}{4.8} - \frac{14.7(777 - 51)}{12}$$

$$= 3807 \text{ ft-lb.}$$

This work performed in the compression of the fuel-air mixture is energy lost from the total potential energy of the ram. Thus the amount of energy available as kinetic energy at ram impact is significantly reduced. It should be noted that this compression energy loss is a constant regardless of the bounce chamber pressure and depends only on the atmospheric pressure. Thus, the proportion of the potential energy available as kinetic energy is greatly reduced as the bounce chamber pressures, and therefore the potential energies, become lower. For example, a bounce chamber pressure of 20 psig recorded at sea level yields a total potential energy of 6804 ft-lb. By subtracting the compression energy loss (3807 ft-lb.), the impact kinetic energy becomes 2994 ft-lb. However, a bounce chamber pressure of 15 psig recorded at sea level

yields a total potential energy of about 5530 ft-lb. and an impact kinetic energy of about 1720 ft-lb. In general:

Impact Kinetic Energy = Total Potential Energy - Compression Loss

or

$$E_{IKE} = E_{PE} - E_C$$

Thus:

for $(BP)_{SL}$ = 20 psig, Impact Kinetic Energy = 6804 - 3907 = 2997 ft-lb

for $(BP)_{SL}$ = 15 psig, Impact Kinetic Energy = 5530 - 3807 = 1723 ft-lb

Thus the Impact Kinetic Energy is significantly less than the Potential Energy and this difference must be considered in evaluating the effective energy determining the penetration resistance of the casing.

EARTHQUAKE ENGINEERING RESEARCH CENTER REPORTS

NOTE: Numbers in parentheses are Accession Numbers assigned by the National Technical Information Service; these are followed by a price code. Copies of the reports may be ordered from the National Technical Information Service, 5285 Port Royal Road, Springfield, Virginia, 22161. Accession Numbers should be quoted on orders for reports (PB --- ---) and remittance must accompany each order. Reports without this information were not available at time of printing. The complete list of EERC reports (from EERC 67-1) is available upon request from the Earthquake Engineering Research Center, University of California, Berkeley, 47th Street and Hoffman Boulevard, Richmond, California 94804.

UCB/EERC-79/01 "Hysteretic Behavior of Lightweight Reinforced Concrete Beam-Column Subassemblages," by B. Forzani, E.P. Popov and V.V. Bertero - April 1979(PB 298 267)A06

UCB/EERC-79/02 "The Development of a Mathematical Model to Predict the Flexural Response of Reinforced Concrete Beams to Cyclic Loads, Using System Identification," by J. Stanton & H. McNiven - Jan. 1979(PB 295 875)A10

UCB/EERC-79/03 "Linear and Nonlinear Earthquake Response of Simple Torsionally Coupled Systems," by C.L. Kan and A.K. Chopra - Feb. 1979(PB 298 262)A06

UCB/EERC-79/04 "A Mathematical Model of Masonry for Predicting its Linear Seismic Response Characteristics," by Y. Mengi and H.D. McNiven - Feb. 1979(PB 298 266)A06

UCB/EERC-79/05 "Mechanical Behavior of Lightweight Concrete Confined by Different Types of Lateral Reinforcement," by M.A. Manrique, V.V. Bertero and E.P. Popov - May 1979(PB 301 114)A06

UCB/EERC-79/06 "Static Tilt Tests of a Tall Cylindrical Liquid Storage Tank," by R.W. Clough and A. Niwa - Feb. 1979 (PB 301 167)A06

UCB/EERC-79/07 "The Design of Steel Energy Absorbing Restrainers and Their Incorporation into Nuclear Power Plants for Enhanced Safety: Volume 1 - Summary Report," by P.N. Spencer, V.F. Zackay, and E.R. Parker - Feb. 1979(UCB/EERC-79/07)A09

UCB/EERC-79/08 "The Design of Steel Energy Absorbing Restrainers and Their Incorporation into Nuclear Power Plants for Enhanced Safety: Volume 2 - The Development of Analyses for Reactor System Piping,""Simple Systems" by M.C. Lee, J. Penzien, A.K. Chopra and K, Suzuki "Complex Systems" by G.H. Powell, E.L. Wilson, R.W. Clough and D.G. Row - Feb. 1979(UCB/EERC-79/08)A10

UCB/EERC-79/09 "The Design of Steel Energy Absorbing Restrainers and Their Incorporation into Nuclear Power Plants for Enhanced Safety: Volume 3 - Evaluation of Commercial Steels," by W.S. Owen, R.M.N. Pelloux, R.O. Ritchie, M. Faral, T. Ohhashi, J. Toplosky, S.J. Hartman, V.F. Zackay and E.R. Parker - Feb. 1979(UCB/EERC-79/09)A04

UCB/EERC-79/10 "The Design of Steel Energy Absorbing Restrainers and Their Incorporation into Nuclear Power Plants for Enhanced Safety: Volume 4 - A Review of Energy-Absorbing Devices," by J.M. Kelly and M.S. Skinner - Feb. 1979(UCB/EERC-79/10)A04

UCB/EERC-79/11 "Conservatism In Summation Rules for Closely Spaced Modes," by J.M. Kelly and J.L. Sackman - May 1979(PB 301 328)A03

UCB/EERC-79/12 "Cyclic Loading Tests of Masonry Single Piers; Volume 3 - Height to Width Ratio of 0.5," by P.A. Hidalgo, R.L. Mayes, H.D. McNiven and R.W. Clough - May 1979(PB 301 321)A08

UCB/EERC-79/13 "Cyclic Behavior of Dense Course-Grained Materials in Relation to the Seismic Stability of Dams," by N.G. Banerjee, H.B. Seed and C.K. Chan - June 1979(PB 301 373)A13

UCB/EERC-79/14 "Seismic Behavior of Reinforced Concrete Interior Beam-Column Subassemblages," by S. Viwathanatepa, E.P. Popov and V.V. Bertero - June 1979(PB 301 326)A10

UCB/EERC-79/15 "Optimal Design of Localized Nonlinear Systems with Dual Performance Criteria Under Earthquake Excitations," by M.A. Bhatti - July 1979(PB 80 167 109)A06

UCB/EERC-79/16 "OPTDYN - A General Purpose Optimization Program for Problems with or without Dynamic Constraints," by M.A. Bhatti, E. Polak and K.S. Pister - July 1979(PB 80 167 091)A05

UCB/EERC-79/17 "ANSR-II, Analysis of Nonlinear Structural Response, Users Manual," by D.P. Mondkar and G.H. Powell July 1979(PB 80 113 301)A05

UCB/EERC-79/18 "Soil Structure Interaction in Different Seismic Environments," A. Gomez-Masso, J. Lysmer, J.-C. Chen and H.B. Seed - August 1979(PB 80 101 520)A04

UCB/EERC-79/19 "ARMA Models for Earthquake Ground Motions," by M.K. Chang, J.W. Kwiatkowski, R.F. Nau, R.M. Oliver and K.S. Pister - July 1979(PB 301 166)A05

UCB/EERC-79/20 "Hysteretic Behavior of Reinforced Concrete Structural Walls," by J.M. Vallenas, V.V. Bertero and E.P. Popov - August 1979(PB 80 165 905)A12

UCB/EERC-79/21 "Studies on High-Frequency Vibrations of Buildings - 1: The Column Effect," by J. Lubliner - August 1979 (PB 80 158 553)A03

UCB/EERC-79/22 "Effects of Generalized Loadings on Bond Reinforcing Bars Embedded in Confined Concrete Blocks," by S. Viwathanatepa, E.P. Popov and V.V. Bertero - August 1979(PB 81 124 018)A14

UCB/EERC-79/23 "Shaking Table Study of Single-Story Masonry Houses, Volume 1: Test Structures 1 and 2," by P. Gülkan, R.L. Mayes and R.W. Clough - Sept. 1979 (HUD-000 1763)A12

UCB/EERC-79/24 "Shaking Table Study of Single-Story Masonry Houses, Volume 2: Test Structures 3 and 4," by P. Gülkan, R.L. Mayes and R.W. Clough - Sept. 1979 (HUD-000 1836)A12

UCB/EERC-79/25 "Shaking Table Study of Single-Story Masonry Houses, Volume 3: Summary, Conclusions and Recommendations," by R.W. Clough, R.L. Mayes and P. Gülkan - Sept. 1979 (HUD-000 1837)A06

UCB/EERC-79/26 "Recommendations for a U.S.-Japan Cooperative Research Program Utilizing Large-Scale Testing Facilities," by U.S.-Japan Planning Group - Sept. 1979(PB 301 407)A06

UCB/EERC-79/27 "Earthquake-Induced Liquefaction Near Lake Amatitlan, Guatemala," by H.B. Seed, I. Arango, C.K. Chan, A. Gomez-Masso and R. Grant de Ascoli - Sept. 1979(NUREG-CR1341)A03

UCB/EERC-79/28 "Infill Panels: Their Influence on Seismic Response of Buildings," by J.W. Axley and V.V. Bertero Sept. 1979(PB 80 163 371)A10

UCB/EERC-79/29 "3D Truss Bar Element (Type 1) for the ANSR-II Program," by D.P. Mondkar and G.H. Powell - Nov. 1979 (PB 80 169 709)A02

UCB/EERC-79/30 "2D Beam-Column Element (Type 5 - Parallel Element Theory) for the ANSR-II Program," by D.G. Row, G.H. Powell and D.P. Mondkar - Dec. 1979(PB 80 167 224)A03

UCB/EERC-79/31 "3D Beam-Column Element (Type 2 - Parallel Element Theory) for the ANSR-II Program," by A. Riahi, G.H. Powell and D.P. Mondkar - Dec. 1979(PB 80 167 216)A03

UCB/EERC-79/32 "On Response of Structures to Stationary Excitation," by A. Der Kiureghian - Dec. 1979(PB 80166 929)A03

UCB/EERC-79/33 "Undisturbed Sampling and Cyclic Load Testing of Sands," by S. Singh, H.B. Seed and C.K. Chan Dec. 1979(ADA 087 298)A07

UCB/EERC-79/34 "Interaction Effects of Simultaneous Torsional and Compressional Cyclic Loading of Sand," by P.M. Griffin and W.N. Houston - Dec. 1979(ADA 092 352)A15

UCB/EERC-80/01 "Earthquake Response of Concrete Gravity Dams Including Hydrodynamic and Foundation Interaction Effects," by A.K. Chopra, P. Chakrabarti and S. Gupta - Jan. 1980(AD-A087297)A10

UCB/EERC-80/02 "Rocking Response of Rigid Blocks to Earthquakes," by C.S. Yim, A.K. Chopra and J. Penzien - Jan. 1980 (PB80 166 002)A04

UCB/EERC-80/03 "Optimum Inelastic Design of Seismic-Resistant Reinforced Concrete Frame Structures," by S.W. Zagajeski and V.V. Bertero - Jan. 1980(PB80 164 635)A06

UCB/EERC-80/04 "Effects of Amount and Arrangement of Wall-Panel Reinforcement on Hysteretic Behavior of Reinforced Concrete Walls," by R. Iliya and V.V. Bertero - Feb. 1980(PB81 122 525)A09

UCB/EERC-80/05 "Shaking Table Research on Concrete Dam Models," by A. Niwa and R.W. Clough - Sept. 1980(PB81 122 368)A06

UCB/EERC-80/06 "The Design of Steel Energy-Absorbing Restrainers and their Incorporation into Nuclear Power Plants for Enhanced Safety (Vol 1A): Piping with Energy Absorbing Restrainers: Parameter Study on Small Systems," by G.H. Powell, C. Oughourlian and J. Simons - June 1980

UCB/EERC-80/07 "Inelastic Torsional Response of Structures Subjected to Earthquake Ground Motions," by Y. Yamazaki April 1980(PB81 122 327)A08

UCB/EERC-80/08 "Study of X-Braced Steel Frame Structures Under Earthquake Simulation," by Y. Ghanaat - April 1980 (PB81 122 335)A11

UCB/EERC-80/09 "Hybrid Modelling of Soil-Structure Interaction," by S. Gupta, T.W. Lin, J. Penzien and C.S. Yeh May 1980(PB81 122 319)A07

UCB/EERC-80/10 "General Applicability of a Nonlinear Model of a One Story Steel Frame," by B.I. Sveinsson and H.D. McNiven - May 1980(PB81 124 877)A06

UCB/EERC-80/11 "A Green-Function Method for Wave Interaction with a Submerged Body," by W. Kioka - April 1980 (PB81 122 269)A07

UCB/EERC-80/12 "Hydrodynamic Pressure and Added Mass for Axisymmetric Bodies," by F. Nilrat - May 1980(PB81 122 343)A08

UCB/EERC-80/13 "Treatment of Non-Linear Drag Forces Acting on Offshore Platforms," by B.V. Dao and J. Penzien May 1980(PB81 153 413)A07

UCB/EERC-80/14 "2D Plane/Axisymmetric Solid Element (Type 3 - Elastic or Elastic-Perfectly Plastic) for the ANSR-II Program," by D.P. Mondkar and G.H. Powell - July 1980(PB81 122 350)A03

UCB/EERC-80/15 "A Response Spectrum Method for Random Vibrations," by A. Der Kiureghian - June 1980(PB81 122 301)A03

UCB/EERC-80/16 "Cyclic Inelastic Buckling of Tubular Steel Braces," by V.A. Zayas, E.P. Popov and S.A. Mahin June 1980(PB81 124 885)A10

UCB/EERC-80/17 "Dynamic Response of Simple Arch Dams Including Hydrodynamic Interaction," by C.S. Porter and A.K. Chopra - July 1980(PB81 124 000)A13

UCB/EERC-80/18 "Experimental Testing of a Friction Damped Aseismic Base Isolation System with Fail-Safe Characteristics," by J.M. Kelly, K.E. Beucke and M.S. Skinner - July 1980(PB81 148 595)A04

UCB/EERC-80/19 "The Design of Steel Energy-Absorbing Restrainers and their Incorporation into Nuclear Power Plants for Enhanced Safety (Vol 1B): Stochastic Seismic Analyses of Nuclear Power Plant Structures and Piping Systems Subjected to Multiple Support Excitations," by M.C. Lee and J. Penzien - June 1980

UCB/EERC-80/20 "The Design of Steel Energy-Absorbing Restrainers and their Incorporation into Nuclear Power Plants for Enhanced Safety (Vol 1C): Numerical Method for Dynamic Substructure Analysis," by J.M. Dickens and E.L. Wilson - June 1980

UCB/EERC-80/21 "The Design of Steel Energy-Absorbing Restrainers and their Incorporation into Nuclear Power Plants for Enhanced Safety (Vol 2): Development and Testing of Restraints for Nuclear Piping Systems," by J.M. Kelly and M.S. Skinner - June 1980

UCB/EERC-80/22 "3D Solid Element (Type 4-Elastic or Elastic-Perfectly-Plastic) for the ANSR-II Program," by D.P. Mondkar and G.H. Powell - July 1980(PB81 123 242)A03

UCB/EERC-80/23 "Gap-Friction Element (Type 5) for the ANSR-II Program," by D.P. Mondkar and G.H. Powell - July 1980 (PB81 122 285)A03

UCB/EERC-80/24 "U-Bar Restraint Element (Type 11) for the ANSR-II Program," by C. Oughourlian and G.H. Powell July 1980(PB81 122 293)A03

UCB/EERC-80/25 "Testing of a Natural Rubber Base Isolation System by an Explosively Simulated Earthquake," by J.M. Kelly - August 1980(PB81 201 360)A04

UCB/EERC-80/26 "Input Identification from Structural Vibrational Response," by Y. Hu - August 1980(PB81 152 308)A05

UCB/EERC-80/27 "Cyclic Inelastic Behavior of Steel Offshore Structures," by V.A. Zayas, S.A. Mahin and E.P. Popov August 1980(PB81 196 180)A15

UCB/EERC-80/28 "Shaking Table Testing of a Reinforced Concrete Frame with Biaxial Response," by M.G. Oliva October 1980(PB81 154 304)A10

UCB/EERC-80/29 "Dynamic Properties of a Twelve-Story Prefabricated Panel Building," by J.G. Bouwkamp, J.P. Kollegger and R.M. Stephen - October 1980(PB82 117 128)A06

UCB/EERC-80/30 "Dynamic Properties of an Eight-Story Prefabricated Panel Building," by J.G. Bouwkamp, J.P. Kollegger and R.M. Stephen - October 1980(PB81 200 313)A05

UCB/EERC-80/31 "Predictive Dynamic Response of Panel Type Structures Under Earthquakes," by J.P. Kollegger and J.G. Bouwkamp - October 1980(PB81 152 316)A04

UCB/EERC-80/32 "The Design of Steel Energy-Absorbing Restrainers and their Incorporation into Nuclear Power Plants for Enhanced Safety (Vol 3): Testing of Commercial Steels in Low-Cycle Torsional Fatigue," by P. Spencer, E.R. Parker, E. Jongewaard and M. Drory

UCB/EERC-80/33 "The Design of Steel Energy-Absorbing Restrainers and their Incorporation into Nuclear Power Plants for Enhanced Safety (Vol 4): Shaking Table Tests of Piping Systems with Energy-Absorbing Restrainers," by S.F. Stiemer and W.G. Godden - Sept. 1980

UCB/EERC-80/34 "The Design of Steel Energy-Absorbing Restrainers and their Incorporation into Nuclear Power Plants for Enhanced Safety (Vol 5): Summary Report," by P. Spencer

UCB/EERC-80/35 "Experimental Testing of an Energy-Absorbing Base Isolation System," by J.M. Kelly, M.S. Skinner and K.E. Beucke - October 1980(PB81 154 072)A04

UCB/EERC-80/36 "Simulating and Analyzing Artificial Non-Stationary Earthquake Ground Motions," by R.F. Nau, R.M. Oliver and K.S. Pister - October 1980(PB81 153 397)A04

UCB/EERC-80/37 "Earthquake Engineering at Berkeley - 1980," - Sept. 1980(PB81 205 874)A09

UCB/EERC-80/38 "Inelastic Seismic Analysis of Large Panel Buildings," by V. Schricker and G.H. Powell - Sept. 1980 (PB81 154 338)A13

UCB/EERC-80/39 "Dynamic Response of Embankment, Concrete-Gravity and Arch Dams Including Hydrodynamic Interaction," by J.F. Hall and A.K. Chopra - October 1980(PB81 152 324)A11

UCB/EERC-80/40 "Inelastic Buckling of Steel Struts Under Cyclic Load Reversal," by R.G. Black, W.A. Wenger and E.P. Popov - October 1980(PB81 154 312)A08

UCB/EERC-80/41 "Influence of Site Characteristics on Building Damage During the October 3, 1974 Lima Earthquake," by P. Repetto, I. Arango and H.B. Seed - Sept. 1980(PB81 161 739)A05

UCB/EERC-80/42 "Evaluation of a Shaking Table Test Program on Response Behavior of a Two Story Reinforced Concrete Frame," by J.M. Blondet, R.W. Clough and S.A. Mahin

UCB/EERC-80/43 "Modelling of Soil-Structure Interaction by Finite and Infinite Elements," by F. Medina - December 1980(PB81 229 270)A04

UCB/EERC-81/01 "Control of Seismic Response of Piping Systems and Other Structures by Base Isolation," edited by J.M. Kelly - January 1981 (PB81 200 735)A05

UCB/EERC-81/02 "OPTNSR - An Interactive Software System for Optimal Design of Statically and Dynamically Loaded Structures with Nonlinear Response," by M.A. Bhatti, V. Ciampi and K.S. Pister - January 1981 (PB81 218 851)A09

UCB/EERC-81/03 "Analysis of Local Variations in Free Field Seismic Ground Motions," by J.-C. Chen, J. Lysmer and H.B. Seed - January 1981 (AD-A099508)A13

UCB/EERC-81/04 "Inelastic Structural Modeling of Braced Offshore Platforms for Seismic Loading," by V.A. Zayas, P.-S.B. Shing, S.A. Mahin and E.P. Popov - January 1981(PB82 138 777)A07

UCB/EERC-81/05 "Dynamic Response of Light Equipment in Structures," by A. Der Kiureghian, J.L. Sackman and B. Nour-Omid - April 1981 (PB81 218 497)A04

UCB/EERC-81/06 "Preliminary Experimental Investigation of a Broad Base Liquid Storage Tank," by J.G. Bouwkamp, J.P. Kollegger and R.M. Stephen - May 1981(PB82 140 385)A03

UCB/EERC-81/07 "The Seismic Resistant Design of Reinforced Concrete Coupled Structural Walls," by A.E. Aktan and V.V. Bertero - June 1981(PB82 113 358)A11

UCB/EERC-81/08 "The Undrained Shearing Resistance of Cohesive Soils at Large Deformations," by M.R. Pyles and H.B. Seed - August 1981

UCB/EERC-81/09 "Experimental Behavior of a Spatial Piping System with Steel Energy Absorbers Subjected to a Simulated Differential Seismic Input," by S.F. Stiemer, W.G. Godden and J.M. Kelly - July 1981

UCB/EERC-81/10 "Evaluation of Seismic Design Provisions for Masonry in the United States," by B.I. Sveinsson, R.L. Mayes and H.D. McNiven - August 1981 (PB82 166 075)A08

UCB/EERC-81/11 "Two-Dimensional Hybrid Modelling of Soil-Structure Interaction," by T.-J. Tzong, S. Gupta and J. Penzien - August 1981(PB82 142 118)A04

UCB/EERC-81/12 "Studies on Effects of Infills in Seismic Resistant R/C Construction," by S. Brokken and V.V. Bertero - September 1981 (PB82 166 190)A09

UCB/EERC-81/13 "Linear Models to Predict the Nonlinear Seismic Behavior of a One-Story Steel Frame," by H. Valdimarsson, A.H. Shah and H.D. McNiven - September 1981(PB82 138 793)A07

UCB/EERC-81/14 "TLUSH: A Computer Program for the Three-Dimensional Dynamic Analysis of Earth Dams," by T. Kagawa, L.H. Mejia, H.B. Seed and J. Lysmer - September 1981(PB82 139 940)A06

UCB/EERC-81/15 "Three Dimensional Dynamic Response Analysis of Earth Dams," by L.H. Mejia and H.B. Seed - September 1981 (PB82 137 274)A12

UCB/EERC-81/16 "Experimental Study of Lead and Elastomeric Dampers for Base Isolation Systems," by J.M. Kelly and S.B. Hodder - October 1981 (PB82 166 182)A05

UCB/EERC-81/17 "The Influence of Base Isolation on the Seismic Response of Light Secondary Equipment," by J.M. Kelly - April 1981 (PB82 255 266)A04

UCB/EERC-81/18 "Studies on Evaluation of Shaking Table Response Analysis Procedures," by J. Marcial Blondet - November 1981 (PB82 197 278)A10

UCB/EERC-81/19 "DELIGHT.STRUCT: A Computer-Aided Design Environment for Structural Engineering," by R.J. Balling, K.S. Pister and E. Polak - December 1981 (PB82 218 496)A07

UCB/EERC-81/20 "Optimal Design of Seismic-Resistant Planar Steel Frames," by R.J. Balling, V. Ciampi, K.S. Pister and E. Polak - December 1981 (PB82 220 179)A07

UCB/EERC-82/01 "Dynamic Behavior of Ground for Seismic Analysis of Lifeline Systems," by T. Sato and A. Der Kiureghian - January 1982 (PB82 218 926)A05

UCB/EERC-82/02 "Shaking Table Tests of a Tubular Steel Frame Model," by Y. Ghanaat and R. W. Clough - January 1982 (PB82 220 161)A07

UCB/EERC-82/03 "Behavior of a Piping System under Seismic Excitation: Experimental Investigations of a Spatial Piping System supported by Mechanical Shock Arrestors and Steel Energy Absorbing Devices under Seismic Excitation," by S. Schneider, H.-M. Lee and W. G. Godden - May 1982 (PB83 172 544)A09

UCB/EERC-82/04 "New Approaches for the Dynamic Analysis of Large Structural Systems," by E. L. Wilson - June 1982 (PB83 148 080)A05

UCB/EERC-82/05 "Model Study of Effects of Damage on the Vibration Properties of Steel Offshore Platforms," by F. Shahrivar and J. G. Bouwkamp - June 1982 (PB83 148 742)A10

UCB/EERC-82/06 "States of the Art and Practice in the Optimum Seismic Design and Analytical Response Prediction of R/C Frame-Wall Structures," by A. E. Aktan and V. V. Bertero - July 1982 (PB83 147 736)A05

UCB/EERC-82/07 "Further Study of the Earthquake Response of a Broad Cylindrical Liquid-Storage Tank Model," by G. C. Manos and R. W. Clough - July 1982 (PB83 147 744)A11

UCB/EERC-82/08 "An Evaluation of the Design and Analytical Seismic Response of a Seven Story Reinforced Concrete Frame - Wall Structure," by F. A. Charney and V. V. Bertero - July 1982(PB83 157 628)A09

UCB/EERC-82/09 "Fluid-Structure Interactions: Added Mass Computations for Incompressible Fluid," by J. S.-H. Kuo - August 1982 (PB83 156 281)A07

UCB/EERC-82/10 "Joint-Opening Nonlinear Mechanism: Interface Smeared Crack Model," by J. S.-H. Kuo - August 1982 (PB83 149 195)A05

UCB/EERC-82/11 "Dynamic Response Analysis of Techi Dam," by R. W. Clough, R. M. Stephen and J. S.-H. Kuo - August 1982 (PB83 147 496)A06

UCB/EERC-82/12 "Prediction of the Seismic Responses of R/C Frame-Coupled Wall Structures," by A. E. Aktan, V. V. Bertero and M. Piazza - August 1982 (PB83 149 203)A09

UCB/EERC-82/13 "Preliminary Report on the SMART 1 Strong Motion Array in Taiwan," by B. A. Bolt, C. H. Loh, J. Penzien, Y. B. Tsai and Y. T. Yeh - August 1982 (PB83 159 400)A10

UCB/EERC-82/14 "Shaking-Table Studies of an Eccentrically X-Braced Steel Structure," by M. S. Yang - September 1982 (PB83 260 778)A12

UCB/EERC-82/15 "The Performance of Stairways in Earthquakes," by C. Roha, J. W. Axley and V. V. Bertero - September 1982 (PB83 157 693)A07

UCB/EERC-82/16 "The Behavior of Submerged Multiple Bodies in Earthquakes," by W.-G. Liao - Sept. 1982 (PB83 158 709)A07

UCB/EERC-82/17 "Effects of Concrete Types and Loading Conditions on Local Bond-Slip Relationships," by A. D. Cowell, E. P. Popov and V. V. Bertero - September 1982 (PB83 153 577)A04

UCB/EERC-82/18 "Mechanical Behavior of Shear Wall Vertical Boundary Members: An Experimental Investigation," by M. T. Wagner and V. V. Bertero - October 1982 (PB83 159 764)A05

UCB/EERC-82/19 "Experimental Studies of Multi-support Seismic Loading on Piping Systems," by J. M. Kelly and A. D. Cowell - November 1982

UCB/EERC-82/20 "Generalized Plastic Hinge Concepts for 3D Beam-Column Elements," by P. F.-S. Chen and G. H. Powell - November 1982 (PB83 247 981)A13

UCB/EERC-82/21 "ANSR-III: General Purpose Computer Program for Nonlinear Structural Analysis," by C. V. Oughourlian and G. H. Powell - November 1982 (PB83 251 330)A12

UCB/EERC-82/22 "Solution Strategies for Statically Loaded Nonlinear Structures," by J. W. Simons and G. H. Powell - November 1982 (PB83 197 970)A06

UCB/EERC-82/23 "Analytical Model of Deformed Bar Anchorages under Generalized Excitations," by V. Ciampi, R. Eligehausen, V. V. Bertero and E. P. Popov - November 1982 (PB83 169 532)A06

UCB/EERC-82/24 "A Mathematical Model for the Response of Masonry Walls to Dynamic Excitations," by H. Sucuoğlu, Y. Mengi and H. D. McNiven - November 1982 (PB83 169 011)A07

UCB/EERC-82/25 "Earthquake Response Considerations of Broad Liquid Storage Tanks," by F. J. Cambra - November 1982 (PB83 251 215)A09

UCB/EERC-82/26 "Computational Models for Cyclic Plasticity, Rate Dependence and Creep," by B. Mosaddad and G. H. Powell - November 1982 (PB83 245 829)A08

UCB/EERC-82/27 "Inelastic Analysis of Piping and Tubular Structures," by M. Mahasuverachai and G. H. Powell - November 1982 (PB83 249 987)A07

UCB/EERC-83/01 "The Economic Feasibility of Seismic Rehabilitation of Buildings by Base Isolation," by J. M. Kelly - January 1983 (PB83 197 988)A05

UCB/EERC-83/02 "Seismic Moment Connections for Moment-Resisting Steel Frames," by E. P. Popov - January 1983 (PB83 195 412)A04

UCB/EERC-83/03 "Design of Links and Beam-to-Column Connections for Eccentrically Braced Steel Frames," by E. P. Popov and J. O. Malley - January 1983 (PB83 194 811)A04

UCB/EERC-83/04 "Numerical Techniques for the Evaluation of Soil-Structure Interaction Effects in the Time Domain," by E. Bayo and E. L. Wilson - February 1983 (PB83 245 605)A09

UCB/EERC-83/05 "A Transducer for Measuring the Internal Forces in the Columns of a Frame-Wall Reinforced Concrete Structure," by R. Sause and V. V. Bertero - May 1983 (PB84 119 494)A06

UCB/EERC-83/06 "Dynamic Interactions between Floating Ice and Offshore Structures," by P. Croteau - May 1983 (PB84 119 486)A16

UCB/EERC-83/07 "Dynamic Analysis of Multiply Tuned and Arbitrarily Supported Secondary Systems," by T. Igusa and A. Der Kiureghian - June 1983 (PB84 118 272)A11

UCB/EERC-83/08 "A Laboratory Study of Submerged Multi-body Systems in Earthquakes," by G. R. Ansari - June 1983 (PB83 261 842)A17

UCB/EERC-83/09 "Effects of Transient Foundation Uplift on Earthquake Response of Structures," by C.-S. Yim and A. K. Chopra - June 1983 (PB83 261 396)A07

UCB/EERC-83/10 "Optimal Design of Friction-Braced Frames under Seismic Loading," by M. A. Austin and K. S. Pister - June 1983 (PB84 119 288)A06

UCB/EERC-83/11 "Shaking Table Study of Single-Story Masonry Houses: Dynamic Performance under Three Component Seismic Input and Recommendations," by G. C. Manos, R. W. Clough and R. L. Mayes - June 1983

UCB/EERC-83/12 "Experimental Error Propagation in Pseudodynamic Testing," by P. B. Shing and S. A. Mahin - June 1983 (PB84 119 270)A09

UCB/EERC-83/13 "Experimental and Analytical Predictions of the Mechanical Characteristics of a 1/5-scale Model of a 7-story R/C Frame-Wall Building Structure," by A. E. Aktan, V. V. Bertero, A. A. Chowdhury and T. Nagashima - August 1983 (PB84 119 213)A07

UCB/EERC-83/14 "Shaking Table Tests of Large-Panel Precast Concrete Building System Assemblages," by M. G. Oliva and R. W. Clough - August 1983

UCB/EERC-83/15 "Seismic Behavior of Active Beam Links in Eccentrically Braced Frames," by K. D. Hjelmstad and E. P. Popov - July 1983 (PB84 119 676)A09

UCB/EERC-83/16 "System Identification of Structures with Joint Rotation," by J. S. Dimsdale and H. D. McNiven - July 1983

UCB/EERC-83/17 "Construction of Inelastic Response Spectra for Single-Degree-of-Freedom Systems," by S. Mahin and J. Lin - July 1983

UCB/EERC-83/18 "Interactive Computer Analysis Methods for Predicting the Inelastic Cyclic Behaviour of Structural Sections," by S. Kaba and S. Mahin - July 1983 (PB84 192 012) A06

UCB/EERC-83/19 "Effects of Bond Deterioration on Hysteretic Behavior of Reinforced Concrete Joints," by F.C. Filippou, E.P. Popov and V.V. Bertero - August 1983 (PB84 192 020) A10

UCB/EERC-83/20 "Analytical and Experimental Correlation of Large-Panel Precast Building System Performance," by M.G. Oliva, R.W. Clough, M. Velkov, P. Gavrilovic and J. Petrovski - November 1983

UCB/EERC-83/21 "Mechanical Characteristics of Materials Used in a 1/5 Scale Model of a 7-Story Reinforced Concrete Test Structure," by V.V. Bertero, A.E. Aktan, H.G. Harris and A.A. Chowdhury - September 1983 (PB84 193 697) A05

UCB/EERC-83/22 "Hybrid Modelling of Soil-Structure Interaction in Layered Media," by T.-J. Tzong and J. Penzien - October 1983 (PB84 192 178) A08

UCB/EERC-83/23 "Local Bond Stress-Slip Relationships of Deformed Bars under Generalized Excitations," by R. Eligehausen, E.P. Popov and V.V. Bertero - October 1983 (PB84 192 848) A09

UCB/EERC-83/24 "Design Considerations for Shear Links in Eccentrically Braced Frames," by J.O. Malley and E.P. Popov - November 1983 (PB84 192 186) A07

UCB/EERC-84/01 "Pseudodynamic Test Method for Seismic Performance Evaluation: Theory and Implementation," by P.-S. B. Shing and S. A. Mahin - January 1984 (PB84 190 644) A08

UCB/EERC-84/02 "Dynamic Response Behavior of Xiang Hong Dian Dam," by R.W. Clough, K.-T. Chang, H.-Q. Chen, R.M. Stephen, G.-L. Wang, and Y. Ghanaat - April 1984

UCB/EERC-84/03 "Refined Modelling of Reinforced Concrete Columns for Seismic Analysis," by S.A. Kaba and S.A. Mahin - April, 1984

UCB/EERC-84/04 "A New Floor Response Spectrum Method for Seismic Analysis of Multiply Supported Secondary Systems," by A. Asfura and A. Der Kiureghian - June 1984

UCB/EERC-84/05 "Earthquake Simulation Tests and Associated Studies of a 1/5th-scale Model of a 7-Story R/C Frame-Wall Test Structure," by V.V. Bertero, A.E. Aktan, F.A. Charney and R. Sause - June 1984

UCB/EERC-84/06 "R/C Structural Walls: Seismic Design for Shear," by A.E. Aktan and V.V. Bertero

UCB/EERC-84/07 "Behavior of Interior and Exterior Flat-Plate Connections subjected to Inelastic Load Reversals," by H.L. Zee and J.P. Moehle

UCB/EERC-84/08 "Experimental Study of the Seismic Behavior of a two-story Flat-Plate Structure," by J.W. Diebold and J.P. Moehle.

UCB/EERC-84/09 "Phenomenological Modeling of Steel Braces under Cyclic Loading," by K. Ikeda, S.A. Mahin and S.N. Dermitzakis - May 1984

UCB/EERC-84/10 "Earthquake Analysis and Response of Concrete Gravity Dams," by G. Fenves and A.K. Chopra - August 1984

UCB/EERC-84/11 "EAGD-84: A Computer Program for Earthquake Analysis of Concrete Gravity Dams," by G. Fenves and A.K. Chopra - August 1984

UCB/EERC-84/12 "A Refined Physical Theory Model for Predicting the Seismic Behavior of Braced Steel Frames," by K. Ikeda and S.A. Mahin - July 1984

UCB/EERC-84/13 "Earthquake Engineering Research at Berkeley - 1984" - August 1984

UCB/EERC-84/14 "Moduli and Damping Factors for Dynamic Analyses of Cohesionless Soils," by H.B. Seed, R.T. Wong, I.M. Idriss and K. Tokimatsu - September 1984

UCB/EERC-84/15 "The Influence of SPT Procedures in Soil Liquefaction Resistance Evaluations," by H. B. Seed, K. Tokimatsu, L. F. Harder and R. M. Chung - October 1984

UCB/EERC-84/16 "Simplified Procedures for the Evaluation of Settlements in Sands Due to Earthquake Shaking," by K. Tokimatsu and H. B. Seed - October 1984

UCB/EERC-84/17 "Evaluation and Improvement of Energy Absorption Characteristics of Bridges under Seismic Conditions," by R. A. Imbsen and J. Penzien - November 1984

UCB/EERC-84/18 "Structure-Foundation Interactions under Dynamic Loads," by W. D. Liu and J. Penzien - November 1984

UCB/EERC-84/19 "Seismic Modelling of Deep Foundations," by C.-H. Chen and J. Penzien - November 1984

UCB/EERC-84/20 "Dynamic Response Behavior of Quan Shui Dam," by R. W. Clough, K.-T. Chang, H.-Q. Chen, R. M. Stephen, Y. Ghanaat and J.-H. Qi - November 1984

NA UCB/EERC-85/01 "Simplified Methods of Analysis for Earthquake Resistant Design of Buildings," by E.F. Cruz and A.K. Chopra - Feb. 1985 (PB86 112299/AS) A12

UCB/EERC-85/02 "Estimation of Seismic Wave Coherency and Rupture Velocity using the SMART 1 Strong-Motion Array Recordings," by N.A. Abrahamson - March 1985

UCB/EERC-85/03 "Dynamic Properties of a Thirty Story Condominium Tower Building," by R.M. Stephen, E.L. Wilson and N. Stander - April 1985 (PB86 118965/AS) A06

UCB/EERC-85/04 "Development of Substructuring Techniques for On-Line Computer Controlled Seismic Performance Testing," by S. Dermitzakis and S. Mahin - February 1985 (PB86 132941/AS) A08

UCB/EERC-85/05 "A Simple Model for Reinforcing Bar Anchorages under Cyclic Excitations," by F.C. Filippou - March 1985 (PB86 112919/AS) A05

UCB/EERC-85/06 "Racking Behavior of Wood-Framed Gypsum Panels under Dynamic Load," by M.G. Oliva - June 1985

UCB/EERC-85/07 "Earthquake Analysis and Response of Concrete Arch Dams," by K.-L. Fok and A.K. Chopra - June 1985 (PB86 139672/AS) A10

UCB/EERC-85/08 "Effect of Inelastic Behavior on the Analysis and Design of Earthquake Resistant Structures," by J.P. Lin and S.A. Mahin - June 1985 (PB86 135340/AS) A08

UCB/EERC-85/09 "Earthquake Simulator Testing of a Base-Isolated Bridge Deck," by J.M. Kelly, I.G. Buckle and H.-C. Tsai - January 1986

UCB/EERC-85/10 "Simplified Analysis for Earthquake Resistant Design of Concrete Gravity Dams," by G. Fenves and A.K. Chopra - September 1985

UCB/EERC-85/11 "Dynamic Interaction Effects in Arch Dams," by R.W. Clough, K.-T. Chang, H.-Q. Chen and Y. Ghanaat - October 1985 (PB86 135027/AS) A05

UCB/EERC-85/12 "Dynamic Response of Long Valley Dam in the Mammoth Lake Earthquake Series of May 25-27, 1980," by S. Lai and H.B. Seed - November 1985 (PB86 142304/AS) A05

UCB/EERC-85/13 "A Methodology for Computer-Aided Design of Earthquake-Resistant Steel Structures," by M.A. Austin, K.S. Pister and S.A. Mahin - December 1985 (PB86 159480/AS) A10

UCB/EERC-85/14 "Response of Tension-Leg Platforms to Vertical Seismic Excitations," by G.-S. Liou, J. Penzien and R.W. Yeung - December 1985

UCB/EERC-85/15 "Cyclic Loading Tests of Masonry Single Piers: Volume 4 - Additional Tests with Height to Width Ratio of 1," by H. Sucuoglu, H.D. McNiven and B. Sveinsson - December 1985

UCB/EERC-85/16 "An Experimental Program for Studying the Dynamic Response of a Steel Frame with a Variety of Infill Partitions," by B. Yanev and H.D. McNiven - December 1985

UCB/EERC-86/01 "A Study of Seismically Resistant Eccentrically Braced Steel Frame Systems," by K. Kasai and E.P. Popov - January 1986

UCB/EERC-86/02 "Design Problems in Soil Liquefaction," by H.B. Seed - February 1986

UCB/EERC-86/03 "Lessons Learned from Recent Earthquakes and Research, and Implications for Earthquake Resistant Design of Building Structures in the United States," by V.V. Bertero - March 1986

UCB/EERC-86/04 "The Use of Load Dependent Vectors for Dynamic and Earthquake Analyses," by P. Léger, E.L. Wilson and R.W. Clough - March 1986

UCB/EERC-86/05 "Two Beam-To-Column Web Connections," by K.-C. Tsai and E.P. Popov - April 1986

UCB/EERC-86/06 "Determination of Penetration Resistance for Coarse-Grained Soils using the Becker Hammer Drill," by L.F. Harder and H.B. Seed - May 1986